

SEISMIC CHARACTERISTICS OF PALEO-POCKMARKS  
AT GREAT SOUTH BASIN, NEW ZEALAND



A Thesis Submitted in Partial Fulfillment of the Requirements  
for the Degree of Master of Science in Geology  
Department of Geology  
Faculty of Science  
Chulalongkorn University  
Academic Year 2018  
Copyright of Chulalongkorn University

ลักษณะเฉพาะทางคลื่นไหวสะเทือนของร่องหลุมโบราณบริเวณแอ่งเกรทเซาท์ ประเทศนิวซีแลนด์



วิทยานิพนธ์นี้เป็นส่วนหนึ่งของการศึกษาตามหลักสูตรปริญญาวิทยาศาสตรมหาบัณฑิต

สาขาวิชาธรณีวิทยา ภาควิชาธรณีวิทยา

คณะวิทยาศาสตร์ จุฬาลงกรณ์มหาวิทยาลัย

ปีการศึกษา 2561

ลิขสิทธิ์ของจุฬาลงกรณ์มหาวิทยาลัย

Thesis Title SEISMIC CHARACTERISTICS OF PALEO-  
POCKMARKS AT GREAT SOUTH BASIN, NEW  
ZEALAND  
By Miss Arunee Karaket  
Field of Study Geology  
Thesis Advisor Assistant Professor PIYAPHONG CHENRAI, Ph.D.

---

Accepted by the Faculty of Science, Chulalongkorn University in Partial  
Fulfillment of the Requirement for the Master of Science

..... Dean of the Faculty of Science  
(Professor POLKIT SANGVANICH, Ph.D.)

THESIS COMMITTEE

..... Chairman  
(Assistant Professor VICHAI CHUTAKOSITKANON,  
Ph.D.)  
..... Thesis Advisor  
(Assistant Professor PIYAPHONG CHENRAI, Ph.D.)  
..... Examiner  
(Professor MONTRI CHOOWONG, Ph.D.)  
..... External Examiner  
(Songkhun Boonchaisuk, Ph.D.)



จุฬาลงกรณ์มหาวิทยาลัย  
CHULALONGKORN UNIVERSITY

อรุณี การะเกตุ : ลักษณะเฉพาะทางคลื่นไหวสะเทือนของร่องหลุมโบราณบริเวณแอ่ง  
เกรทเซาท์ ประเทศนิวซีแลนด์. ( SEISMIC CHARACTERISTICS  
OF PALEO-POCKMARKS AT GREAT SOUTH  
BASIN, NEW ZEALAND) อ.ที่ปรึกษาหลัก : ผศ. ดร.ปิยพงษ์ เซน  
รัมย์

ร่องหลุมโบราณ และร่องหลุมปัจจุบัน เป็นลักษณะร่องรอยที่พบได้หลากหลายพื้นที่ ทั้งบริเวณในชายฝั่งทะเลและนอกชายฝั่งทะเลทั่วโลก ซึ่งร่องหลุมเหล่านี้สามารถใช้เป็นตัวบ่งชี้ถึงกระบวนการไหลของของไหลผ่านชั้นตะกอนที่ยังไม่แข็งตัวในแอ่งสะสมตะกอนได้ โดยในบริเวณแอ่งเกรทเซาท์ ประเทศนิวซีแลนด์ เป็นหนึ่งในแอ่งสะสมตะกอนที่มีการสำรวจพบร่องหลุมโบราณกระจายตัวครอบคลุมพื้นที่นอกชายฝั่งทางด้านตะวันออกเฉียงใต้ของเกาะใต้ บริเวณใต้พื้นผิวที่ความลึกประมาณ 1.5 วินาที (TWT) ดังนั้นงานวิจัยนี้ถูกจัดทำขึ้นโดยมีวัตถุประสงค์เพื่อศึกษาลักษณะเฉพาะทางคลื่นไหวสะเทือนของร่องหลุมโบราณในพื้นที่แอ่งเกรทเซาท์ และอภิปรายของชนิดของของไหลที่สามารถเป็นต้นกำเนิด รวมทั้งกระบวนการเกิดร่องหลุมโบราณในพื้นที่

ร่องหลุมโบราณในพื้นที่ศึกษาถูกพบอยู่บนชั้นตะกอนละเอียดสมัยอีโอซีนตอนกลางของหมวดหินแลง มีลักษณะการกระจายตัวในทิศทางตะวันตกเฉียงใต้ไปยังตะวันออกเฉียงเหนือซึ่งสอดคล้องกับรูปร่างของตะกอนรูปพัด พื้นที่ของร่องหลุมโบราณถูกแบ่งออกเป็น 3 ส่วน เพื่อศึกษารูปร่างลักษณะและความหนาแน่นของร่องหลุมโบราณ ซึ่งประกอบไปด้วยพื้นที่ส่วนต้นของตะกอนรูปพัด (โซน 1) ส่วนกลาง (โซน 2) และส่วนปลาย (โซน 3) ตัวอย่างร่องหลุมโบราณจำนวน 94 ร่องหลุม ถูกเลือกโดยการสุ่มจากทั้ง 3 ส่วน เพื่อใช้ในการวัดขนาดของร่องหลุมโบราณในพื้นที่ จากการศึกษาสรุปว่าร่องหลุมโบราณในพื้นที่ศึกษาถูกจำแนกเป็นชนิด “ร่องหลุมแบบปกติ” ที่มีรูปร่างจากมุมบนเป็นลักษณะกึ่งกลมถึงกลม และจากมุมด้านข้างเป็นรูปร่างคล้ายตัววีและตัวยู โดยมีความกว้างตั้งแต่ 131 ถึง 481 เมตร และลึกตั้งแต่ 15 ถึง 45 มิลลิวินาที (TWT) พบว่าร่องหลุมโบราณมีความหนาแน่นประมาณ 13.4 ร่องหลุมต่อพื้นที่ 1 ตารางกิโลเมตร กระจายตัวหนาแน่นโดยเฉพาะบริเวณตอนกลางของพื้นที่ศึกษา นอกจากนี้ยังพบว่าตำแหน่งที่พบและลักษณะการกระจายตัวของร่องหลุมโบราณสามารถสันนิษฐานได้ว่าของไหลที่เป็นต้นกำเนิดของร่องหลุมโบราณนี้ประกอบไปด้วย ไมโครเบียลมีเทนเป็นของไหลต้นกำเนิดหลักที่ทำให้เกิดลักษณะการกระจายตัวกว้างของร่องหลุมโบราณสมัยอีโอซีนตอนกลางในสภาวะที่มีอุณหภูมิต่ำได้ ในขณะที่น้ำที่สะสมตัวในชั้นตะกอนละเอียดที่ถูกบีบอัด ประกอบไปด้วยหมวดหินวิกคลิฟสมัยครีเทเชียสตอนปลายถึงพาลีโอซีนตอนต้น และหมวดหินแลงสมัยอีโอซีนตอนต้นถึงตอนกลาง มีความเป็นไปได้ที่จะเป็นหนึ่งในของไหลต้นกำเนิดที่ก่อให้เกิดร่องหลุมโบราณในพื้นที่ศึกษาได้เช่นกัน

จุฬาลงกรณ์มหาวิทยาลัย  
CHULALONGKORN UNIVERSITY

สาขาวิชา ธรณีวิทยา

ลายมือชื่อนิติ

ปีการศึกษา 2561

ลายมือชื่อ อ.ที่ปรึกษาหลัก



## 5972093423 : MAJOR GEOLOGY

KEYWORD: middle Eocene paleo-pockmarks, fluid flow feature, Laing formation, New Zealand

Arunee Karaket : SEISMIC CHARACTERISTICS OF PALEO-POCKMARKS AT GREAT SOUTH BASIN, NEW ZEALAND. Advisor: Asst. Prof. PIYAPHONG CHENRAI, Ph.D.

Paleo-pockmarks and present-day pockmarks are founded in several varieties both onshore and offshore worldwide. These features can be used as an indicator of fluid flow process which expulses through an unconsolidated sediment within the basin. The Great South Basin, New Zealand is one of the basins that paleo-pockmarks are observed covering the southeast offshore of South Island at around 1.5 s (TWT) depth beneath the surface. This study aims to identify seismic characteristics of paleo-pockmarks in the Great South Basin and predict the possible fluid origins and their mechanism. The numerous paleo-pockmarks are identified and imaged by using 3D seismic interpretation.

Paleo-pockmarks in the study area are observed on the fine-grained sedimentary succession of middle Eocene as known Laing formation. The paleo-pockmark distribution is aligned from the southwest toward northeast direction coincident with fan shaped geometry. Paleo-pockmark area are divided within 3 major zones to study morphology and density of paleo-pockmarks. There are zone 1 located in the proximal fan, zone 2 located in the middle fan, and zone 3 located in the distal fan. The 94 paleo-pockmark samples are randomly chosen from 3 zones for size measurement. Paleo-pockmarks in the study area are identified as “normal pockmark” with sub-round to round on the top view, V-shape and U-shape in profile view. Their size ranges from 131 to 481 m in diameter and 15 to 45 ms (TWT) in depth. Paleo-pockmarks are observed to have high density around 13.4 paleo-pockmarks per a square kilometer at the central part of the study area (zone B). Furthermore, location distribution of paleo-pockmarks is interpreted to be caused by two possible fluid origins. Microbial methane is the main fluid origins which generate more widespread middle Eocene paleo-pockmarks in low temperature condition. While pore water in compacted fine-grained sedimentary layers, including late Cretaceous to early Paleocene Wickcliffe formation and early to middle Eocene Laing formation, are possible to be one of the fluid sources of paleo-pockmarks in the study area as well.

CHULALONGKORN UNIVERSITY

Field of Study: Geology  
Academic Year: 2018

Student's Signature .....  
Advisor's Signature .....

## ACKNOWLEDGEMENTS

I would like to thank Department of Geology, Chulalongkorn University for give me the opportunity to pursue master degree in geology program.

I wish to express my sincere thanks to my advisor: Assistant Professor Dr.Piyaphong Chenrai who support my work in this way and helped me get results of better quality. His advice, invaluable suggestions and critical comments are very much appreciated. I also would like to thank all committee members who give me an advice and supported my work.

I am deeply thank to my family for their support and blessing. I also would like to thank my friend for their cheer up and inspire me.

Finally, I would like to thank all staff at Faculty of Science and Department of geology who helped me manage all the important document.

Arunee Karaket

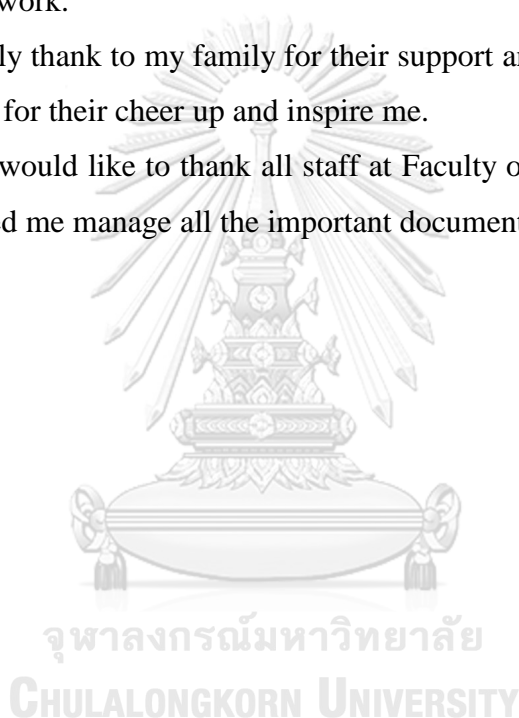


# TABLE OF CONTENTS

	<b>Page</b>
ABSTRACT (THAI) .....	iii
ABSTRACT (ENGLISH).....	iv
ACKNOWLEDGEMENTS.....	v
TABLE OF CONTENTS.....	vi
LIST OF TABLES .....	ix
LIST OF FIGURES .....	x
CHAPTER 1 .....	1
INTRODUCTION .....	1
1.1 Overviews of pockmarks .....	4
1.1.1 Pockmark definition .....	4
1.1.2 Pockmark characteristics and classification .....	5
1.1.3 Cause of fluid expulsion.....	10
1.2 Research objectives .....	13
1.3 Research benefits .....	13
CHAPTER 2 .....	14
GEOLOGICAL SETTING AND STRATIGRAPHY .....	14
2.1 Geological setting .....	15
2.2 Sedimentary sequences .....	18
2.3 Marine weather and sea conditions of the South Island .....	20
CHAPTER 3 .....	22
METHODOLOGY .....	22
3.1 Step 1 : Surface Attribute .....	25
3.1.1 RMS amplitude.....	26
3.2 Step 2 : Volume Attribute.....	27
3.2.1 Variance attribute .....	27

3.2.2 Consistent dip .....	27
3.2.3 3D Curvature .....	28
3.3 well log analysis .....	28
3.3.1 Gamma ray log pattern interpretation .....	30
3.3.2 Well log correlation .....	31
CHAPTER 4 .....	33
RESULTS .....	33
4.1 Stratigraphic correlation .....	33
4.2 Paleo-pockmark distribution .....	37
4.3. Seismic characteristics of paleo-pockmarks and size measurement.....	38
4.3.1 Paleo-pockmark characteristics in zone A .....	41
4.3.2 Paleo-pockmark characteristics in zone 2 .....	44
4.3.3 Paleo-pockmark characteristics in zone 3 .....	52
4.4 Density .....	55
4.5 Well log analysis.....	56
4.5.1 Marker picking .....	56
CHAPTER 5 .....	62
DISCUSSIONS .....	62
5.1 Paleo-pockmark classification .....	62
5.1.1 Type of the paleo-pockmarks .....	62
5.1.2 Density of the paleo-pockmarks and their location.....	66
5.2 The possible fluid sources .....	70
5.2.1 Pore water .....	70
5.2.2 Hydrothermal fluid .....	71
5.2.3 Biogenic Methane.....	72
5.3 Migration pathway .....	74
5.3.1 Polygonal fault system .....	75
5.3.2 Progradational clinoform.....	75
5.4 Other external factors .....	75

5.4.1 Sea-level change.....	75
5.5 Mechanism of middle Eocene Paleo-pockmarks.....	76
5.6 Petroleum application .....	78
CHAPTER 6 .....	80
CONCLUSIONS.....	80
REFERENCES .....	82
VITA.....	87



## LIST OF TABLES

	<b>Page</b>
Table 1 well data used in this study .....	23
Table 2 The statistic information of representative paleo-pockmarks from zone 1.....	43
Table 3 The statistic information of representative paleo-pockmarks from zone 2.....	51
Table 4 The statistic information of representative paleo-pockmarks from zone 3.....	54
Table 5 The characteristic comparison of three type pockmarks .....	66



## LIST OF FIGURES

	<b>Page</b>
Figure 1 Schematic illustration and seismic characteristic of fluid flow features show which are divided into three major groups (Andresen, 2012). .....	2
Figure 2 show (right) 3D seismic time slice at 1490 ms (TWT) in the Great South Basin, New Zealand showed the distribution of uncommon features around the area, and (left) enlargement of the feature in yellow frame. ....	4
Figure 3 show the fluid flow process model of pockmarks formation by (Judd and Hovland, 2009) .....	5
Figure 4 show illustration of the major group of pockmarks modified from Hovland et al. (2002).....	6
Figure 5 Representation of pockmark-families in the Norwegian Trough by using shaded relief digital terrain model (DTM) (Hovland et al., 2010).....	7
Figure 6 Maps of (a) high-density normal pockmarks in the Barents Sea (Mazzini et al., 2017) and (b) North Sea (Nickel et al., 2012), and (c) low-density normal pockmarks in the North Island, New Zealand (Chenrai and Huuse, 2017). ....	8
Figure 7 show (a) the relationship of circulation pattern, bathymetric map and (b) distribution of elongated pockmarks, and (c) the long axis direction of elongated pockmarks on the southern slope of Norwegian Trend (Bøe et al., 1998). ....	9
Figure 8 show illustrate model of the evolution of elongated pockmarks (Puchala, 2014). ....	9
Figure 9 show the evolution of crescent pockmarks is explained into 5 stages (S1-S5). S1; fluid escape generated small pockmarks on the fine grain surface. S2; strings of pockmarks are growth by slides and slumps in slope area, S3-S5; pockmarks developed to larger pockmark and remodel to crescent pockmarks in finally (Chen et al., 2015). ....	10
Figure 10 Illustrate models show mechanism of pockmark formation in the Levant Basin (southeastern Mediterranean). A) natural gas accumulated in the turbiditic sand lenses, B) gas venting through sediment layer upward to the seabed and developed to large pockmarks in the final stage (Bertoni et al., 2013). ....	13
Figure 11 The evolution of New Zealand's plate tectonic from early Cretaceous to present day (NZP&M, 2015). ....	16

Figure 12 Map of New Zealand’s sedimentary basin cover North Island and South Island (NZP&M, 2015).....	17
Figure 13 Schematic model of sequenced stratigraphy in GSB (NZP&M, 2015).....	20
Figure 14 A schematic map shows the large-scale anti-clockwise circulation and current in New Zealand (left). Mean current model (right) show two dominant currents around the South Island. Southland Current (SC) flows northward and Antarctic Circumpolar Current (ACC) flows eastward. (Gorman et al., 2005).....	21
Figure 15 Map of the Great South Basin, New Zealand (study area). 3D seismic line located on black polygonal, 2D seismic show in blue line, and wells exploration show in black- dots (Chenrai and Huuse, 2017). ....	24
Figure 16 Workflow shows two major steps for the paleo-pockmark study in the study area. ....	25
Figure 17 The comparison between general seismic volume (A) and RMS amplitude attribute volume (B) high-value indicate high amplitude anomaly (Koson et al., 2014). ....	26
Figure 18 Variance attribute image as dark to hot colors displays fault characteristics (red arrow) on the seismic section (Pigott et al., 2013). ....	27
Figure 19 Sign convention of curvature attribute. Grey arrows are defined as vectors (Schlumberger Petrel 2014). ....	28
Figure 20 Well log sample shows physical parameters which used to identify lithology, porosity, and fluid type (Schlumberger, 2006). ....	30
Figure 21 Schematic model of log shapes shows the relationship between gamma-ray log patterns and depositional environments (Odundun and Nton, 2012). ....	31
Figure 22 The sample of three selected three well which was correlated by using schlumberger Petrel software.....	32
Figure 23 2D and 3D seismic section which is used for horizon picking and seismic interpretation correlated with Pakaha-1 well. Five color lines on both figures are the top formation, which the name label on the right .....	36
Figure 24 Seismic profiles show sequence stratigraphy, structural pattern and the important features in the study area. The paleo-pockmark layer (number 4) is detected on the top of Laing formation (green layer). The lower part of Laing formation shows progradation pattern (number 5). Polygonal fault system (number 3) is located at the eastern part of the study area. ....	37
Figure 25 (a) Characteristics of paleo-pockmarks are shown both on the top view and (b) side view. Paleo-pockmark width and depth are measured in seismic section.	



Width is measure from the left shoulder (A) to the right shoulder (A'), while depth is measure from paleo-pockmark cluster to the bottom (b).....	38
Figure 26 (a) RMS amplitude map shows paleo-pockmark distribution as fan shape in the study area. The variance (var) and consistent dip (dip) images show (b)the sample images of paleo-pockmark from zone 1, (c) zone 2, and (d) zone 3. White dashed lines are the boundary of fan shape. ....	39
Figure 27 Variance map shows the location of each zone to study characteristics of paleo-pockmarks. There are three major zones, including two red frames located in zone 1, four green frames located in zone 2, and a purple frame located in zone 3. ...	40
Figure 28 Variance map (left) shows sub-round to round in shapes on the top view with medium to high values (0.5 to 0.8 value) of discontinuity. While consistent dip map (right) shows 7 to 15 degrees of paleo-pockmark dip angle (medium to high value).....	41
Figure 29 Seismic sections (1-S1 to 1-S3) show the shape of nine paleo-pockmarks (Pm1-Pm9) in section view. Pm1 and Pm2 are V-shape pockmarks, while Pm3 to Pm9 are mostly U-shape pockmarks. Their size ranges from 204 to 382 m (width), and 19 to 45 ms (TWT) (depth). See seismic profiles in Figure 28. ....	42
Figure 30 Variance map (left) shows sub-round to round in shapes on the top view with medium values (around 0.5 value) of discontinuity. While consistent dip map (right) shows 6 to 7 degrees of paleo-pockmark dip angle (medium value). ....	42
Figure 31 Seismic sections show characteristics of paleo-pockmarks 10 to 18 (Pm10-Pm18). All paleo-pockmarks in these sections are U-shape pockmarks. Their size ranges from 333 to 481 m (width), and 15 to 34 ms (TWT) (depth). Moreover, the progradational pattern of clastic sediment is founded beneath paleo-pockmarks layer. See seismic profiles in Figure 30. ....	43
Figure 32 Variance map (left) displays low to high value (0.3 to 0.8 value) with mostly sub-round in shape on the top view. While consistent dip map (right) shows 4 to 15 degrees of paleo-pockmark dip angle (low to high value). ....	45
Figure 33 Seismic sections show characteristics of paleo-pockmarks 19 to 28 (Pm19-Pm28). All paleo-pockmarks in these sections are U-shape pockmarks. Their size ranges from 138 to 189 m (width), and 15 to 24 ms (TWT) (depth). Moreover, progradational pattern of clastic sediment is founded beneath paleo-pockmarks layer. See seismic profiles in Figure 32. ....	45
Figure 34 Variance map (left) displays low to high value (0.3 to 0.8 value) with mostly sub-round in shape on the top view. While consistent dip map (right) shows 4 to 15 degrees of paleo-pockmark dip angle (low to high value). ....	46

- Figure 35 Seismic sections show characteristics of paleo-pockmarks 29 to 39 (Pm29-Pm39). All paleo-pockmarks in these sections are V-shape to U-shape pockmarks. Their size ranges from 131 to 340 m (width), and 16 to 33 ms (TWT) (depth). Moreover, progradational pattern of clastic sediment is founded beneath paleo-pockmarks layer. See seismic profiles in Figure 34.....46
- Figure 36 Seismic sections show characteristics of paleo-pockmarks 40 to 54 (Pm40-Pm54). All paleo-pockmarks in these sections are U-shape pockmarks. Their size ranges from 222 to 350 m (width), and 29 to 45 ms (TWT) (depth). Moreover, progradational pattern of clastic sediment is founded beneath paleo-pockmarks layer. See seismic profiles in Figure 34. ....47
- Figure 37 Variance map (left) displays low to medium value (0.3 to 0.5 value) with mostly sub-round in shape on the top view. While, consistent dip map (right) shows 7 to 15 degrees of paleo-pockmark dip angle (medium to high value).....48
- Figure 38 Seismic sections show characteristics of paleo-pockmarks 55 to 62 (Pm55-Pm62). Paleo-pockmarks in these sections are mostly V-shape pockmarks. Their size ranges from 166 to 239 m (width), and 20 to 30 ms (TWT) (depth). Moreover, progradational pattern of clastic sediment is founded beneath paleo-pockmarks layer. See seismic profiles in Figure 37.....48
- Figure 39 Seismic sections show characteristics of paleo-pockmarks 63 to 74 (Pm63-Pm74). Almost paleo-pockmarks in these sections are V-shape pockmarks (Pm65-Pm70 and Pm72-Pm73). Their size ranges from 141 to 330 m (width), and 19 to 42 ms (TWT) (depth). Moreover, progradational pattern of clastic sediment is founded beneath paleo-pockmarks layer. See seismic profiles in Figure 37. ....49
- Figure 40 Variance map (left) displays low to medium value (0.3 to 0.8 value) with sub-round to round in shape on the top view. While, consistent dip map (right) shows 4 to 7 degrees of paleo-pockmark dip angle (low to medium value).....50
- Figure 41 Seismic sections show characteristics of paleo-pockmarks 75 to 81 (Pm75-Pm81). Paleo-pockmarks in these sections are V-shape to U-shape pockmarks. Their size ranges from 152 to 292 m (width), and 19 to 21 ms (TWT) (depth). See seismic profiles in Figure 40.....50
- Figure 42 Variance map (left) displays low to medium value (0.3 to 0.5 value) with sub-round to round in shape on the top view. While, consistent dip map (right) shows 4 to 7 degrees of paleo-pockmark dip angle (low to medium value).....53
- Figure 43 Seismic sections show characteristics of paleo-pockmarks 82 to 88 (Pm82-Pm88). All paleo-pockmarks in these sections are U-shape pockmarks. Their size ranging from 163 to 225 m (width), and 18 to 22 ms (TWT) (depth). Polygonal faults are founded on the upper portion of the seismic section. See seismic profiles in Figure 42. ....53

- Figure 44 Seismic sections show characteristics of paleo-pockmarks 89 to 94 (Pm89-Pm94). Paleo-pockmarks in these sections are V-shape to U-shape pockmarks. Their size ranges from 163 to 281 m (width), and 16 to 37 ms (TWT) (depth). Polygonal faults are founded on the upper portion of the seismic section. ....54
- Figure 45 Characteristics of paleo-pockmarks of three zones are described by curvature dip map, including (a) zone 1, (b) zone 2, and (c) zone 3 see the location in the red rectangle (d). Black dashed rectangles are the total area of three zones. Characteristics of paleo-pockmarks are shown in a dashed circle (blue color is pockmark edge and the red color is pockmark bottom). ....55
- Figure 46 Log patterns and marker picking of Pakaha-1 and Kawau-1 well. Paleo-pockmarks are founded on the surface of unit C (Laing formation). While unit B founded hydrocarbon in the Waipawan Black Shale (upper part of unit B). ....59
- Figure 47 Well correlation of 3 wells in the Great South Basin show the pattern of log pattern and regional correlation. Paleo-pockmarks are founded on the surface of Laing formation (middle Eocene time). ....61
- Figure 48 Graph illustrates the order of dimension of pockmarks from 57 published. Single points are pockmark measurement or average measurement. Error bars show the range of size from each field. Red point and red error bars show the boundary of size ranging of the paleo-pockmarks in the study area. modified from (Pilcher and Argent, 2007). ....65
- Figure 49 The bar graph shows the comparison of paleo-pockmark density in five square kilometers areas ( $\text{pm} / 25 \text{ km}^2$ ) from zone 1, zone 2, and zone 3. It should be noted that zone B seems to be the highest density, while zone C has the lowest density than the other zones. ....67
- Figure 50 Seismic sections show termination patterns of sedimentary layers in the Great South Basin. The upper part of Waipawan Black Shale (blue layer) shows downlap pattern (blue arrows) from NW to SE direction. Laing formation (green layer) shows onlap pattern (red arrow) on Waipawan Black Shale formation. While Tucker Cove formation (yellow layer) and Penrod Group (grey layer) show parallel pattern overlay on Laing formation. ....69
- Figure 51 Turbidite facies model (Bouma Sequence) shows characteristics of sediment in a sub-marine fan. This sediment sequences relate with size and density of paleo-pockmarks in the study area (Shanmugam, 1997). ....70
- Figure 52 Schematic model of hydrocarbon maturation shows stage of biogenic gas and thermogenic gas, which occur in different temperature and pressure (Bjørlykke, 1989). ....73

Figure 53 Example of pockmarks migrated through normal fault and generate pockmarks on the hanging wall (Pilcher and Argent, 2007). .....	74
Figure 54 The comparison between global sea-level curve and local sea-level curve in the Great South Basin shows sea-level drop for short-term around middle Eocene (Uruski, 2017).....	76
Figure 55 Model of Mechanism of middle Eocene paleo-pockmarks in the study area during early middle Eocene to recent. ....	78



# CHAPTER 1

## INTRODUCTION

Sediment remobilization and fluid flow features are discovered on the subsurface over the past century. In the early period, understanding of these features is not clear because of limitation of survey tools. Nowadays, high-resolution seismic survey and geological programs has become the main tools to study these features. Sediment remobilization and fluid flow features are observed in several geological setting worldwide. Characteristics of these features are generated in different morphologies depend on external factors, origins, and their mechanism. In the present-day, the study of sediment remobilization and fluid flow features is one of the important studies because of these features related with the important conditions and global events. For example, 1) hydrocarbon plumping system (Andresen, 2012; Judd and Hovland, 2009); 2) tectonic and structural deformation (Hovland et al., 2002); 3) compaction and diagenesis process (Cartwright, 2007; Morgan et al., 2015); 4) sea-level change (Riboulot et al., 2013); 5) dissolve gas hydrate (Nakajima et al., 2014); 6) physical and biological erosion (Nicholas et al., 2016); and 7) rapid sediment loading environment (Chenrai and Huuse, 2017). Generally, fluids both liquid and gas, can move laterally and vertically directions depending on the physical properties of the fluids and other factors.

Fluid escapes are founded in different forms such as hot fluid (thermogenic) escape as vents, cold fluid (oil and gas) escape as seeps, and groundwater escape as springs (Judd and Hovland, 2009). Sediment remobilization and fluid flow features had been reported and named at the very first time of thus research area as sand intrusion (Murchison, 1827), pockmarks (King and MacLEAN, 1970), gas hydrate (Nakajima et al., 2014), mud volcano (Milkov, 2000), methane-derived authigenic carbonate (MDAC) (Boetius et al., 2000), and Hydrocarbon-related diagenetic zones (HRDZs) (Cowley and O'brien, 2000). Andresen (2012) gathered and classified seismic characteristics of sediment remobilization and fluid flow features which are shown in Figure 1.

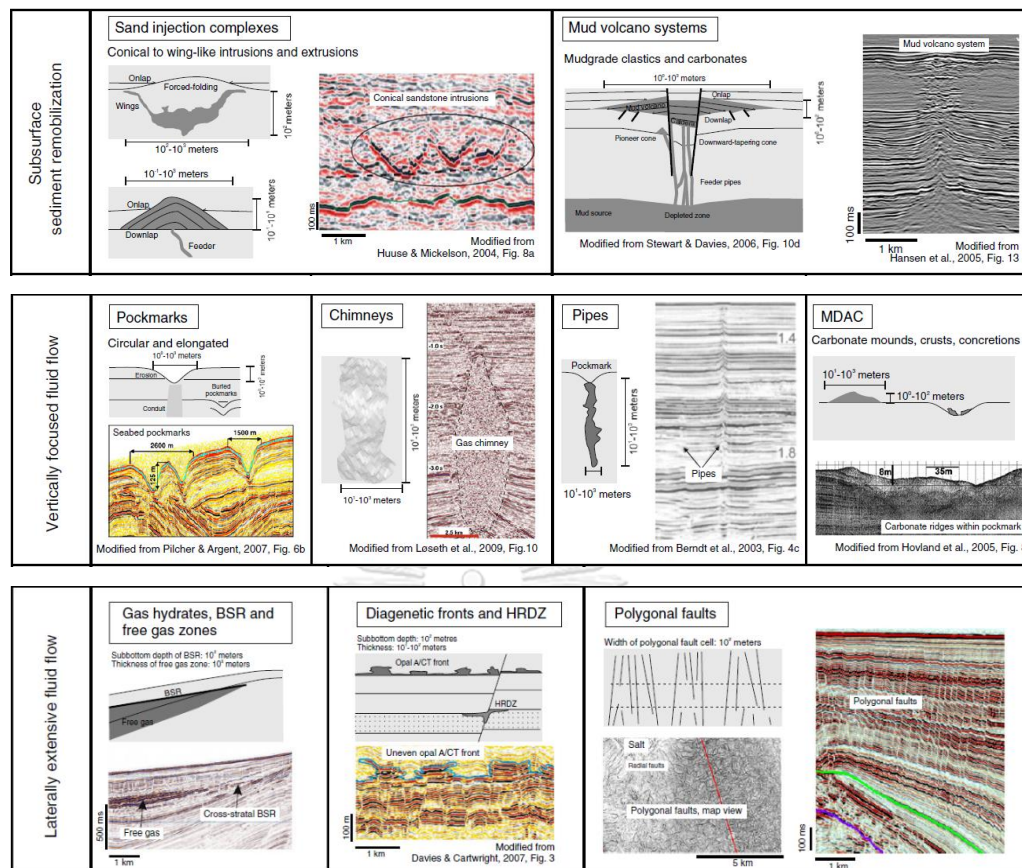


**Figure 1** Schematic illustration and seismic characteristic of fluid flow features show which are divided into three major groups (Andresen, 2012).

Sediment remobilization and Fluid flow features were divided within three major groups base on geometry, lithology, and characteristics of the hosting sediment (Andresen, 2012; Cartwright, 2007). There are subsurface sediment remobilization, vertically focused fluid flow, and laterally extensive fluid flow (Figure 1). Characteristics and detail of these features are described in detail below.

### a) Subsurface sediment remobilization

The fluid flow features in this group are generated cause of an overpressure change (Andresen, 2012). It means fluid possible to move or flow when overpressure decrease. There are included clastic sediment remobilization (e.g. sand intrusion and mud volcano system), and non-clastic sediment remobilization (e.g. mud-grade carbonate volcanoes).

### **b) Vertically focused fluid flow**

The fluid flow features in this group are formed because of fluid venting. It means fluid can disturb and erode sediment both surfaces and vertical direction. These features consist of pockmarks, chimneys, pipes, and Methane-derived authigenic carbonates (MDAC) (Andresen, 2012). In general, characteristics of fluid flow features in this group shows high-amplitude anomalies in vertical direction on seismic section as shown in Figure 1.

### **c) Laterally extensive fluid flow**

Fluid flow features in this group show high-amplitude anomalies in lateral direction on seismic section. There are founded in a specific condition, for example, high porosity layer, and specific pressure and temperature, etc. These features include gas hydrates, free gas, diagenetic fronts, hydrocarbon-related diagenetic zone (HRDZs), and bottom simulating reflections (BSRs) (Andresen, 2012).

However, fluid flow features in sedimentary basin are possible to be generated as an isolated feature or related with other features. For example, there are the relationship of pockmarks, gas chimneys, and mud volcanoes in the salt mini-basin; the relationship of polygonal fault and buried pockmarks in the sedimentary basin (Morgan et al., 2015). Fluid flow features might be able to tell us about the evolution of basin in terms of 1) timing of fluid flow event, 2) the origin of fluid sources, 3) fluid migration pathway, 4) major trigger which control the formation of fluid flow features in the area (Andresen, 2012). In the Great South Basin of the South Island, the high-resolution 3D seismic survey discovered uncommon features at around 1500 ms (TWT). This feature occurs associated with polygonal fault system as shown in Figure 1 and 2. Seismic characteristics of this feature are likely to be pockmarks which is one of the fluid flow features that occur worldwide. Thus, we need to study about definition and characteristics of pockmark in detail below.

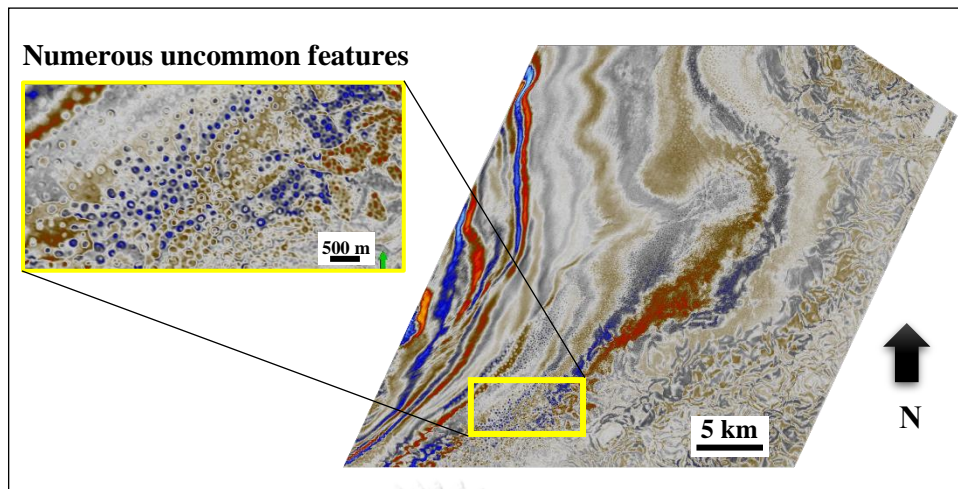


**Figure 2** show (right) 3D seismic time slice at 1490 ms (TWT) in the Great South Basin, New Zealand showed the distribution of uncommon features around the area, and (left) enlargement of the feature in yellow

## 1.1 Overviews of pockmarks

### 1.1.1 Pockmark definition

The definition of pockmarks is seafloor depression which are generated by fluid or gas expulsion through unconsolidated fine-grained sediments (Killops et al., 1997; King and MacLEAN, 1970). Pockmarks are usually distributed both onshore and offshore such as shallow coastal areas, continental shelves, deep water areas and freshwater lakes (Judd and Hovland, 2009). Pockmarks are one of the fluid flow features which can indicate subsurface fluid flow processes (Chenrai and Huuse, 2017; Hovland and Svensen, 2006), basin evolution (Andresen, 2012), methane generation (Hovland et al., 1987), and global climate change event (Hovland et al., 2002) within the areas. Furthermore, Hovland et al. (2002) suggested that pockmarks are possible to use as an indicator of potential or non-potential petroleum fields. Pockmarks distribution are observed both random (Riboulot et al., 2013; Sun et al., 2011; Tasianas et al., 2018), semi-random (Harrington, 1985), and non-random pattern (Chenrai and Huuse, 2017) worldwide.

Judd and Hovland (2009) suggested mechanism model of pockmarks formation and divided it within three stages (Figure 3). The first stage, fluid accumulates under the seabed by outer parameter stimulation. After that fluid



migrates in a vertical direction and creates a dome shape near the surface. The second stage, the large amount of fluid created high pressure which affects to the cracking of seabed. Then fluid and sediment break out from the seabed, and the final stage, fine grain sediments were transported from the pockmark crater by oceanic bottom current and some of the coarse grain sediments may fall back to the bottom of pockmarks. Moreover, Bøe et al. (1998) gave a definition of ancient pockmarks, buried pockmarks or paleo-pockmarks are the pockmarks which buried by younger sediment. Thus, pockmark characteristics can help identify the fluid sources and migration pathway such as gas associated with methane and porewater (Chenrai and Huuse, 2017; Mazzini et al., 2017; Nickel et al., 2012).

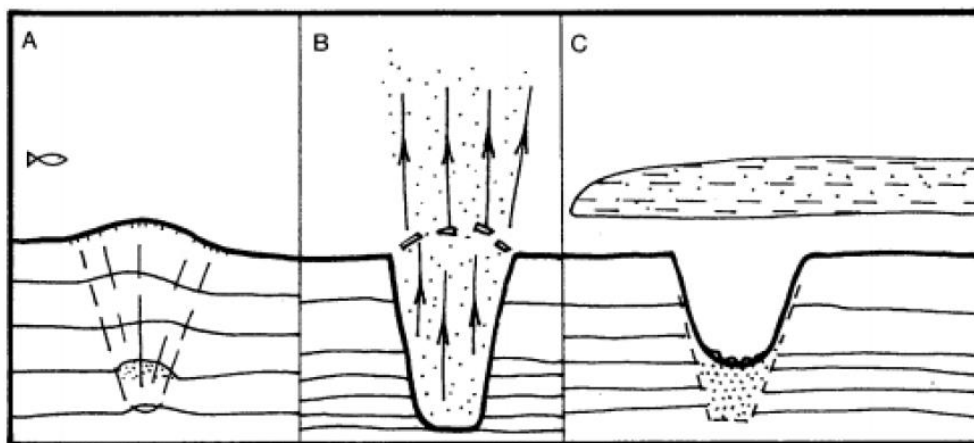


**Figure 3** show the fluid flow process model of pockmarks formation by (Judd and Hovland, 2009)

### 1.1.2 Pockmark characteristics and classification

Characteristics of pockmarks were identified for the first time in 1970 and reported as circular and elliptical in shapes (King and MacLEAN, 1970) after that other shapes of pockmarks have been founded and classified (Chen et al., 2015; Killops et al., 1997). Various shapes of pockmarks depend on the fluid source and external factors (Hovland et al., 2002). For example, circular pockmarks are the common shape that is created by both porewater and free gas expulsion (Chen et al., 2015), elongated pockmarks are developed by the oceanic bottom current (Bøe et al., 1998), eyed pockmarks are generated by biogenic carbonate and porewater expulsion

(Andresen and Huuse, 2011). Size of pockmarks can expand from a meter to several hundred meters in diameters and depths. Characteristic of pockmarks was classified within 6 classes including a unit pockmark, normal pockmarks, elongated pockmarks, eyed pockmarks, strings of pockmarks, and complex pockmarks (Hovland et al., 2002) (Figure 4).

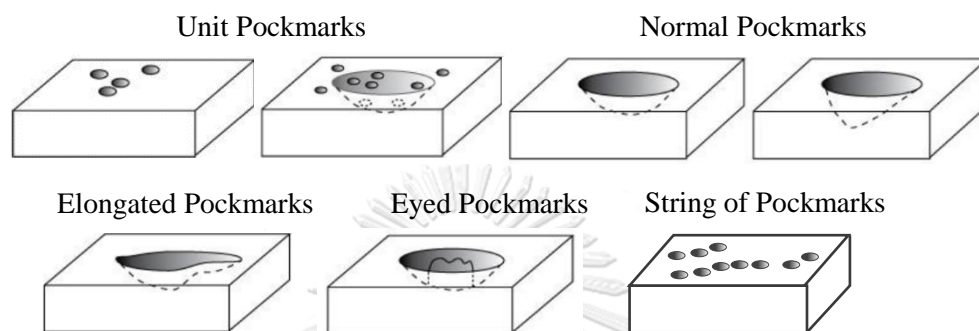


**Figure 4** show illustration of the major group of pockmarks modified from Hovland et al. (2002)

#### **a) A Unit pockmarks**

The unit pockmark is the smallest depression which occurs as an isolated feature on the seafloor and possible to occur associated with normal pockmarks and other shapes. The shape of a unit pockmark is circular to sub-circular in generally (Hovland et al., 2002). Their size ranges from 1 to 10 meters in width and deep up to 0.5 meters. Researchers found that a unit pockmark manifest at the first stage of fluid seepage and developed to the larger size such as normal pockmarks and the other shapes (e.g.)(Chen et al., 2015; Harrington, 1985; Hovland et al., 2010). The example of the unit pockmarks was founded associate with normal pockmarks in the Norwegian Trough by Hovland et al. (2010) (Figure 5).

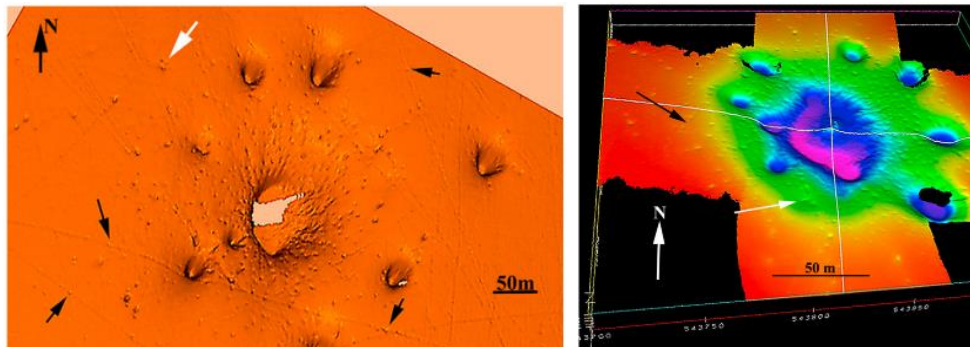


**Figure 5** Representation of pockmark-families in the Norwegian Trough by using shaded relief digital terrain model (DTM) (Hovland et al.,

### **b) Normal pockmarks**

Normal pockmarks are founded commonly worldwide. Normal pockmarks are described for general pockmarks which have circular or elliptical in shape, their size can expand from 10 to 700 meters in diameters and deep up to 45 meters (Hovland et al., 2002). Normal pockmark is used as an indicator of both porewater and gas expulsions. This feature is founded in the basin which has low-energy of bottom current (Chenrai and Huuse, 2017; Mazzini et al., 2017; Nickel et al., 2012). Moreover, the density of normal pockmarks can help to identify the fluid source in the basin. For example, high-density normal pockmarks are founded mostly in the large gas field, such as the Barents Sea (Figure 6a) and the North Sea (Figure 6b) (Mazzini et al., 2017; Nickel et al., 2012). While, low-density normal pockmarks associated with porewater are found in New Zealand (Figure 6c) (Chenrai and Huuse, 2017).

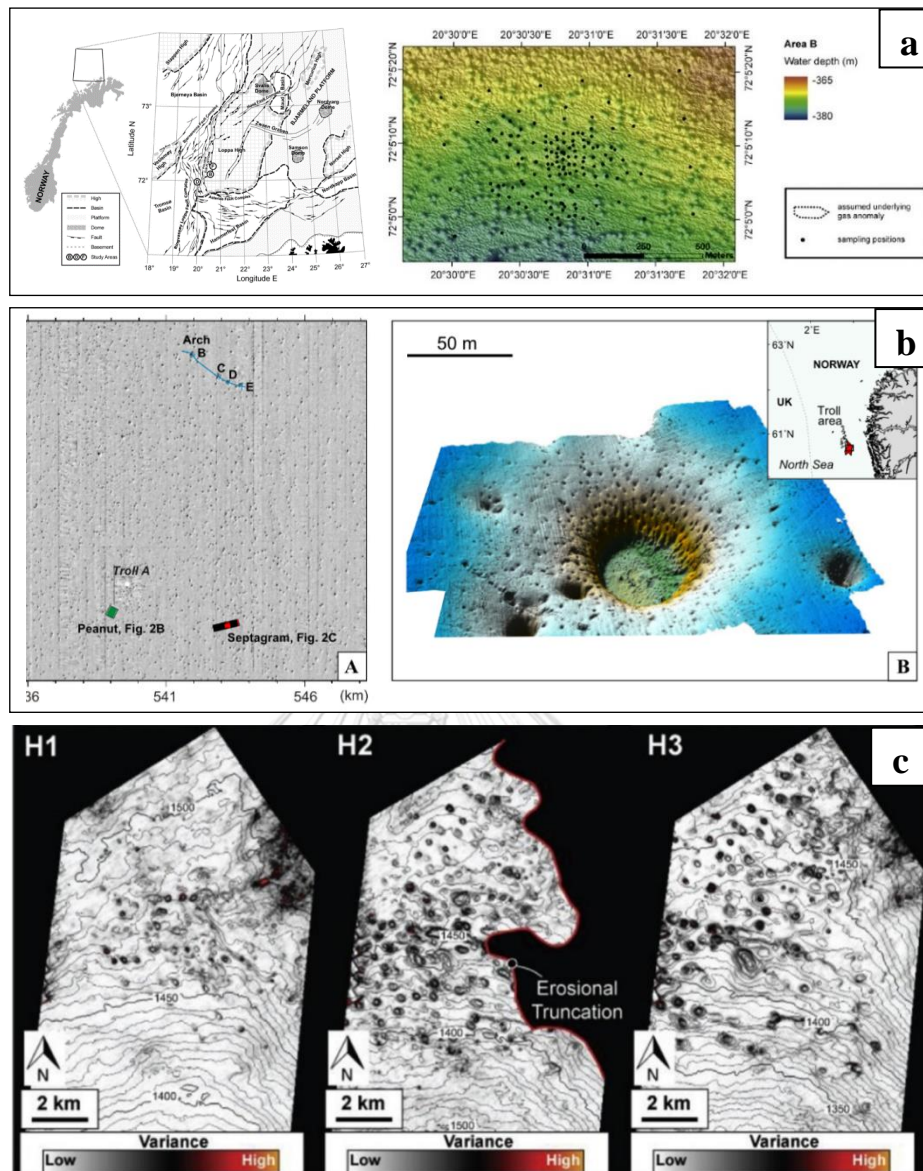


**Figure 6** Maps of (a) high-density normal pockmarks in the Barents Sea (Mazzini et al., 2017) and (b) North Sea (Nickel et al., 2012), and (c) low-density normal pockmarks in the North Island, New Zealand (Chenrai and Huuse, 2017).

### c) Elongated pockmarks

The definition of elongated pockmarks is one axis longer than the other axis (Hovland et al., 2002). Shape of this pockmarks are usually controlled by bottom current activity and there are often combined with shallow fluid expulsion (Hovland, 1983; Hovland et al., 2002). The longest axis related to bottom current direction

which erodes and transport fine-grain sediment away from pockmark crater (Bøe et al., 1998; Puchała, 2014) (Figure 7). Puchała (2014) illustrated the model of elongated pockmark evolution and suggested that at the first stage of dewatering process, unit pockmarks manifest on the fine-grained seabed and then strong bottom current eroded and suspended sediments around the unit pockmark craters by one main direction. Then, unit pockmarks are remodeled to elongated pockmarks at the last stage (Figure 8).

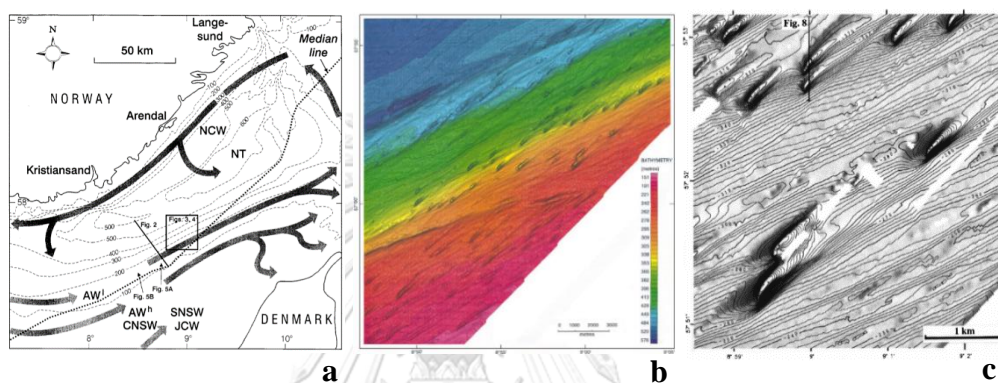


**Figure 7** show (a) the relationship of circulation pattern, bathymetric map and (b) distribution of elongated pockmarks, and (c) the long axis direction of elongated pockmarks on the southern slope of Norwegian Trend (Bøe et al., 1998).

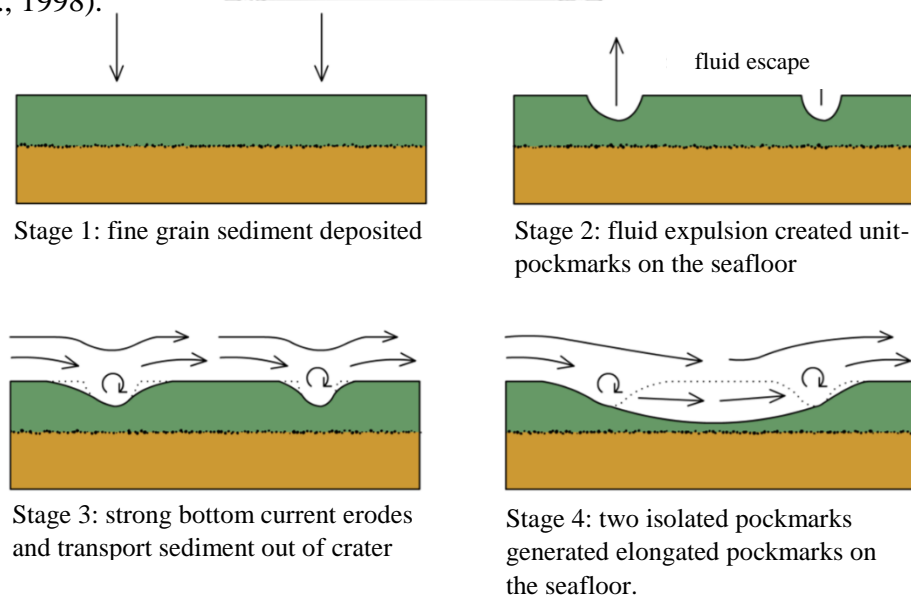


**Figure 8** show illustrate model of the evolution of elongated pockmarks (Puchała, 2014).



#### d) Eyed pockmarks

Characteristic of eyed pockmarks are described like an ordinary pockmark. An Eyed pockmark has a circular or sub-circular in plain view with dome shape of carbonate or coarse materials composed within the central part of the pockmark (Hovland et al., 2002). Eyed pockmark is possible to indicate long-term of erosion process, biological deposition, carbonate precipitation, and biogenic methane generation (Andresen and Huuse, 2011; Hovland et al., 2002).

#### e) Other shapes

##### Crescent pockmarks

In 2015, crescent pockmarks are the new shape of pockmarks which were founded in the northern Zhongjiannan Basin, South China Sea (Chen et al., 2015). Crescent pockmarks in this area are generated by fluid in the basin (Chen et al., 2015). This type of pockmark shows the evolution of size and shape from unit pockmark at the early stage which has a small size to the larger size of crescent pockmark at the final stage as follows (Figure 9).

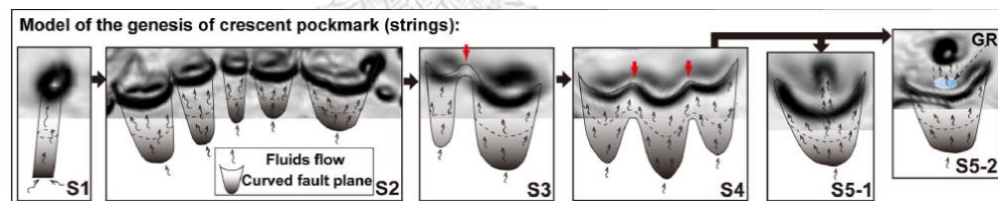


**Figure 9** show the evolution of crescent pockmarks is explained into 5 stages (S1-S5). S1; fluid escape generated small pockmarks on the fine grain surface. S2; strings of pockmarks are growth by slides and slumps in slope area, S3-S5; pockmarks developed to larger pockmark and remodel to crescent pockmarks in finally (Chen et al., 2015).

#### 1.1.3 Cause of fluid expulsion

Characteristics of pockmarks are generated and controlled by several factors, for instance, the bottom current, faults and fractures, geological conditions, and the other parameters. Furthermore, King and MacLEAN (1970) suggested that pockmarks were perhaps formed by rising of gas or water leakage from sedimentary successions

at the coastal plain. The important causes of fluid expulsion are chosen within five main causes below.

**a) Tectonic and structural deformations**

Tectonic and structural deformations are the important cause which leads to fluid expulsion in some area. For example, earthquake and fault are the main tectonic and structural events which occur related to pockmarks in some areas (e.g.) (Hovland et al., 2002). Earthquake is the trigger of fluid accumulation in the sedimentary layer, while the fault is usually founded as a migration pathway of fluid expulsion. In 1980, pockmarks debut in the northern of California both during active an earthquake and ten days after an earthquake event (Hovland et al., 2002). Supporting data were recorded such as temperature increase during the earthquake at northern Peleonnesos of Greece in 1993 and gas bubbling from deeper part to water surface at the Gulf of Corinth in 1995 (Hovland et al., 2002). Hovland et al. (2002) concluded that pockmarks regularly active before and during earthquakes because there is a higher rate of gas venting from the sea-surface during the earthquake. Furthermore, pockmarks were founded on the hanging-wall of shallow faults at the West African continental margin (Pilcher and Argent, 2007). These data indicate that tectonic and structural deformation (earthquake and fault) are possible to be an important trigger for pockmark generation.

**b) Diagenesis and dewatering processes of formation**

Diagenesis process is a stage of sedimentary compaction. Sediments are compressed by hydrostatic pressure and overburden pressure, and its effects to decrease of porosity and permeability of the rock. Dewatering is an effect after diagenesis process. Pore-fluid between sediment grain is expelled both upward and downward to higher permeable bed (Chapman, 1987). Thus, diagenesis and dewatering processes lead to fluid accumulation and expulsion in sedimentary formation. The evidence of diagenesis and dewatering process are founded in term of fluid flow features in several areas. For example, polygonal fault and buried pockmarks in the Lower Congo Basin, offshore Angola (Morgan et al., 2015); pockmarks in the Taranaki Basin, New Zealand (Chenrai and Huuse, 2017).

### c) Dissolve gas hydrate

Dissolve gas hydrate is one of the important triggers that generated pockmarks formation. Gas hydrate is a compound of water and gas in a solid stage (Hovland et al., 2005). There are occur in a specific condition (low temperature and overpressure) associated with external factors such as the gas compound, the salinity of the water, geothermal gradient (Chand et al., 2008). Dissolve of gas hydrate is possible to create natural gas venting upward through sedimentary layer and leads to pockmark generation on the fine-grained seafloor (Skarke et al., 2014). For example, mounds and pockmarks at the eastern margin of the Sea of Japan were founded associated gas hydrate (Nakajima et al., 2014). These features occurred during sea-level fall and transgressive because of hydrostatic pressure release.

### d) Physical and biological erosion

Pockmark formation possible to create not only fluid flow system but also living things. Nicholas et al. (2016) discovered small pockmarks on the seafloor which are built-up by fish. The researcher founded fish remains around an isolate pockmark. This evidence shows that pockmarks are possible to occur associated with biological activities such as fish. Size and shape of pockmarks which occur by fish depend on the difference of fish habit and timing (Nicholas et al., 2016).

### e) Methane escape

Methane venting is one of the important process that indicates hydrocarbon accumulation in the basin and relates directly to seafloor depression built up (Andresen, 2012). Methane gas is generated within three possible origins. First, biogenic methane: microbial activity generates regional methane gas in organic-rich sediments which deposited in a source rock layer. Second, thermogenic methane which is generated by temperature and pressure which directly variation to depth of source rock. Third, abiogenic methane which is generated as a result of igneous activities such as serpentinization, degassing, and cooling of igneous rock (Judd, 2003). Pockmark is an indicator for petroleum exploration in several basins (Nickel et al., 2012). In some cases, pockmarks occurred by the association between methane venting and sea-level drawdown (Bertoni et al., 2013) (Figure 10).



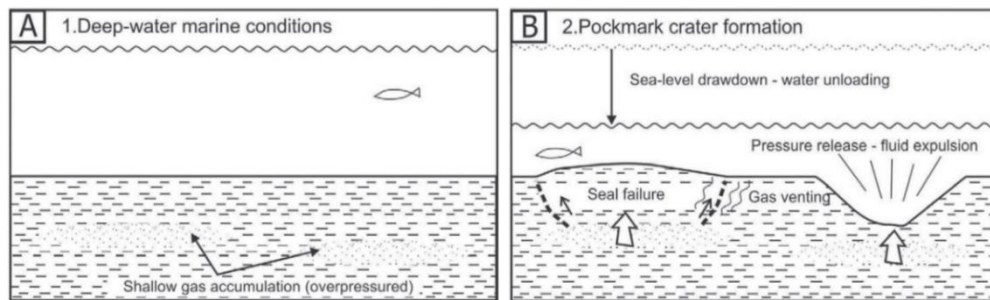


**Figure 10** Illustrate models show mechanism of pockmark formation in the Levant Basin (southeastern Mediterranean). A) natural gas accumulated in the turbiditic sand lenses, B) gas venting through sediment layer upward to the seabed and developed to large pockmarks in the final stage (Bertoni et al., 2013).

## 1.2 Research objectives

The main objectives of this thesis focus on seismic characteristics of paleo-pockmarks in the Great South Basin, New Zealand by using seismic interpretation. This thesis carries out the fluid flow knowledge for paleo-pockmarks formation in the area. Thus, this thesis aims to;

2.1) To describe the seismic characteristics of middle Eocene paleo-pockmarks at the Great South Basin, New Zealand.

2.2) To predict the fluid origin and mechanism of paleo-pockmarks in the study area.

## 1.3 Research benefits

This thesis will full fill the fluid flow knowledge on the seabed at the Great South Basin, New Zealand. In addition, it helps to analyse petroleum status and timing of hydrocarbon in the study area.

## CHAPTER 2

### GEOLOGICAL SETTING AND STRATIGRAPHY

The study area is located in the Great South Basin (GSB) where pockmarks and other interesting features are appeared and is situated in south-east offshore, South Island (Figure 12 and 15). The Great South Basin covers an offshore area of approximately 85,000 km<sup>2</sup> with water depth from 600 to 800 meters. The basin is occurred from an intra-continental breakup on the eastern margin of Gondwana (Minerals, 2014). Graben and half-graben in northwest to southeast trending in the GSB are formed by the mid Cretaceous extension while New Zealand separated from western Antarctica. The complex subduction zone formed because of convergent plate boundary between the continental plate (Australian Plate) and oceanic plate (Pacific Plate) as the Australian Plate has subducted below the Pacific Plate in the South Island whereas the Pacific has dived under the Australian Plate in the North Island (Ballance, 2009). After an intraplate rifting and thermal subsidence, late Cretaceous to recent sediments are deposited in the GSB area (Killops et al., 1997).

Sedimentary sequences in the GBS area consist of four major groups which deposited from late Cretaceous to recent. The lower sequence of this basin is late Cretaceous non-marine clastic facies of the Hoiho group which deposited during syn-rift phase. The Hoiho group includes conglomerate, sandstone, shale, and coal. After rifting phase, Cretaceous to late Paleocene fluvial, deltaic to shallow marine sediments of Pakaha group are deposited in the basin. The Pakaha group consists of sandstone, siltstone, shale, and minor coal measure and are mostly founded at the western margin. Following by marine sediments of Rakiura group which is deposited in the Eocene to Early Oligocene time, including shale and carbonate sediments dominantly. In the last stage, carbonate sediment sequence of Penrod group deposited during Miocene to recent (Killops et al., 1997; Morley et al., 2017). The detail of geological setting and stratigraphy of the Great South Basin are described in detail below.

## **2.1 Geological setting**

### **Early Cretaceous to Late Cretaceous**

Pacific, Australia, and Antarctic plates separate from Gondwanaland during late Cretaceous (Omosanya and Harishidayat, 2019). The result of this separation is seafloor spreading in an east-west direction between the Tasman Sea and Southern Pacific Ocean (ExxonMobil, 2010; NZP&M, 2015). Australian Plate moves to the north at a few centimeters per year, while the Pacific Plate moves to the south and rotate anticlockwise to the southwest at around 4 centimeters per year which situated to the South Island of New Zealand (Ballance, 2009).

The Great South Basin evolution includes three major phases, that is syn-rift, post-rift, and syn-orogenic (Omosanya and Harishidayat, 2019). The syn-rift phase, the basin extended by horizontal extension during late Cretaceous. The rifting produced graben and half-graben since Early Cretaceous. Sediments are allowed deposit on the margin, coastal plain and shelf including coarse-grain sediments such as conglomerate, sandstone, and coal, while in the central basin was restricted. The post-rift phase follows by regional subsidence and transgression during late Cretaceous. This event affected to marine sequence deposition in Great South Basin and Canterbury Basin (Killops et al., 1997).

### **Paleocene to Oligocene**

Seafloor spreading was extended in Late Cretaceous to Early Eocene following by thermal subsidence and marine transgression (Killops et al., 1997). Post-rift facies were accumulated at around margin, coastal, and shelf area and there are associated with coal deposition which is possible to be source rock of many basins in New Zealand. The Eocene time, sedimentary facies include transgressive sequences following by fine-grained clastic in middle Eocene and carbonate-rich sediments of the Oligocene time (NZP&M, 2015).

### **Oligocene to recent**

The final phase is syn-orogenic tectonic which structures began to develop and mountain build up (Omosanya and Harishidayat, 2019). The rotation of plate boundary was created right-lateral shear at the northern plate border as known

“Alpine Fault zone” and a lot of minor faults along the northern plate edge (ExxonMobil, 2010). The forming of Alpine Fault leads to mountain-building along this fault (Constable et al., 2010).

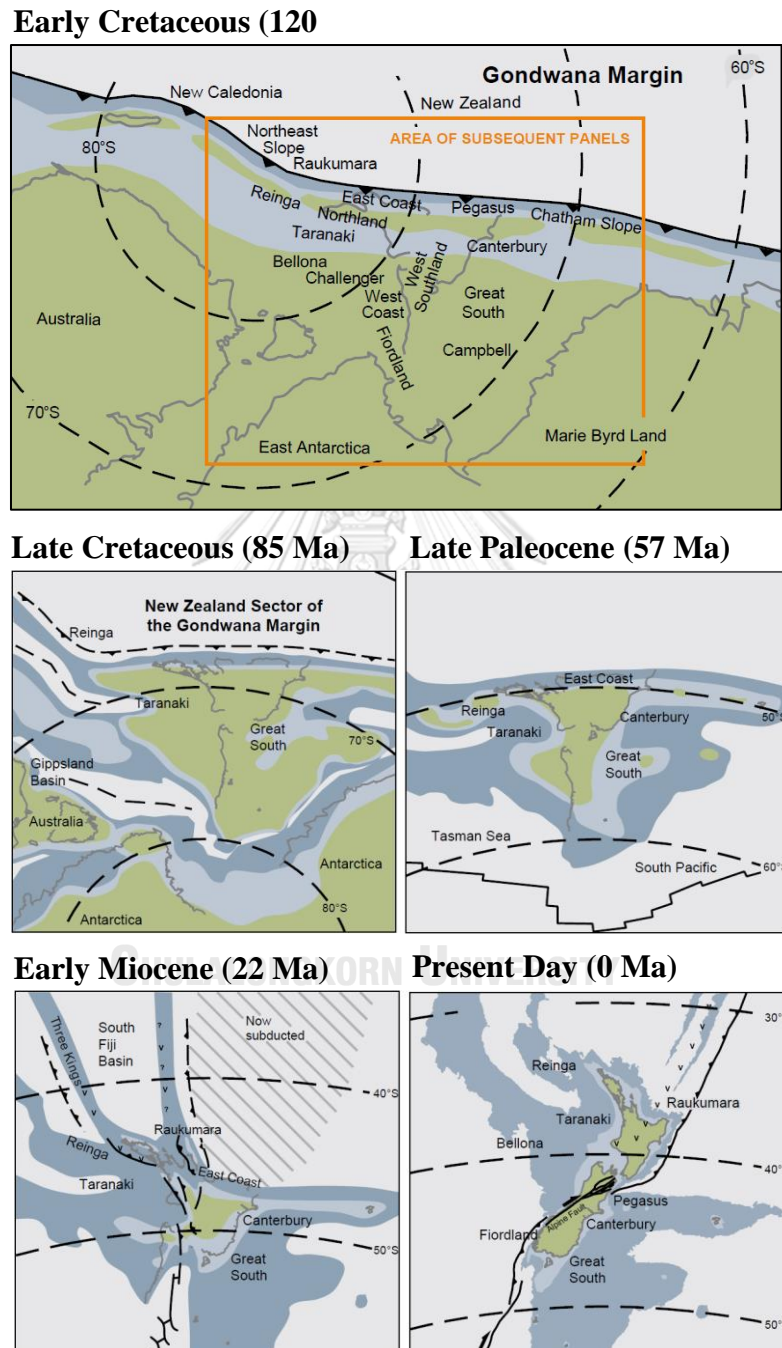


**Figure 11** The evolution of New Zealand’s plate tectonic from early Cretaceous to present day (NZP&M, 2015).



**Figure 12** Map of New Zealand's sedimentary basin cover North Island and South Island (NZP&M, 2015).

## 2.2 Sedimentary sequences

The possible basement rocks in GSB area are reported in two types, there are granitic rock and metamorphosed sediments. Granitic plutonic had founded in Pakaha-1 and Pukaki-1 wells which has Carboniferous to Early Cretaceous age (ExxonMobil, 2010). One of many reports suggested the possible age of basement rocks that had ever found to be 112 Ma by using K-Ar and Ar-Ar dating (Constable et al., 2010). Metamorphosed sediments which have Paleozoic age had founded by seismic line and Kawau-1A (ExxonMobil, 2010). Sedimentary sequences in the Great South Basin began deposited around late Cretaceous to recent. There are four major groups, including Hoiho group, Pakaha group, Rakiura group, and Penrod group. All sedimentary sequences are described in detail below (Figure 13).

### **Hoiho group**

Around late Cretaceous period non-marine and shallow marine clastic facies as known “Hoiho group” deposited around the basin. This group is the oldest sediment sequence in the basin, it deposited overlain on basement rock. In the lower part, alluvial-fluvial, lacustrine, main sedimentary rocks are deposited which consist of sandstone and shale, following by traditional unit which deposited during the last phase of the rifting, high-quality sands and coal are found in this unit interpreted as delta plain (Constable et al., 2010). Moreover, conglomerate distributed in some part of northern and southern of the basin as showed in Tara-1 well and Hoiho-1C (NZP&M, 2015).

### **Pakaha group**

Late Cretaceous to Paleocene sequences showed sedimentary deposition of “Pakaha group”. This group was divided within three major formations, including Kawau formation, Wickliffe formation, and Taratu formation. Kawau formation developed in the early of thermal subsidence phase after rifting had been finished. Kawau formation is includes main sandstone and siltstone, rare shale and coal deposited on the western and south-eastern margins overlain by Wickliffe formation include a thick layer of shale and siltstone deposited in the central part. In addition to Taratu formation includes a thick bed of coal, appeared in the northern part of the

basin and showed in Tara-1 well (NZP&M, 2015). Depositional environment of this part was defined as fluvial, estuarine, deltaic, and shallow marine facies.

### **Rakiura group**

The upper part, Rakiura group deposited during Eocene to early Oligocene time. This group was divided within two formations, including Laing formation and Turker Cove formation. The early stage, Laing formation consists of massive mudstone deposited in regional and marl in the central part which deposited in shelf to bathyal environment overlain by carbonate rock of Turker Cove formation which deposited in bathyal marine environment (Constable et al., 2010; NZP&M, 2015).

### **Penrod group**

The younger sediment of Penrod group deposited in Mid Oligocene to recent, including carbonate sediments. In South Island at around 15 to 20 Ma, the Alpline Fault occurred from convergent plate boundary of Australian Plate and Pacific Plate. Mountain is built up along fault plain and many structures forming in this phase such as uplifting, anticlinal structure and inversion of fault, etc. The Alpline Fault movement and mountain building affect to sediment supply in the basin as a wedge shape from Canterbury basin to Great South Basin. Clastic sediments of shelf-bathyal marine environment deposited mostly in some east part of the offshore area, while the central and other part deposited fine-grained sediments of the deep marine environment (Constable et al., 2010).



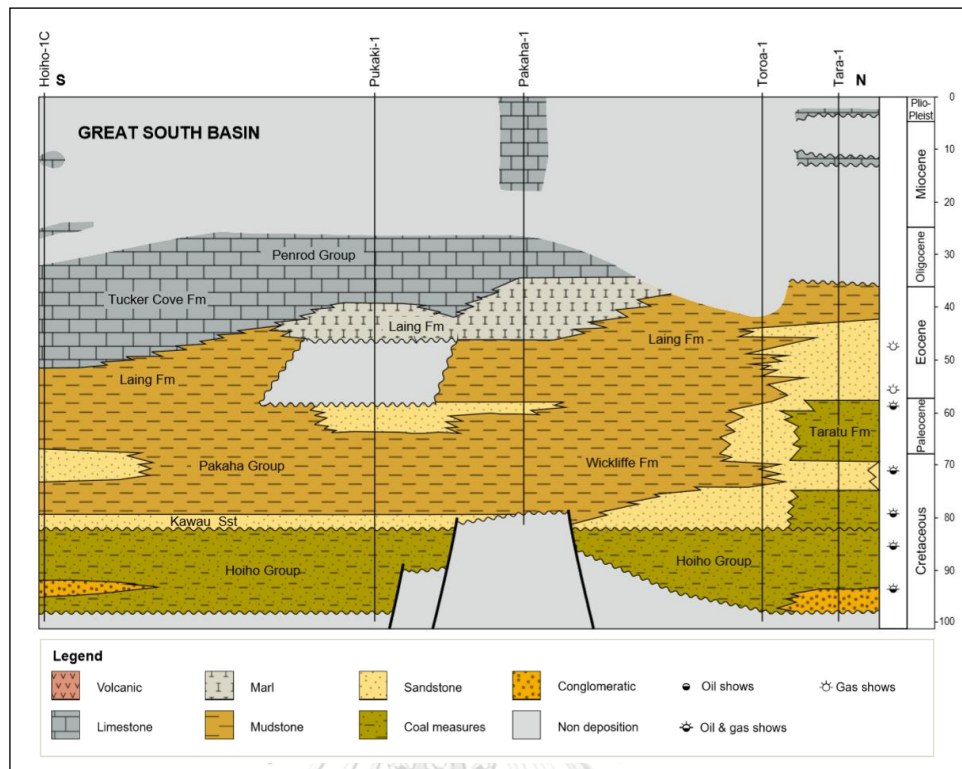


**Figure 13** Schematic model of sequenced stratigraphy in GSB (NZP&M, 2015).

### 2.3 Marine weather and sea conditions of the South Island

Gorman et al. (2005) published marine weather and sea condition report of the Great South Basin, New Zealand. They suggested four main categories such as winds, waves, and circulation and current. This report shows the relationship between wind, wave, and current directions in the South Island.

The results show 30% west wind are predominant with over 10 m/s. In the same time, the high-energy wave is predominant in the west direction with mean height over 3 meters because strong west winds predominate in the water south of New Zealand. The monthly wave means show maximum values in May, and minimum values in October, December, and January.

In the part of circulation and current, the large-scale anti-clockwise circulation in New Zealand is created by the South Pacific subtropical gyre. This gyre includes two wind directions that are the southeast to the north and the west to the south. While



the circulation and current in the Great South Basin are driven by two major currents which are Southland Current (SC) and Antarctic Circumpolar Current (ACC). Southland Current (SC) flows northward along the continental slope of the South Island with speeds around 30 cm/s and Antarctic Circumpolar Current (ACC) flows eastward along the slope of Campbell Plateau with speeds around 50 cm/s (Figure 14).

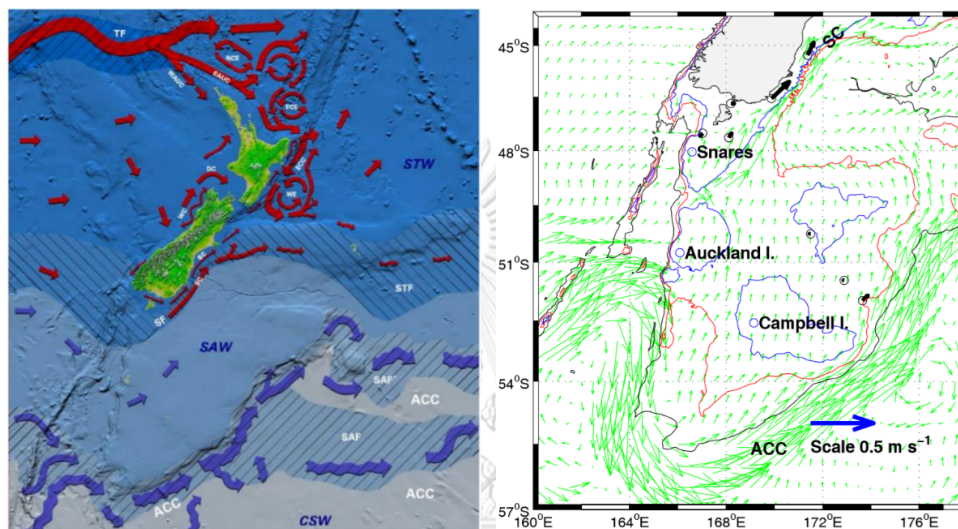


**Figure 14** A schematic map shows the large-scale anti-clockwise circulation and current in New Zealand (left). Mean current model (right) show two dominant currents around the South Island. Southland Current (SC) flows northward and Antarctic Circumpolar Current (ACC) flows eastward. (Gorman et al., 2005)

## CHAPTER 3

### METHODOLOGY

The early days, the seismic data acquisition equipment could not have recorded high-quality images of survey data which made interpretation of origins of fluid flow features unclear. Side scan sonar, multi-frequency echo sounder, multibeam bathymetry data, and the others were used to study morphology, and predict the origin of pockmarks in the past days (Harrington, 1985; Hovland, 1983; Josenhans et al., 1978; King and MacLEAN, 1970). Side scan sonar survey is an equipment which is scattered short pulses of acoustical energy at a low angle to the seafloor. This ray emits deeply in the vertical plane up to 730 meters from the ship (King and MacLEAN, 1970). Nowadays, high-resolution seismic reflection tools were developed with 2D and 3D imaging for ocean exploration. 2D and 3D seismic data are the main methods that researchers used to study structures and stratigraphy in the sedimentary basin. Pockmarks were founded and identified by using side-scan sonar survey at the first time by King and MacLEAN (1970). Pockmarks and paleo-pockmarks were displayed as a strong reflection (dark spot) (King and MacLEAN, 1970) or v-shaped notch (Josenhans et al., 1978) in side view. In the next time, high-resolution seismic reflection surveys are used extensively around the world. Two important data include 2D / 3D seismic data (Andresen and Huuse, 2011; Chenrai and Huuse, 2017) and multibeam bathymetry data (Chen et al., 2015; de Mahiques et al., 2017; Nickel et al., 2012) show pockmarks and paleo-pockmark clearly on the top view and section view, but multibeam bathymetry data show more details in pockmarks shape on the top view than 2D / 3D seismic data. Characteristics of pockmarks and paleo-pockmarks are studied and identified on morphology (shape and size) and distribution (location and density) by using geological programs.

One of the best exploration tools which can record a high quality of image data is geophysics survey as a seismic reflection, therefore, this thesis selects the combination of 2D/3D high-resolution seismic reflection data with well log correlation data and geological support data for study the paleo-pockmarks in the study area. 3D seismic interpretation is the main method that we use for finding

geomorphology and sequence stratigraphy of paleo-pockmarks, and in addition to 2D seismic reflection data and well log correlation data are used for confirming lithology and stratigraphy in the pockmarks interval. There are seven exploration wells located around the study area and the detail of wells shown in table 1.

2D and 3D seismic data and well log data are used as the main data in this study. Total seismic volume covers approximately 1,344 km<sup>2</sup> with water depth around 600 to 800 meters in the Great South Basin. Schlumberger Petrel software is used for seismic interpretation and creating the structural map of paleo-pockmarks. The 3D seismic data include three main planes, that is inline (vertical plane), crossline (vertical plane), and time slice (horizontal plane). Bin spacing is 25 x 12.5 m in incline and crossline direction, respectively. The seismic reflection data are normal polarity (SEG) with the increase in acoustic impedance is shown by peak. The frequencies of seismic data are 40 – 60 Hz. Vertical resolution is 8 to 12.5 meters by using the average of young sediment velocity of 2,000 m/s. The horizontal resolution around 16 to 25 meters which affirms to identify pale-pockmark characteristics in the study area. Stratigraphic sequences were interpreted on 2D seismic sections which correlate to Pakaha-1 well. Pakaha-1 well is the nearest well which located on the east of the 3D seismic area (Figure 15).

**Table 1 well data used in this study**

Well name	Location		Total Depth (m)	Water Depth (m)
	Latitude	Longitude		
Hoiho-1	-49.6151389	169.6228056	2,386.5	656.6
Kawau-1	-48.9289844	169.1011333	3,826.9	683
Rakiura-1	-48.6644444	168.1466667	2,408.5	642.1
Pukaki-1	-48.5586111	170.1519444	3,717.3	879.5
Pakaha-1	-48.2491667	169.5494444	3,389	684.9
Toroa-1	-47.4445487	169.4876264	4,551.6	480.06
Tara-1	-47.3167699	169.1684507	4,416	123.4

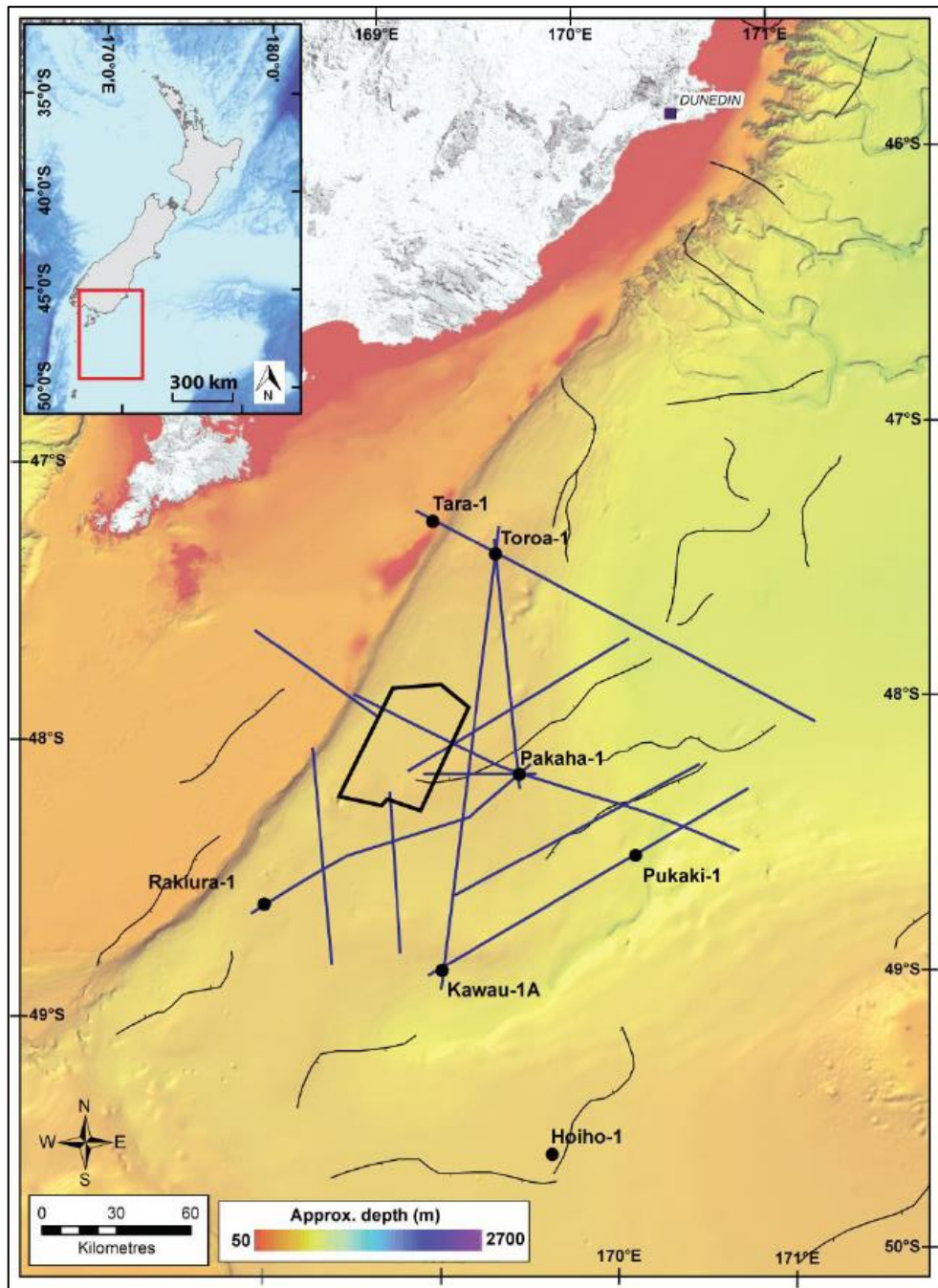


**Figure 15** Map of the Great South Basin, New Zealand (study area). 3D seismic line located on black polygonal, 2D seismic show in blue line, and wells exploration show in black- dots (Chenrai and Huuse, 2017).

Characteristics of paleo-pockmarks are studied by using seismic surface and seismic volume attributes. RMS (Root Mean Square) amplitude attribute was chosen to create the surface of paleo-pockmarks and their distribution on the surface of interest in the study area. While volume attributes include variance, consistent dip, and 3D curvature dip. Variance and consistent dip attributes were chosen to identify paleo-pockmark morphology on the top view. Seismic sections were cut to identify characteristics of paleo-pockmarks in section view. Furthermore, 3D curvature dip attribute was chosen to analyze paleo-pockmark density in the study area. The detail of methodology and all attributes will be described below (Figure 16).

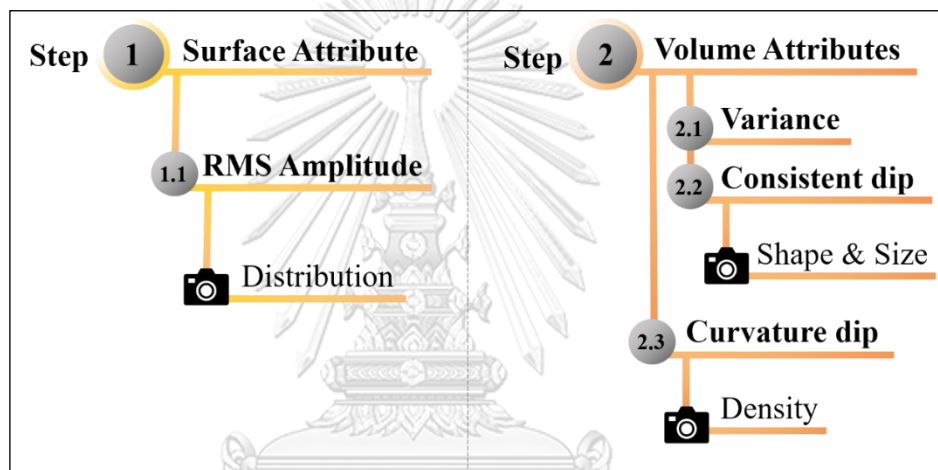


**Figure 16** Workflow shows two major steps for the paleo-pockmark study in the study area.

### 3.1 Step 1 : Surface Attribute

Key horizon picking on both inline and cross line is prepared for morphological and stratigraphic interpretation. Key horizon is picked on the strong seismic reflection which displays when density ( $\rho$ ) and velocity ( $v$ ) of rock change. Top formations of all sediment sequences were identified by using the correlation between well log data (in term of depth) and 2D seismic section (in term of time). We used 2D seismic data which link from 3D seismic area to Pahaka-1 well (east of the 3D seismic area) to identify the key horizons. Continuity and termination of the seismic reflection help to identify the broad scale of the sedimentary package and key horizons are marked on the top formation of each sequence. Then, the timing of



paleo-pockmark surface was founded, and we use this data to build RMS amplitude map to show paleo-pockmark distribution on the surface of interest.

### 3.1.1 RMS amplitude

RMS amplitude is the estimation of varying magnitude in the seismic data. This method will calculate the square root of the summing of all sample average, both the positive and negative amplitude around the surface of interest (Equation 1) (Figure 17). It can display a broad scale of amplitude anomalies, bright spot, facies change, and an unconformity zone in the seismic data. It means high-value of RMS amplitude indicate high amplitude anomaly or more lithological variation (Koson et al., 2014; Meek, 2015). In this thesis, RMS amplitude map is used to show the pattern of paleo-pockmarks on the surface of interest (Laing formation). This attribute estimates the varying magnitude at around 50 ms (TWT) below the surface of middle Eocene paleo-pockmarks. The reason to use 50 ms (TWT) window is that all paleo-pockmarks display on the same surface (middle Eocene surface), and they have the depth less than 50 ms (TWT). ( $X_{RMS}$  is RMS amplitude value; amp is amplitude of each sample; k is the number of sample).

$$X_{RMS} = \sqrt{\frac{\sum_i^n amp^2}{k}} \quad \text{Equation 1.}$$

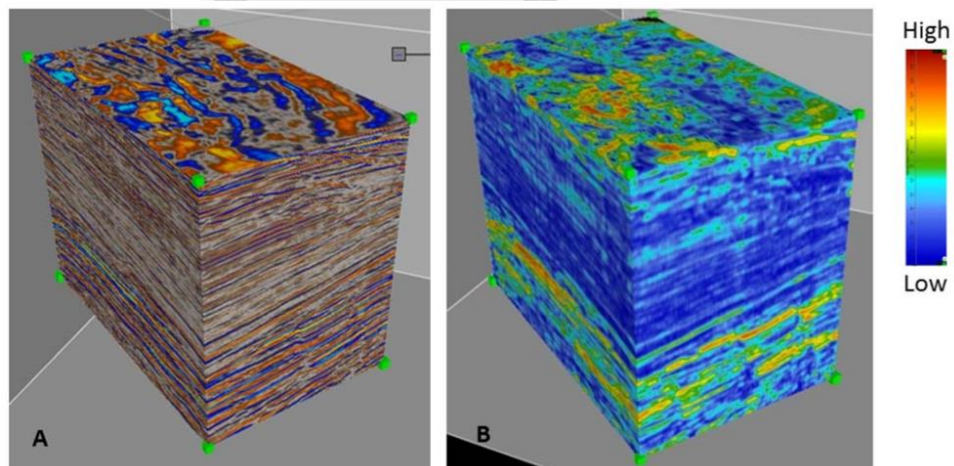


**Figure 17** The comparison between general seismic volume (A) and RMS amplitude attribute volume (B) high-value indicate high amplitude anomaly (Koson et al., 2014).

### 3.2 Step 2 : Volume Attribute

#### 3.2.1 Variance attribute

Variance attribute is a volume attribute which can measure the similarity of seismic wave in both lateral and vertical sections by using mean value calculation (Figure 18). In contrast, the different waveform or discontinuity waveform is also displayed, for example, channels, faults, sequence boundaries, unconformities, and uncommon features (Pigott et al., 2013). Thus, variance attribute is possible to estimate the discontinuity of the whole seismic volume and display the characteristics of paleo-pockmarks (morphology and distribution) and polygonal fault in the study area.

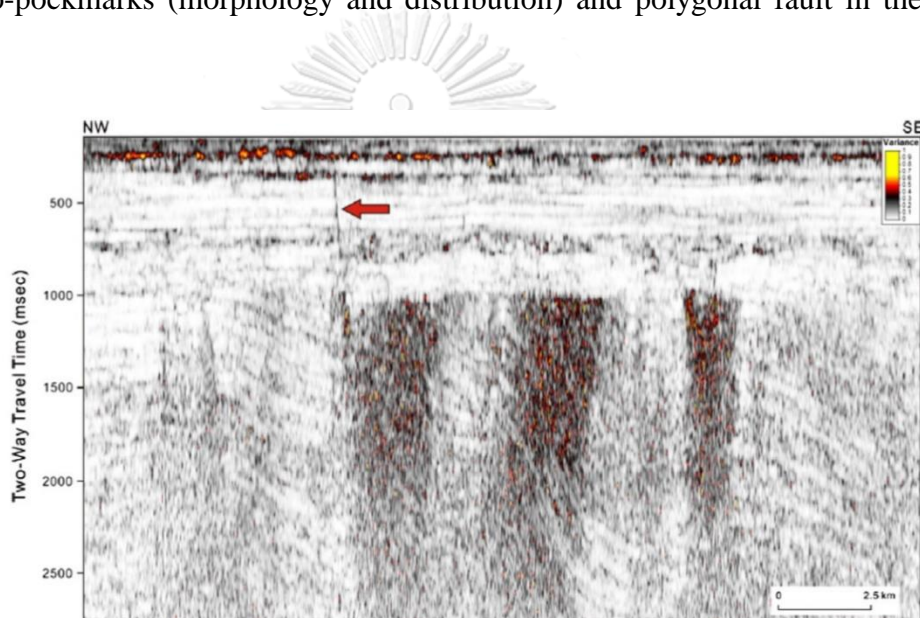


**Figure 18** Variance attribute image as dark to hot colors displays fault characteristics (red arrow) on the seismic section (Pigott et al., 2013).

#### 3.2.2 Consistent dip

The consistent dip is one of the volumetric dip calculations that is essential for many structural attributes. Generally, this method applies a smoothing filter for spatially continuous display by reducing the lateral and vertical resolution. In addition, the consistent dip uses an iterative global optimization method to calculate the dip and honors global consistency constraints of reciprocity, causality, consistency, and continuity (Schlumberger Petrel, 2014). It means consistent dip consider and analyze many properties. For example, 1) The symmetrical of neighboring trace both inline and crossline (Reciprocity); 2) Disturbance by tectonic

or other reasons (Causality); 3) The correct dip from each part of both inline and crossline (Consistency); and 4) The discontinuities due to fault or channel cut or poor signal (Continuity). Thus, this attribute possible to estimate the variation of dip angle of the pockmark craters.

### 3.2.3 3D Curvature

The curvature is a two-dimensional attribute of a curve. It can describe how much the curve deviates from a horizontal plane. This method measures the rate change of curve direction on both inline and crossline. The curvature is zero where the vectors are parallel on a flat plane. The curvature is positive where the vectors diverge on an anticline structure, and the curvature is negative where the vectors converge on a syncline structure (Schlumberger Petrel, 2014) (Figure 19). Thus, this attribute is used to estimate and display edge and bottom of the paleo-pockmarks in the study area.

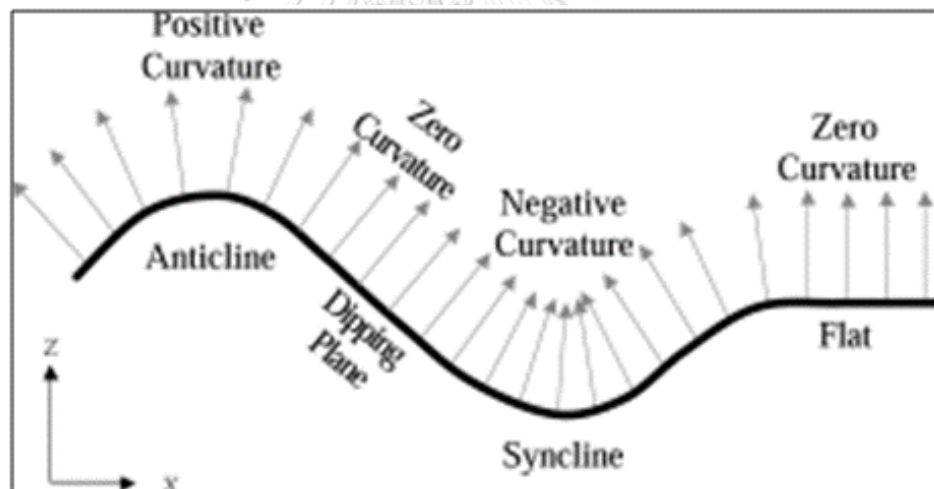


**Figure 19** Sign convention of curvature attribute. Grey arrows are defined as vectors (Schlumberger Petrel 2014).

### 3.3 well log analysis

Well logging is the tool which uses to record characteristics of the rock formation in the well-bore (Serra, 1984). Well log data include gamma-ray log, neutron log, density log, resistivity, and others. Each physical parameter in well log can be used to document different data such as gamma-ray log relating type of lithology (sand or shale), neutron and density log relating porosity of the sediment,



and resistivity log relating fluid type (oil, gas, or brine) (Figure 20). Furthermore, the pattern of gamma-ray log is used to indicate the depositional environment of each sequence as shown in (Figure 21). Generally, well log data are chosen to describe and identify characteristics of lithology, porosity, fluid type, and the depositional environment in the study area. While the oil industries use well log data to find hydrocarbon in the sedimentary formation. In this thesis, the estimation analyzes physical properties of rock in the basin and depositional environment on a regional scale which data is present in three wells. There are Pakaha-1, Kawau-1, and Hoiho-1 wells which located near 3D seismic data. The reason for choosing these well because the direction of well correlation seems to relate with the direction of sediment transportation from proximal fan to distal fan.

The well logs including gamma-ray log, resistivity log, neutron log, and density log were used as the main parameters in this study (Figure 20). The meaning of each parameter was described by (Pernes, 2013). First, Gamma-ray log is used to identify clay composition in a formation. High gamma-ray means sediment has potassium rich, and it measures the percentage of rock to be shale or sandstone. Resistivity log is used to measure the resistivity of rock. High resistivity means that rock is filled by hydrocarbon (oil or gas). Low resistivity means that rock is filled with water (brine). Neutron log is used to estimate the formation porosity and it is possible to imply hydrogen, carbon, oxygen element which fill in the formation. While density log is used to measure the density of the formation. High density means tight rock, and low density means that rock possible to has high porosity and high permeability. Thus, we used these logs to describe physical properties of rocks and find out hydrocarbon traces around the study area.

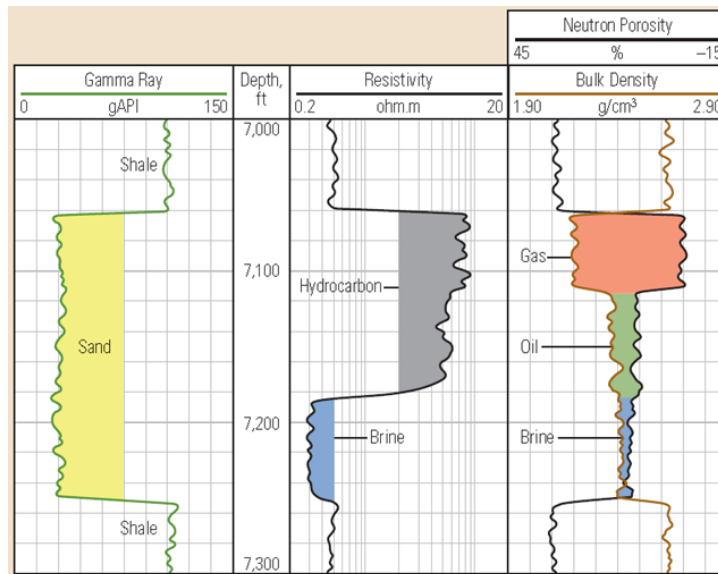


**Figure 20** Well log sample shows physical parameters which used to identify lithology, porosity, and fluid type (Schlumberger, 2006).

### 3.3.1 Gamma ray log pattern interpretation

Gamma-ray log patterns can be used to define the depositional environment of the sedimentary sequences and picking top formation (Odundun and Nton, 2012) in the study area. Gamma-ray log trends are divided within five major shapes, including irregular shape, funnel shape, cylindrical shape, and bell shape (Figure 21). The descriptions of all gamma-ray log patterns are presented below.

#### Cylindrical shape

The cylindrical shape represents the sharp form of gamma-ray log both upper and lower boundaries. It could indicate inner-fan channel and slope channel environments (Odundun and Nton, 2012).

#### Funnel shape

Funnel shape is used as an indicator of coarsening upward sequence and increasing of sand content. The possible depositional environments are progressive barrier bar, marine shelf fan, and delta or crevasse splay (Odundun and Nton, 2012).

#### Bell Shape

Bell shape represents a pattern of fining upward sequence and increasing of clay content. It is used as an indicator of transgressive, tidal channel, fluvial-deltaic channel (Odundun and Nton, 2012)

### Symmetric shape

Symmetric shape shows the transition between coarsening upward sequence and fining upward sequence. It indicates the shallow marine environment because of sea-level change (Kuhasubpasin, 2017).

### Irregular shape

The irregular shape represents the fluctuation pattern of gamma-ray. The trend has not a clear interval of shale or sand aggradation. Sedimentary layers show parallel laminae of clay or silt, it is possible to deposit from suspension, fluvial floodplain, tidal flat, and deep marine slope (Odundun and Nton, 2012).

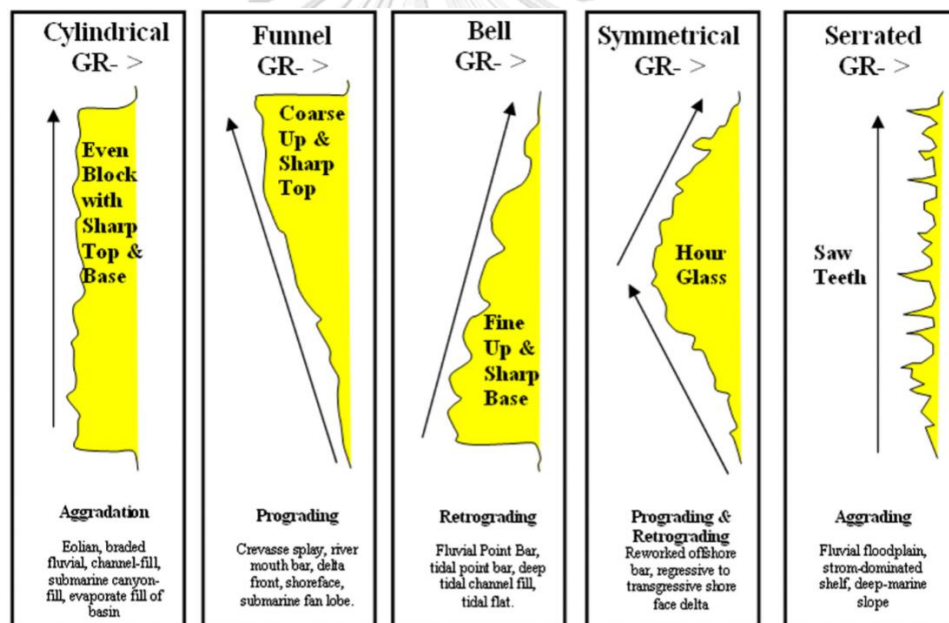


**Figure 21** Schematic model of log shapes shows the relationship between gamma-ray log patterns and depositional environments (Odundun and Nton, 2012).

### 3.3.2 Well log correlation

Well log correlation is used to interpret stratigraphic correlation in a regional scale after picking top formation of each well. In this part, three wells were chosen to make well correlation by using Schlumberger Petrel software, including Pakaha-1,

Kawau-1, and hoiho-1 wells. These wells located in the southern to northern part of the study area. Gamma-ray log patterns are used as the main parameter to correlate top formation of each sequence. The sample of well correlation is shown in Figure 22.

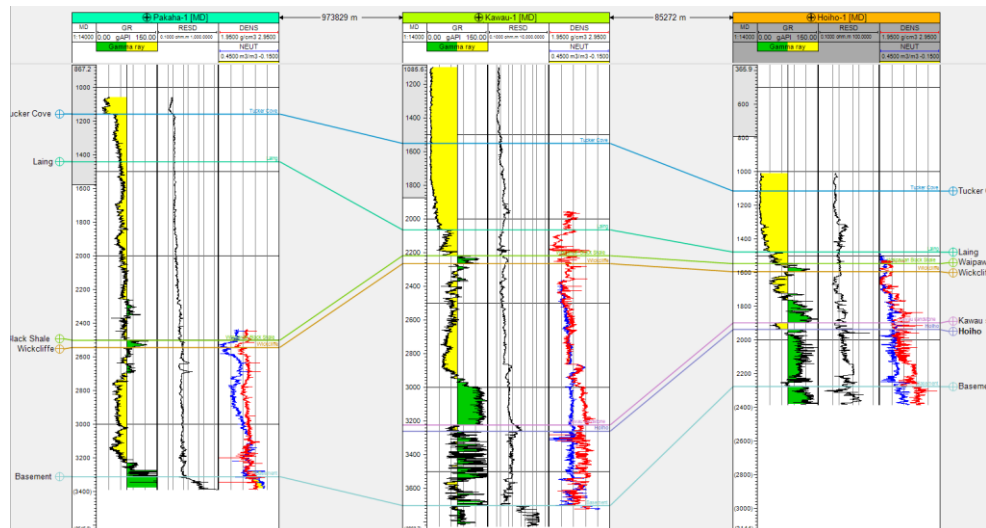


**Figure 22** The sample of three selected three well which was correlated by using schlumberger Petrel software.

## CHAPTER 4

### RESULTS

Characteristics of paleo-pockmarks in this thesis are considered by using seismic interpretation, including 2D and 3D seismic data, and well data. Schlumberger Petrel software is used as the main tool to image seismic characteristics, seismic facies, depositional pattern, and other uncommon features in the study area. This chapter includes stratigraphic correlation, seismic characteristics of paleo-pockmarks both top view and section view, size measurement, depositional environment in the Great South Basin (GSB), paleo-pockmark distribution, paleo-pockmark density, and well log analysis. Pakaha-1 well is only one exploration well which is used for seismic and well correlation. This well located in the eastern part of the study area.

#### 4.1 Stratigraphic correlation

Stratigraphic correlation is the first step for studying seismic characteristics of paleo-pockmarks in this thesis. The result represents stratigraphic sequences, thickness, depositional environment, and the important features in the study area. 2D seismic data and Pakaha-1 well data are used for correlation. The result shows stratigraphic sequences divided into four major groups based on depositional environments (Figure 23). There are Hoiho group, Pakaha group, Rakiura group, and Penrod group. In addition, the important features are founded in all sequences as shown in the seismic profiles which are cut in the northwest to the southeast direction (Figure 24).

Many interesting features are founded associated with paleo-pockmarks in the study area as shown in the seismic section (Figure 4-2). These feature include graben and half-graben (number 7), characteristics of opal-A to opal-CT (number 6), the progradational pattern of clastic sediment (number 5), paleo-pockmarks (number 4), polygonal fault (number 3), channel erosion (number 2), and present-day pockmarks (number 1). Characteristics of these features are described in detail below.

Stratigraphy and observed features in the study area are described in detail below.

### **Hoiho group**

Hoiho group is the oldest non-marine clastic sedimentary sequence in the Great South Basin but it is not found in Pakaha-1 well. The reason is that Pakaha-1 well was drilled on the horst structure which is the highest portion in the basin. Lack of Hoiho group affects to key horizon interpretation in the lowest part and prediction of hydrocarbon in Pakaha-1 well. Graben and half-graben (Figure 24) (label in number 7) are founded in the lower part of stratigraphic sequences.

### **Pakaha group**

Late Cretaceous to early Paleocene package as known Pakaha group is the oldest sedimentary sequence in Pakaha-1 well data deposited in post-rift 2 (Constable et al., 2010). Pakaha group is defined as coastal to shelf facies. This group is divided into two formations which are Wickcliffe and Waipawan black shale. Seismic characteristics of Wickcliffe formation (purple line) represents a thick bed of non-marine to coastal facies which deposited on graben and half-graben of the basement. The top formation of this sequence developed around 2.4 to 2.8 s (TWT). The wedge shape of clastic sediment is founded in the eastern part near Pakaha-1 well. While Waipawan black shale (blue line) represents the pattern of downlap clearly in the upper part as shown in seismic profiles (Figure 24). The top formation of this sequence detected around 1.8 to 2.3 s (TWT). This formation shows decreasing of slope from the northwest to the east directions as shown in (Figure 23).

### **Rakiura group**

The late Paleocene to late Eocene successions of Rakiura group contain basinal deposition and shelf facies, including Laing formation and Tucker Cove formations (Figure 23). Laing formation is the fine-grained marine facies which deposited around late Paleocene to middle Eocene time. The top formation of this sequence developed around 1.4 to 1.7 s (TWT). The seismic section shows increasing of thickness from the northwest to southeast direction. In the lower part of Laing

formation, a progradational pattern of clastic sediments (Figure 24) (label in number 5) is developing at around 1.8 to 2.0 s (TWT) from the southwest (SW) to northeast (NE) direction. Seismic profiles show the pattern of downlap overlain on the top surface of Wipawan black shale as shown in (Figure 24). In the upper part of Laing formation, paleo-pockmarks are observed on the surface of Laing formation and possible seismic characteristics of opal-A to opal-CT (Figure 24) (label in number 6) based on the interpretation of Morley et al. (2017). The cross-cutting reflections between stratigraphic layer and diagenetic front layer is the specific pattern of opal-A to opal-CT caused by density and rigidity increases (Figure 24).

Tucker Cove formation is the fine-grained marine sediments which deposits around late Eocene to early Oligocene time. The top formation of this sequence developed around 1.1 to 1.4 s (TWT) (Figure 23). Seismic profiles show thin parallel beds and pattern of onlap overlain on progradational clinoform as shown in Figure 24. This progradational clinoform are founded in the seismic section (Figure 24) (label in number 5) at around 1.7 to 2.2 s (TWT). Slope angle of this clinoform decreases from northwest to southeast direction. Moreover, polygonal fault features (Figure 4-2) (label in number 3) are also detected on bathyal sediment both Laing and Tucker Cove formations around 1.3 to 2.0 s (TWT). This polygonal fault feature is defined as a regional extensional fault which is developed within the fine-grained sediment sequences (e.g. Gay et al., 2004; Morgan et al., 2015).

### **Penrod group**

In the last stage, the late Oligocene to Recent carbonate package as known Penrod group is deposited overlain on Mashall Paraconformity as presented in Figure 23. Penrod group (gray line) represents two different seismic characteristics including a lower part and upper part. In the lower part, seismic section shows characteristics of channel erosion at around 1.0 to 1.3 s (TWT) (Figure 23 and 24). While, in the upper part, seismic section shows thin parallel layer which has high amplitude anomalies. Thus, the depositional environment of this formation is defined as bathyal facies.



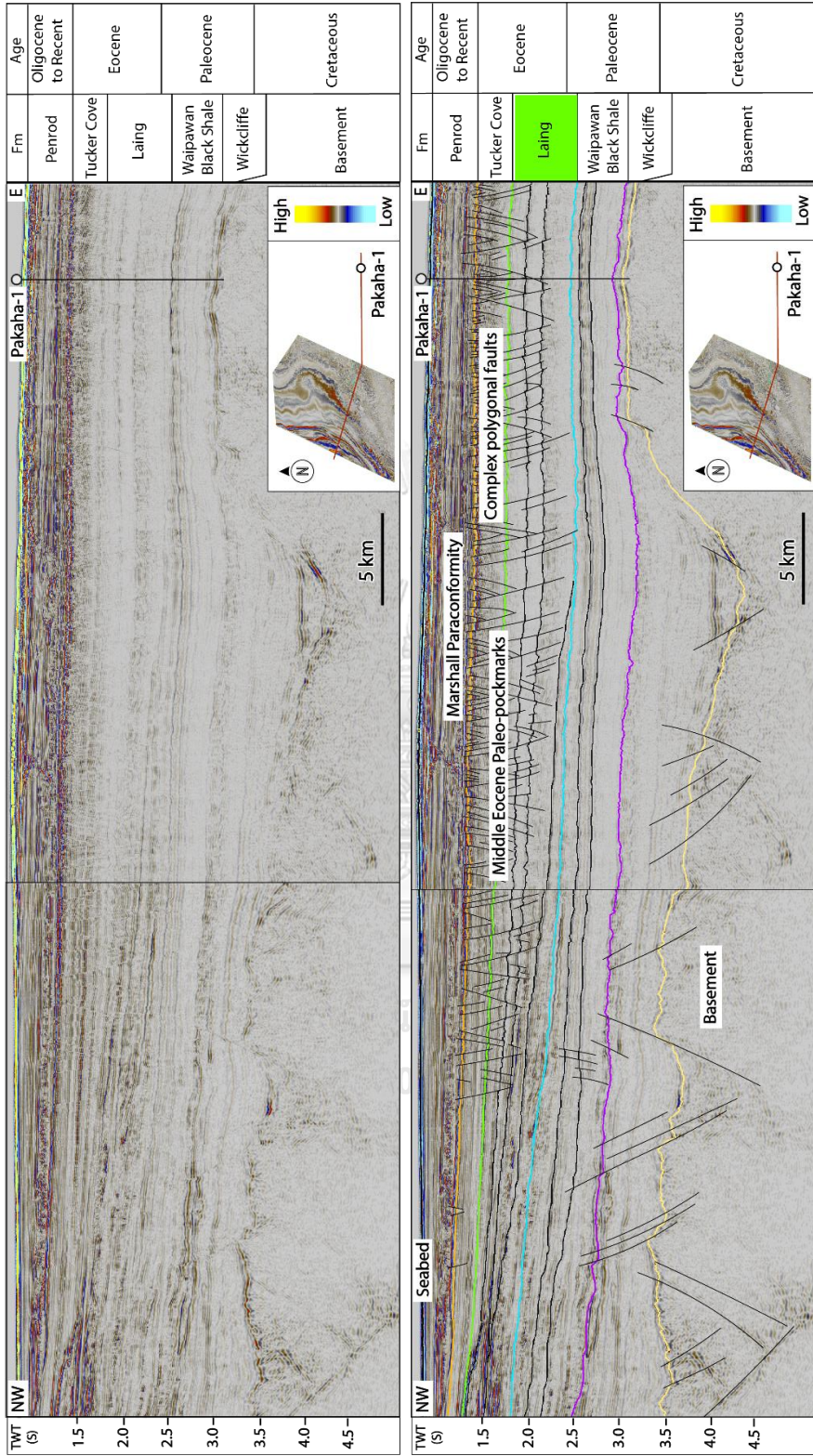


**Figure 23** 2D and 3D seismic section which is used for horizon picking and seismic interpretation correlated with Pakaha-1 well. Five color lines on both figures are the top formation, which the name label on the right



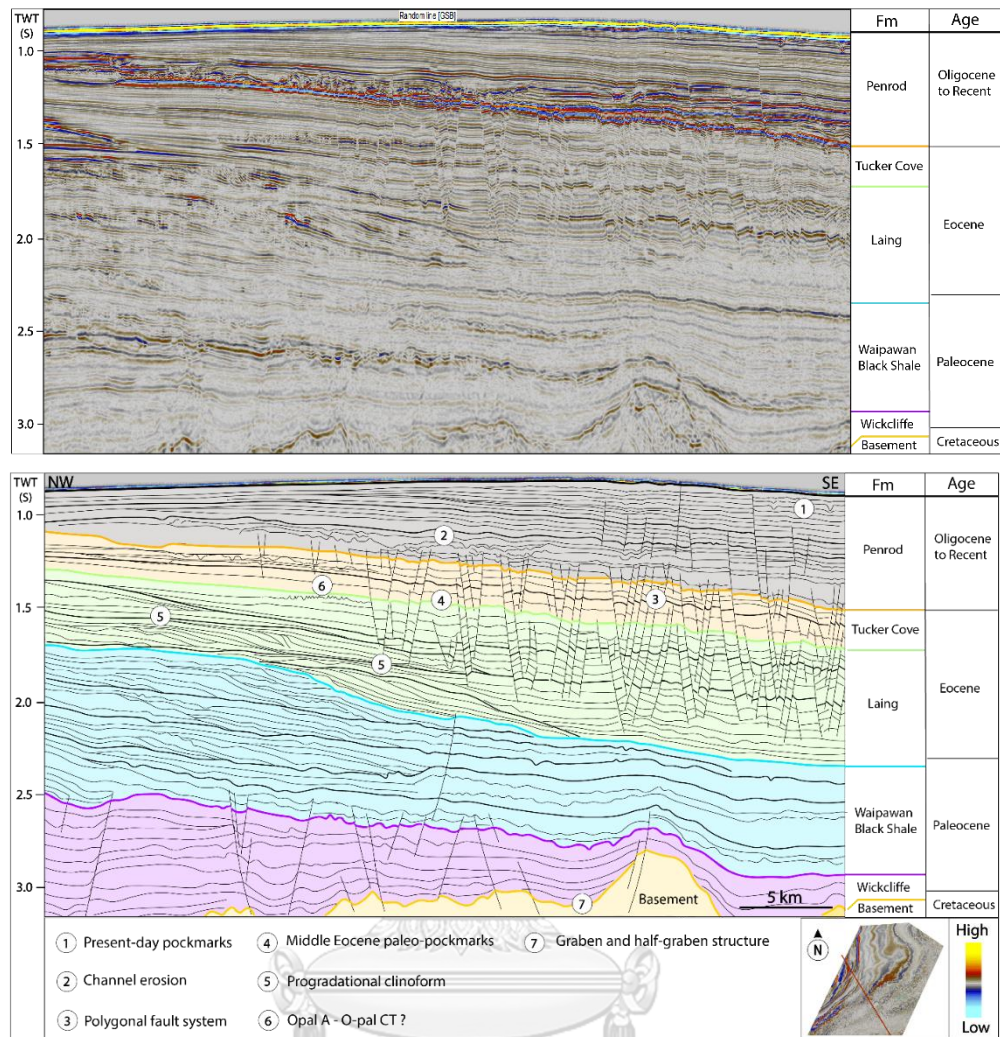


**Figure 24** Seismic profiles show sequence stratigraphy, structural pattern and the important features in the study area. The paleo-pockmark layer (number 4) is detected on the top of Laing formation (green layer). The lower part of Laing formation shows progradation pattern (number 5). Polygonal fault system (number 3) is located at the eastern part of the study area.

#### 4.2 Paleo-pockmark distribution

In this area, numerous paleo-pockmarks are clearly displayed on the paleo-seafloor at time slice of 1492 ms (TWT). RMS amplitude attribute is used to image the depositional pattern of paleo-pockmarks in the study area. This method estimates the various magnitude at around 50 ms (TWT) below the top surface of Laing formation, middle Eocene time.

The result shows high amplitude anomaly of paleo-pockmark formation spreading on a fan shape like feature along the southwest to the northeast direction (from proximal fan to distal fan) as presented in Figure 26. In the body of fan shape, RMS amplitude represents increasing of number of paleo-pockmarks in the central of the fan. Three major zones of the fan shape are chosen randomly to study paleo-pockmark morphology and density including zone 1, zone 2, and zone 3 (Figure 26). Zone 1 located in the proximal fan, zone 2 located in the middle fan, and zone 3 located in the distal fan base on the study of Shanmugam, 2016. Two types of volume attribute are used to image characteristics of paleo-pockmarks in each zone including variance attribute and consistent dip attribute. Variance attribute is used to measure the similarity of seismic reflections, while consistent dip attribute is used to calculate the dip angle of paleo-pockmarks (Figure 26). The results of these attributes are described in the next part for the characteristic of the paleo-pockmarks.

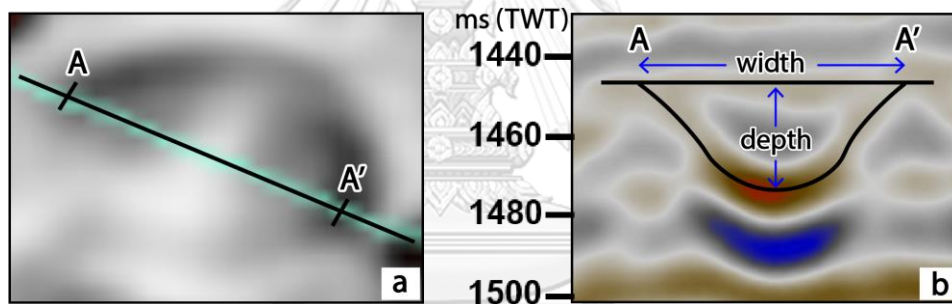


**Figure 25** (a) Characteristics of paleo-pockmarks are shown both on the top view and (b) side view. Paleo-pockmark width and depth are measured in seismic section. Width is measure from the left shoulder (A) to the right shoulder (A'), while depth is measure from paleo-pockmark cluster to the bottom (b).

#### 4.3. Seismic characteristics of paleo-pockmarks and size measurement

Characteristics of paleo-pockmarks are described in shapes, both top view and section view, and sizes for this study. Volume seismic attributes are chosen to image paleo-pockmarks characteristics because they calculate data precisely and show a clear shape of paleo-pockmarks on top view. Size measurement is width and depth of paleo-pockmarks by using measure ruler in Schlumberger Petrel software as shown in Figure 25. Paleo-pockmark width or diameter is a measurement in a lateral direction

on pockmark edge from left shoulder to right shoulder. While depth is the measurement in a vertical direction from pockmark crater to pockmark bottom.

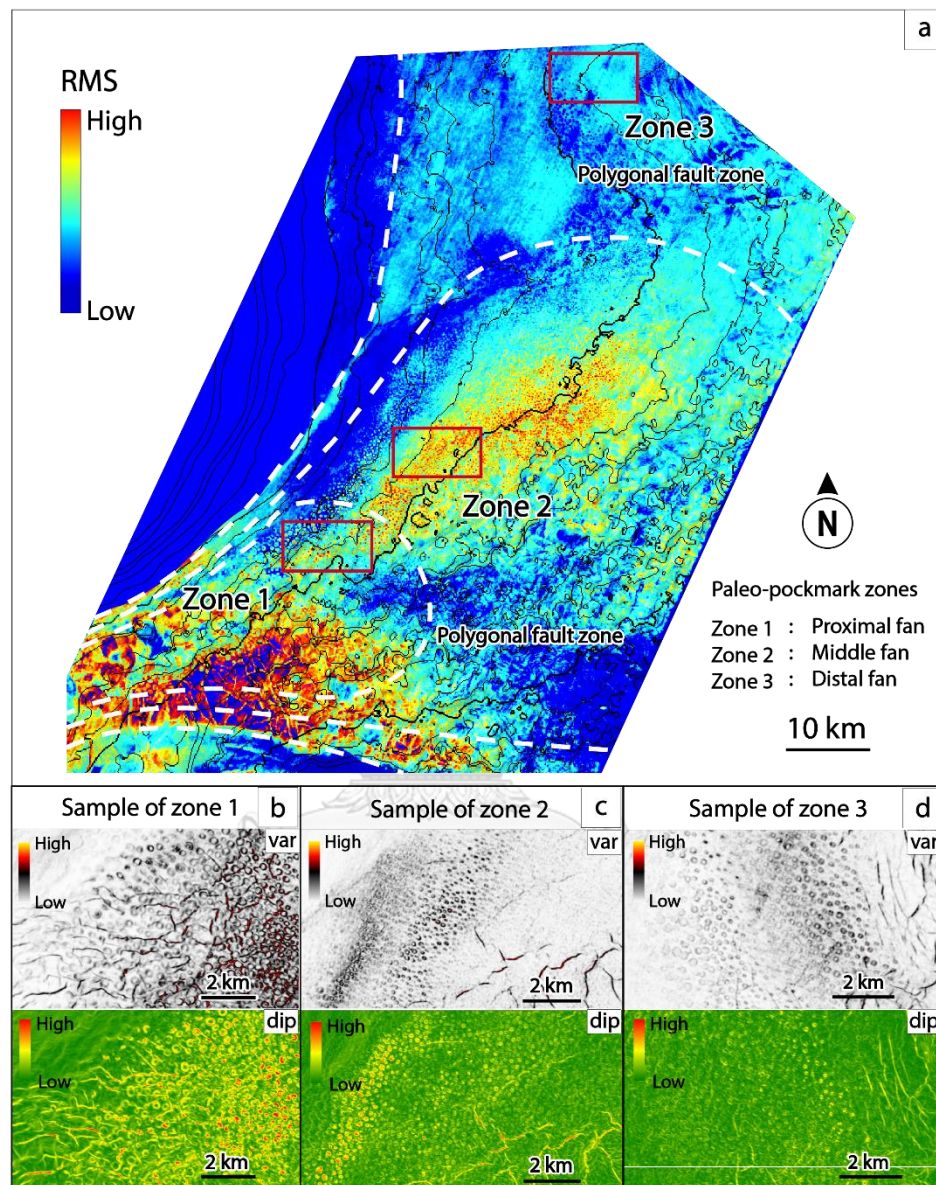


**Figure 26** (a) RMS amplitude map shows paleo-pockmark distribution as fan shape in the study area. The variance (var) and consistent dip (dip) images show (b) the sample images of paleo-pockmark from zone 1, (c) zone 2, and (d) zone 3. White dashed lines are the boundary of



The result shows numerous paleo-pockmarks are buried by the younger sediments at around 1.5 km below the present seabed (using the average velocity of sediment at 2,000 m/s). The 94 paleo-pockmark samples are chosen from zone 1, zone 2, and zone 3 for size measurement (Table 2, 3, and 4). They are classified as “normal pockmarks” with a sub-round to round shape on top view and V-shape to U-shaped in vertical section. Their sizes are mainly ranging from 131 to 481 m in diameter and 15 to 45 ms (TWT) in depth. The smallest paleo-pockmarks are founded in zone B having diameter and depth approximately 131 m and 16 ms (TWT) in depth, respectively. The largest paleo-pockmarks are founded in zone 1 having diameter and depth approximately 481 m and 15 ms (TWT) in depth, respectively. Characteristics of paleo-pockmarks of each zone are described in detail as follows;

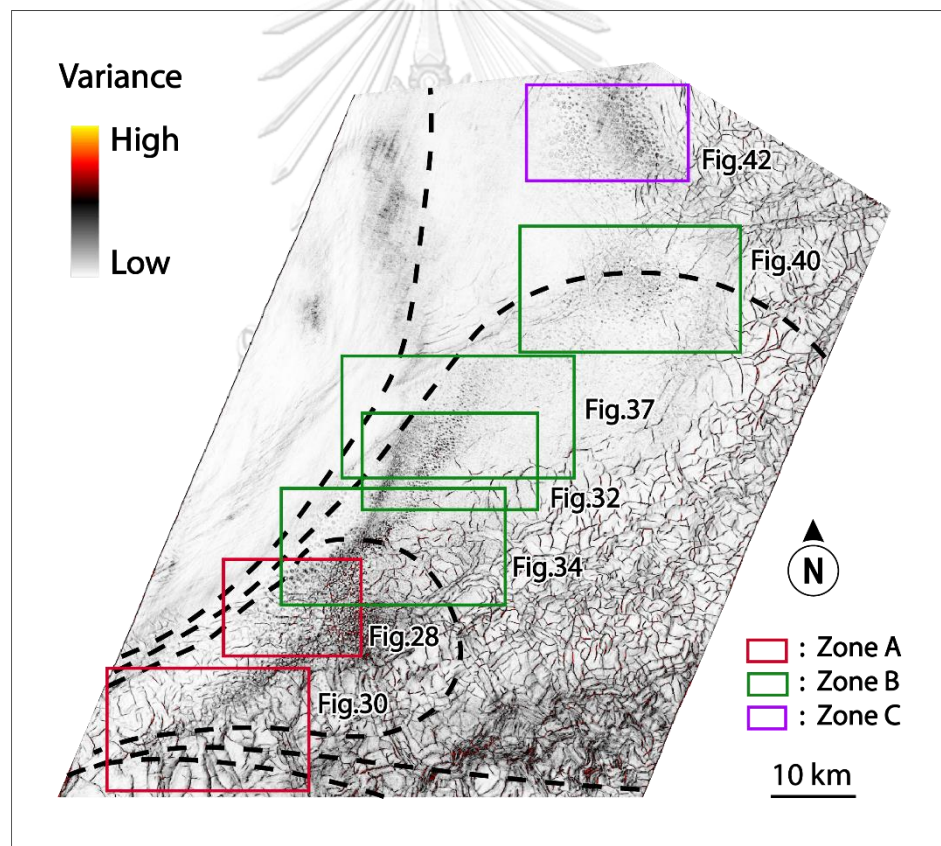


**Figure 27** Variance map shows the location of each zone to study characteristics of paleo-pockmarks. There are three major zones, including two red frames located in zone 1, four green frames located in zone 2, and a purple frame located in zone 3.

### 4.3.1 Paleo-pockmark characteristics in zone A

Paleo-pockmarks in zone 1 are detected and founded the depth are around 1.4 to 1.5 s (TWT). Examples of paleo-pockmarks in this zone include 1-1 and 1-2 with six sub-seismic sections (1-S1 to 1-S6) (Figure 28 to 31). Paleo-pockmark shapes are divided based on two viewpoints, top view and section view. Variance attribute map displays medium to high variance value (0.5 to 0.8 value) with sub-round to round in shapes on the top view see in Figure 28 and 30. The circular black edges in variance maps corresponds to low amplitude contrast of eighteen paleo-pockmarks (Pm1 to Pm18). In section view, U-shaped paleo-pockmarks are commonly observed, except Pm1 and Pm2 are more likely to be V-shape. The paleo-pockmarks in this zone show 7 to 15 degrees of paleo-pockmark dip angle (medium to high value).

The paleo-pockmarks in this zone have their sizes ranging from 204 to 481 m in diameter and 15 to 45 ms (TWT) in depth. Progradation pattern of clastic sediment is founded around 1.8 s (TWT) in seismic beneath the paleo-pockmark layer, and the paleo-pockmarks are likely to be larger than the other zones. The statistic information of representative paleo-pockmarks from zone 1 is shown in Table 2.

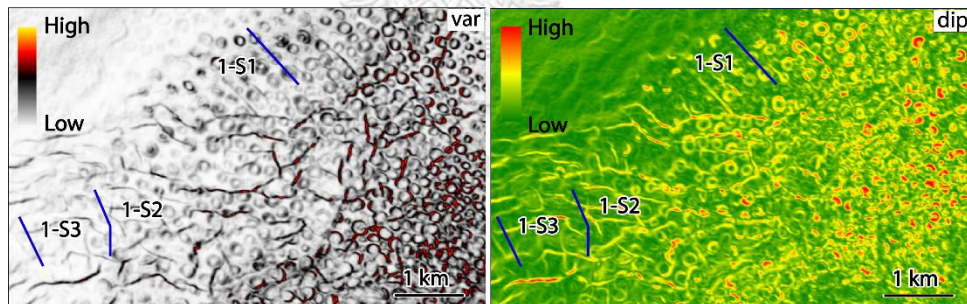


**Figure 28** Variance map (left) shows sub-round to round in shapes on the top view with medium to high values (0.5 to 0.8 value) of discontinuity. While consistent dip map (right) shows 7 to 15 degrees of paleo-pockmark dip angle (medium to high value).

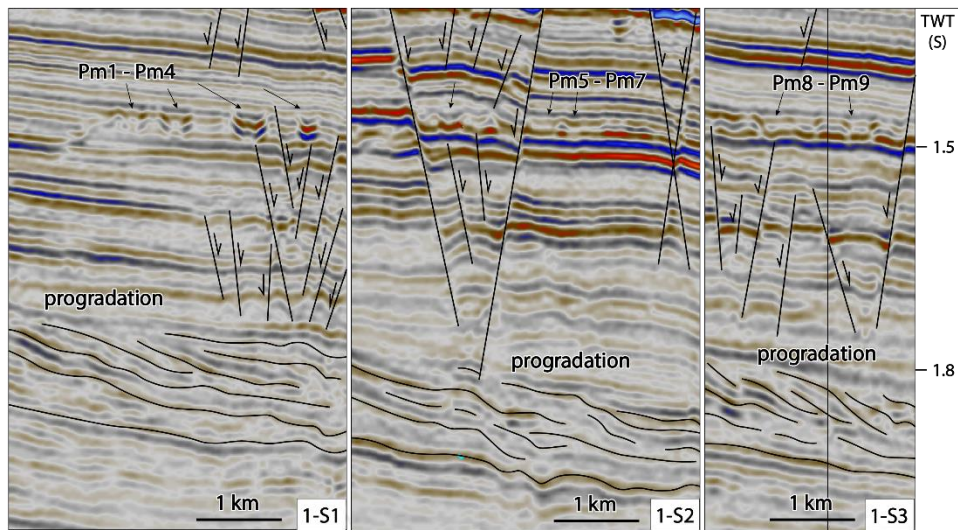


**Figure 29** Seismic sections (1-S1 to 1-S3) show the shape of nine paleopockmarks (Pm1-Pm9) in section view. Pm1 and Pm2 are V-shape pockmarks, while Pm3 to Pm9 are mostly U-shape pockmarks. Their size ranges from 204 to 382 m (width), and 19 to 45 ms (TWT) (depth). See seismic profiles in Figure 28.

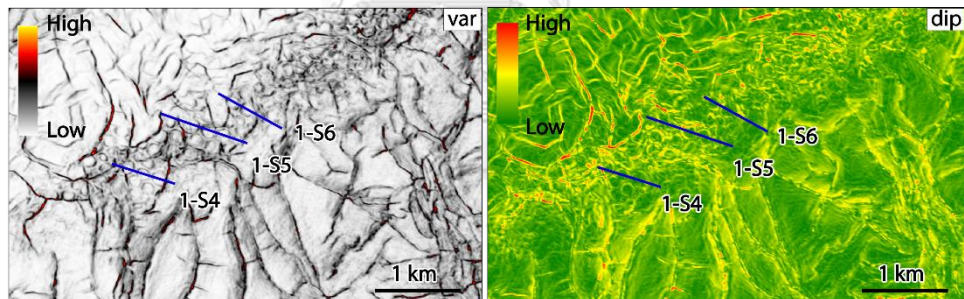


**Figure 30** Variance map (left) shows sub-round to round in shapes on the top view with medium values (around 0.5 value) of discontinuity. While consistent dip map (right) shows 6 to 7 degrees of paleopockmark dip angle (medium value).



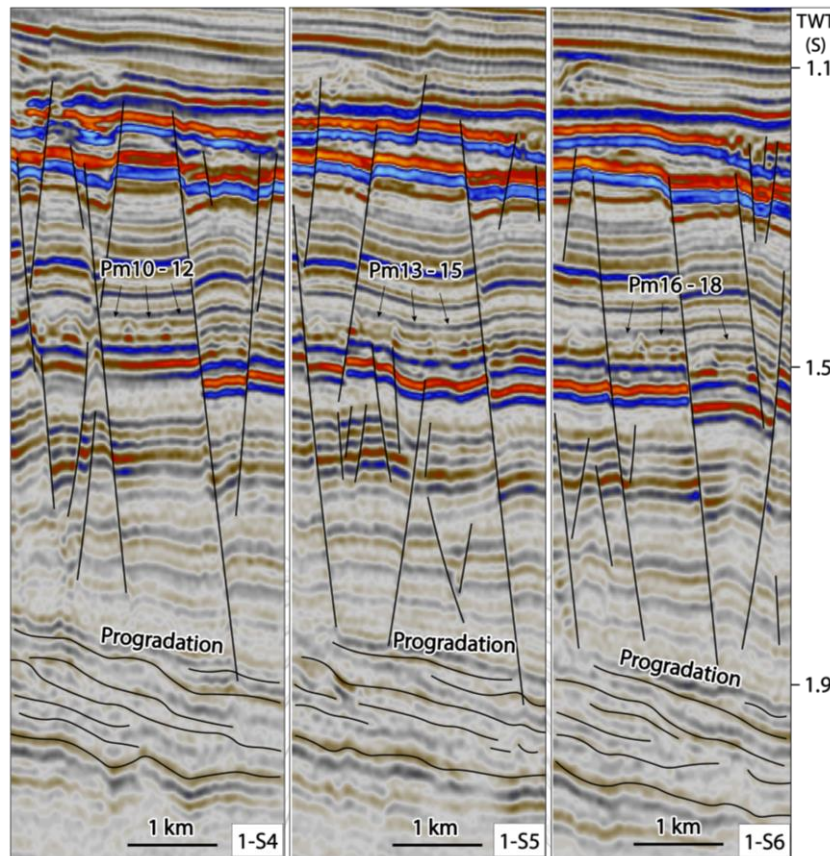


**Figure 31** Seismic sections show characteristics of paleo-pockmarks 10 to 18 (Pm10-Pm18). All paleo-pockmarks in these sections are U-shape pockmarks. Their size ranges from 333 to 481 m (width), and 15 to 34 ms (TWT) (depth). Moreover, the progradational pattern of clastic sediment is founded beneath paleo-pockmarks layer. See seismic profiles in Figure 30.

**Table 2** The statistic information of representative paleo-pockmarks from zone 1

Name	Diameter (m)	Depth (ms)(TWT)	Shape		Section name
			Top view	Section view	
Pm1	293	29	Sub-round	V-shape	1-S1
Pm2	306	25	Round	U-shape	
Pm3	382	45	Round	U-shape	
Pm4	257	38	Round	V-shape	
Pm5	209	20	Sub-round	U-shape	1-S2
Pm6	300	19	Round	U-shape	
Pm7	204	32	Round	U-shape	

Pm8	293	32	Round	U-shape	1-S3
Pm9	300	37	Round	U-shape	
Pm10	358	34	Sub-round	U-shape	1-S4
Pm11	427	15	Sub-round	U-shape	
Pm12	347	16	Sub-round	U-shape	1-S5
Pm13	481	15	Sub-round	U-shape	
Pm14	417	21	Sub-round	U-shape	1-S6
Pm15	405	18	Sub-round	U-shape	
Pm16	333	17	Sub-round	U-shape	1-S6
Pm17	364	15	Sub-round	U-shape	
Pm18	451	15	Sub-round	U-shape	
<b>Average</b>	<b>340.39</b>	<b>24.61</b>			

#### 4.3.2 Paleo-pockmark characteristics in zone 2

Paleo-pockmarks in zone 2 is detected around 1.5 s (TWT). Images of paleo-pockmarks in this zone include 2-1 and 2-4 with fifteen sub-seismic sections (2-S1 to 2-S15) (Figure 32 to 41). Variance attribute map displays low to high (0.3 to 0.8 value) with mostly sub-round in shape on the top view. The circular black edge in variance map corresponds to medium to high amplitude contrast of sixty-three U-shape paleo-pockmarks (Pm19 to Pm81) in seismic sections. The paleo-pockmarks in this zone show 4 to 15 degrees of paleo-pockmark dip angle (low to high value).

Size of paleo-pockmarks ranges from 131 to 350 m in diameter and 15 to 45 ms (TWT) in depth. The smallest paleo-pockmarks is Pm37 which has 131 m in diameter and 16 ms (TWT) in depth and locates in the central part of the zone. Progradation pattern is observed at around 1.7 to 1.8 s (TWT) underneath the paleo-pockmark layer, in the lower part of Laing formation, middle Eocene time. The statistic information of representative paleo-pockmarks from zone 2 is shown in Table 3.



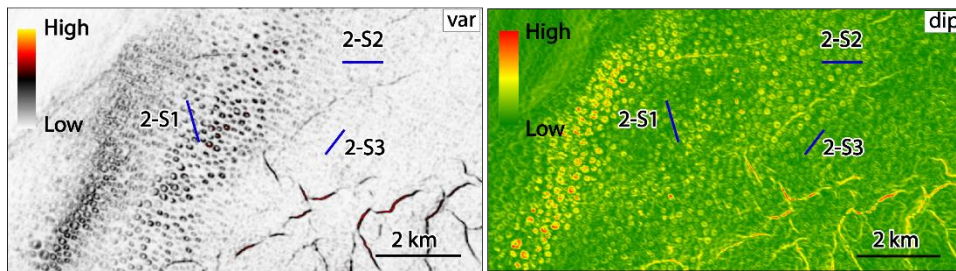


**Figure 32** Variance map (left) displays low to high value (0.3 to 0.8 value) with mostly sub-round in shape on the top view. While consistent dip map (right) shows 4 to 15 degrees of paleo-pockmark dip angle (low to high value).

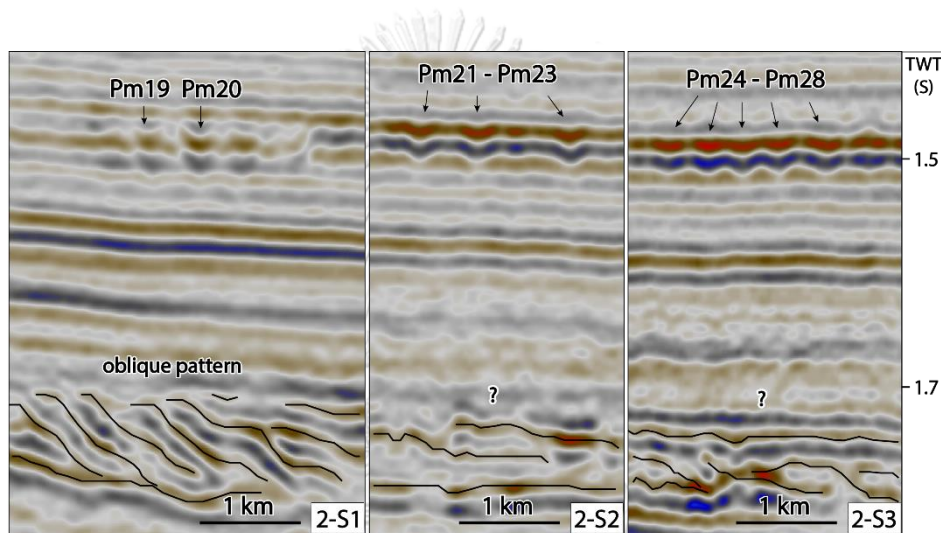


**Figure 33** Seismic sections show characteristics of paleo-pockmarks 19 to 28 (Pm19-Pm28). All paleo-pockmarks in these sections are U-shape pockmarks. Their size ranges from 138 to 189 m (width), and 15 to 24 ms (TWT) (depth). Moreover, progradational pattern of clastic sediment is founded beneath paleo-pockmarks layer. See seismic profiles in Figure 32.

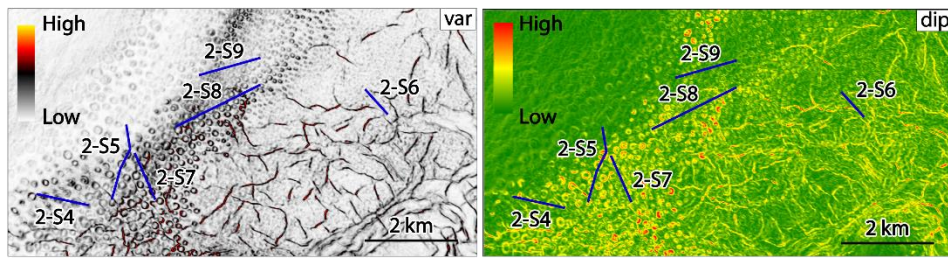


**Figure 34** Variance map (left) displays low to high value (0.3 to 0.8 value) with mostly sub-round in shape on the top view. While consistent dip map (right) shows 4 to 15 degrees of paleo-pockmark dip angle (low to high value).

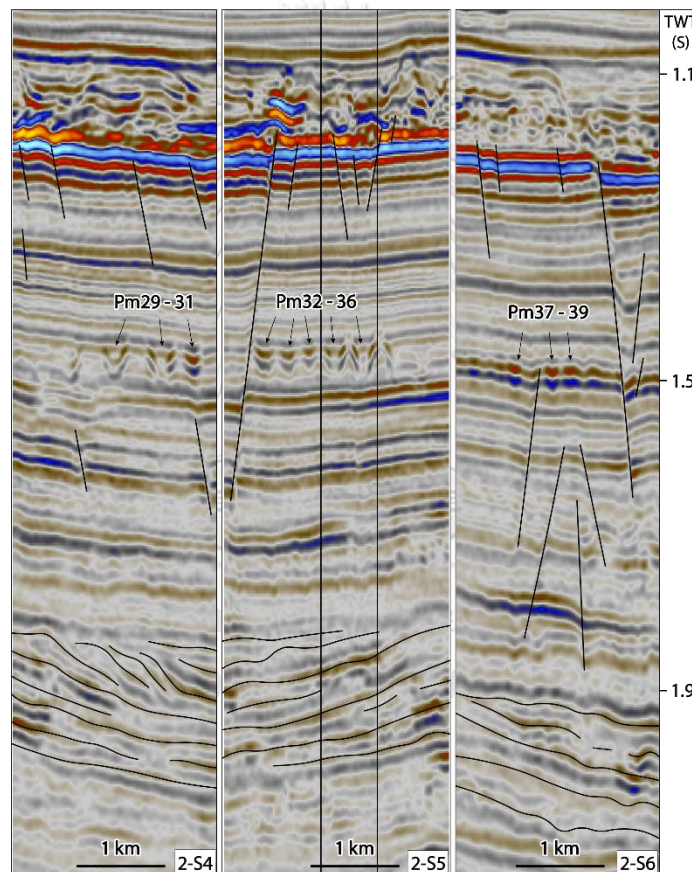


**Figure 35** Seismic sections show characteristics of paleo-pockmarks 29 to 39 (Pm29-Pm39). All paleo-pockmarks in these sections are V-shape to U-shape pockmarks. Their size ranges from 131 to 340 m (width), and 16 to 33 ms (TWT) (depth). Moreover, progradational pattern of clastic sediment is founded beneath paleo-pockmarks layer. See seismic profiles in Figure 34.

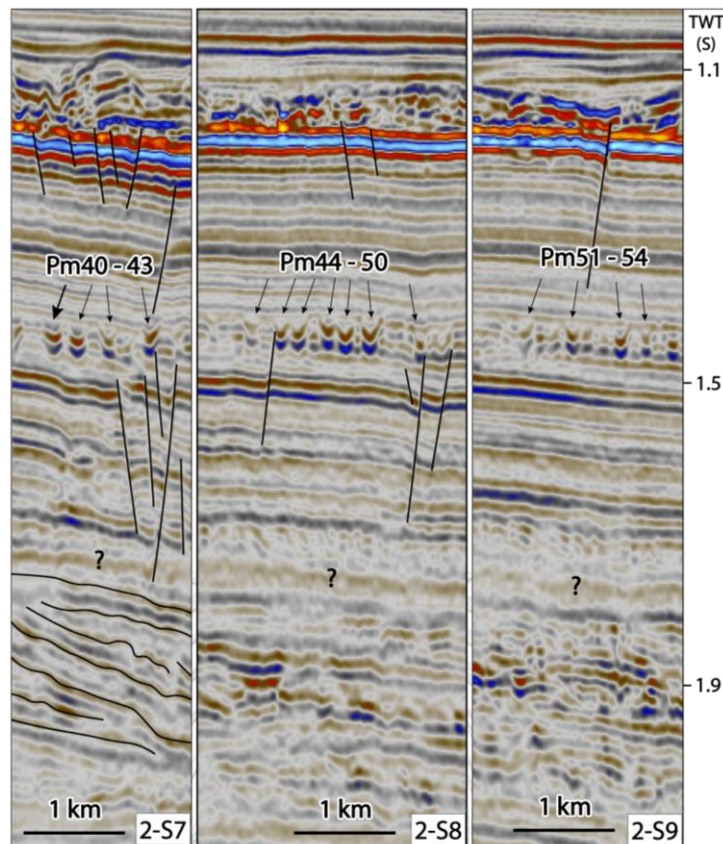


**Figure 36** Seismic sections show characteristics of paleo-pockmarks 40 to 54 (Pm40-Pm54). All paleo-pockmarks in these sections are U-shape pockmarks. Their size ranges from 222 to 350 m (width), and 29 to 45 ms (TWT) (depth). Moreover, progradational pattern of clastic sediment is founded beneath paleo-pockmarks layer. See seismic profiles in Figure 34.



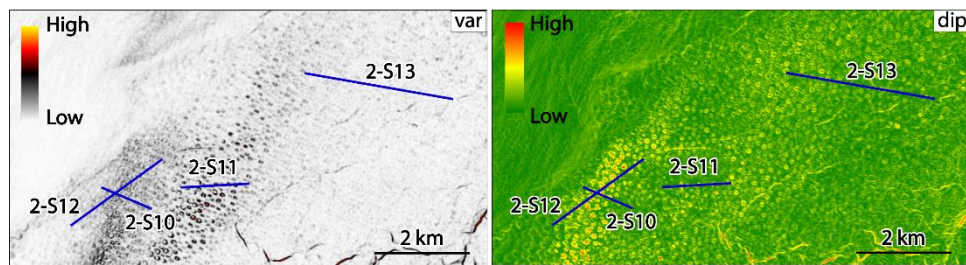


**Figure 37** Variance map (left) displays low to medium value (0.3 to 0.5 value) with mostly sub-round in shape on the top view. While, consistent dip map (right) shows 7 to 15 degrees of paleo-pockmark dip angle (medium to high value).

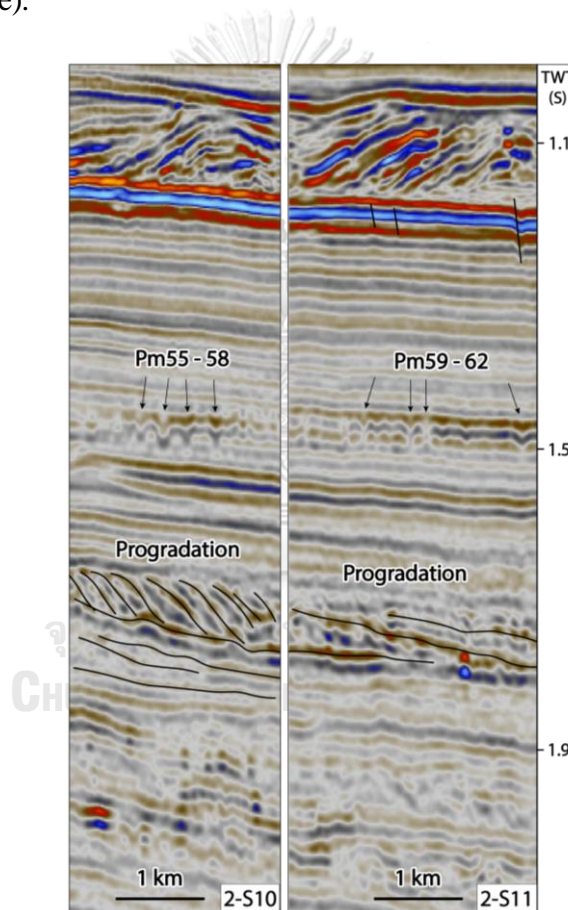


**Figure 38** Seismic sections show characteristics of paleo-pockmarks 55 to 62 (Pm55-Pm62). Paleo-pockmarks in these sections are mostly V-shape pockmarks. Their size ranges from 166 to 239 m (width), and 20 to 30 ms (TWT) (depth). Moreover, progradational pattern of clastic sediment is founded beneath paleo-pockmarks layer. See seismic profiles in Figure 37.

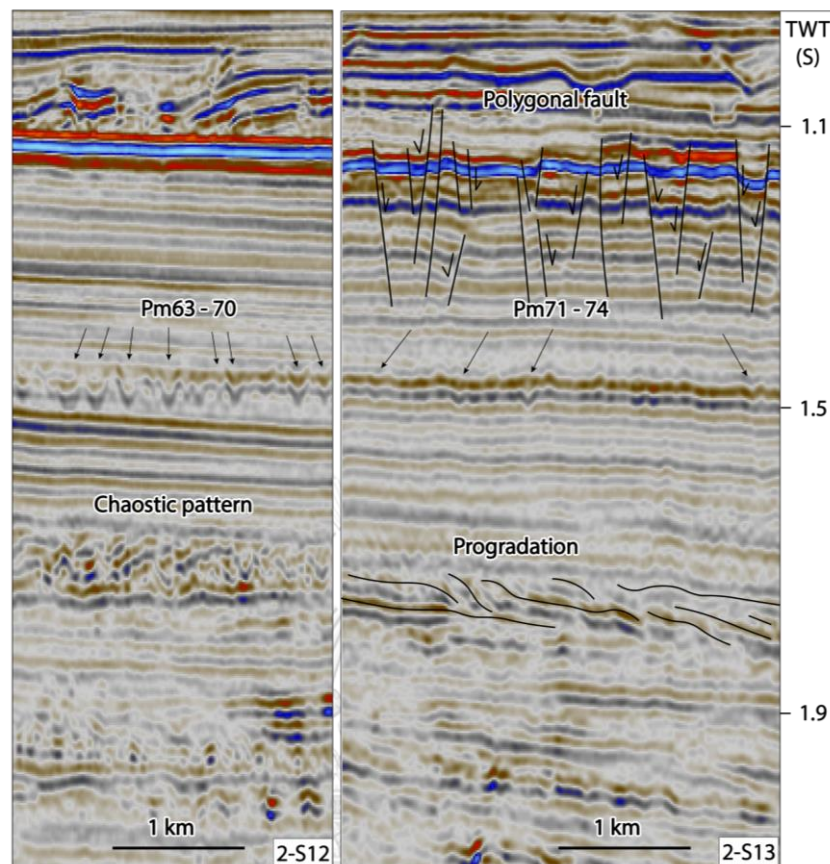


**Figure 39** Seismic sections show characteristics of paleo-pockmarks 63 to 74 (Pm63-Pm74). Almost paleo-pockmarks in these sections are V-shape pockmarks (Pm65-Pm70 and Pm72-Pm73). Their size ranges from 141 to 330 m (width), and 19 to 42 ms (TWT) (depth). Moreover, progradational pattern of clastic sediment is founded beneath paleo-pockmarks layer. See seismic profiles in Figure 37.

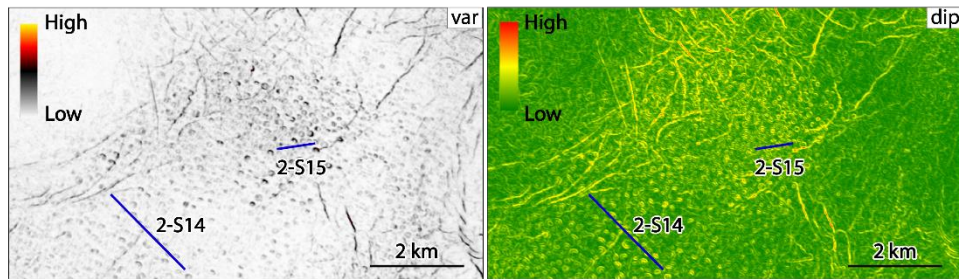


**Figure 40** Variance map (left) displays low to medium value (0.3 to 0.8 value) with sub-round to round in shape on the top view. While, consistent dip map (right) shows 4 to 7 degrees of paleo-pockmark dip angle (low to medium value).

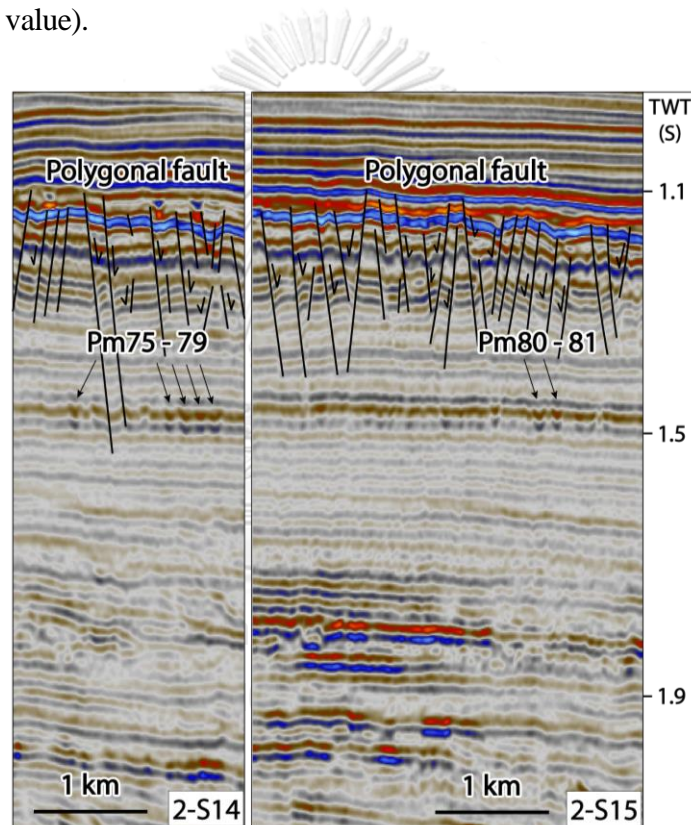


**Figure 41** Seismic sections show characteristics of paleo-pockmarks 75 to 81 (Pm75-Pm81). Paleo-pockmarks in these sections are V-shape to U-shape pockmarks. Their size ranges from 152 to 292 m (width), and 19 to 21 ms (TWT) (depth). See seismic profiles in Figure 40.



**Table 3 The statistic information of representative paleo-pockmarks from zone 2**

Name	Diameter (m)	Depth (ms)(TWT)	Shape		Section name
			Top view	Section view	
Pm19	152	24	Sub-round	U-shape	2-S1
Pm20	158	21	Sub-round	U-shape	
Pm21	197	21	Sub-round	U-shape	2-S2
Pm22	189	21	Sub-round	U-shape	
Pm23	164	21	Sub-round	U-shape	
Pm24	164	16	Sub-round	U-shape	2-S3
Pm25	138	15	Sub-round	U-shape	
Pm26	183	16	Sub-round	U-shape	
Pm27	169	15	Sub-round	U-shape	
Pm28	189	17	Sub-round	U-shape	
Pm29	291	30	Sub-round	U-shape	
Pm30	313	28	Round	V-shape	
Pm31	205	18	Round	U-shape	
Pm32	233	19	Round	U-shape	2-S5
Pm33	201	18	Round	U-shape	
Pm34	170	18	Round	U-shape	
Pm35	260	20	Round	U-shape	
Pm36	340	33	Round	U-shape	
Pm37	131	16	Sub-round	U-shape	
Pm38	142	19	Round	U-shape	2-S6
Pm39	133	17	Sub-round	U-shape	
Pm40	347	45	Round	U-shape	2-S7
Pm41	350	41	Round	U-shape	
Pm42	319	36	Sub-round	V-shape	
Pm43	222	29	Round	V-shape	2-S8
Pm44	309	31	Sub-round	V-shape	
Pm45	264	35	Sub-round	V-shape	
Pm46	315	37	Sub-round	V-shape	
Pm47	251	35	Sub-round	U-shape	
Pm48	275	39	Sub-round	V-shape	
Pm49	295	39	Sub-round	V-shape	
Pm50	242	37	Sub-round	V-shape	
Pm51	289	38	Round	U-shape	2-S9
Pm52	287	36	Sub-round	V-shape	
Pm53	318	38	Round	V-shape	
Pm54	275	33	Sub-round	V-shape	
Pm55	194	25	Sub-round	V-shape	2-S10
Pm56	239	30	Sub-round	V-shape	
Pm57	203	21	Round	U-shape	
Pm58	166	22	Round	U-shape	
Pm59	177	22	Sub-round	V-shape	2-S11

Pm60	232	24	Sub-round	V-shape	
Pm61	212	22	Sub-round	V-shape	
Pm62	205	20	Sub-round	V-shape	
Pm63	330	42	Sub-round	U-shape	
Pm64	291	39	Sub-round	U-shape	
Pm65	272	37	Round	V-shape	
Pm66	258	31	Round	V-shape	2-S12
Pm67	141	19	Round	V-shape	
Pm68	216	23	Round	V-shape	
Pm69	239	27	Round	V-shape	
Pm70	183	23	Round	V-shape	
Pm71	239	20	Sub-round	U-shape	
Pm72	178	19	Sub-round	V-shape	2-S13
Pm73	243	24	Round	V-shape	
Pm74	230	24	Round	V-shape	
Pm75	170	26	Round	V-shape	
Pm76	173	23	Round	V-shape	
Pm77	292	26	Round	V-shape	2-S14
Pm78	184	21	Sub-round	U-shape	
Pm79	187	21	Sub-round	U-shape	
Pm80	180	22	Sub-round	V-shape	2-S15
Pm81	152	19	Sub-round	V-shape	
<b>Average</b>	<b>226.44</b>	<b>26.10</b>			

### 4.3.3 Paleo-pockmark characteristics in zone 3

Paleo-pockmarks in zone 3 cover the northern part of the study area observing at around 1.5 s (TWT). Examples of paleo-pockmarks in this zone are 3-1 and 3-2 with four sub-seismic sections (3-S1 to 3-S4) (Figure 42 to 44). Variance attribute map displays low to medium (0.3 to 0.5 value) with sub-round to round on the top view. The circular black edge in variance map corresponds to low amplitude contrast of thirteen V-shape and U-shape paleo-pockmarks (Pm82 to Pm94) in seismic sections. The paleo-pockmarks in this zone show 4 to 7 degrees of paleo-pockmark dip angle (low to medium value).

Their size ranges from 163 to 281 m in diameter and 16 to 37 ms (TWT) in depth. The smallest paleo-pockmarks is Pm92 having 163 m in diameter and 16 ms (TWT) in depth. Paleo-pockmarks in this zone are observed below the polygonal fault system. The statistic information of representative paleo-pockmarks from zone 3 is shown in Table 4.



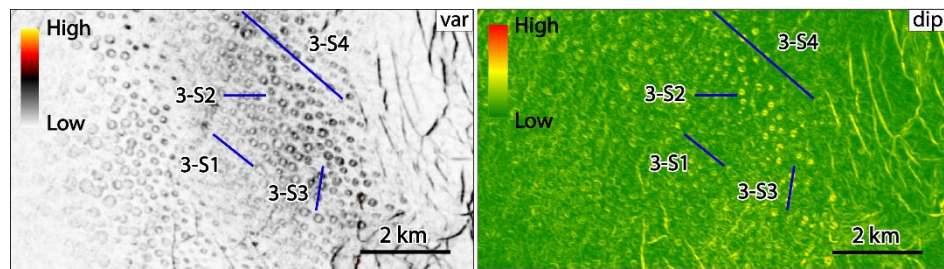


**Figure 42** Variance map (left) displays low to medium value (0.3 to 0.5 value) with sub-round to round in shape on the top view. While, consistent dip map (right) shows 4 to 7 degrees of paleo-pockmark dip angle (low to medium value).

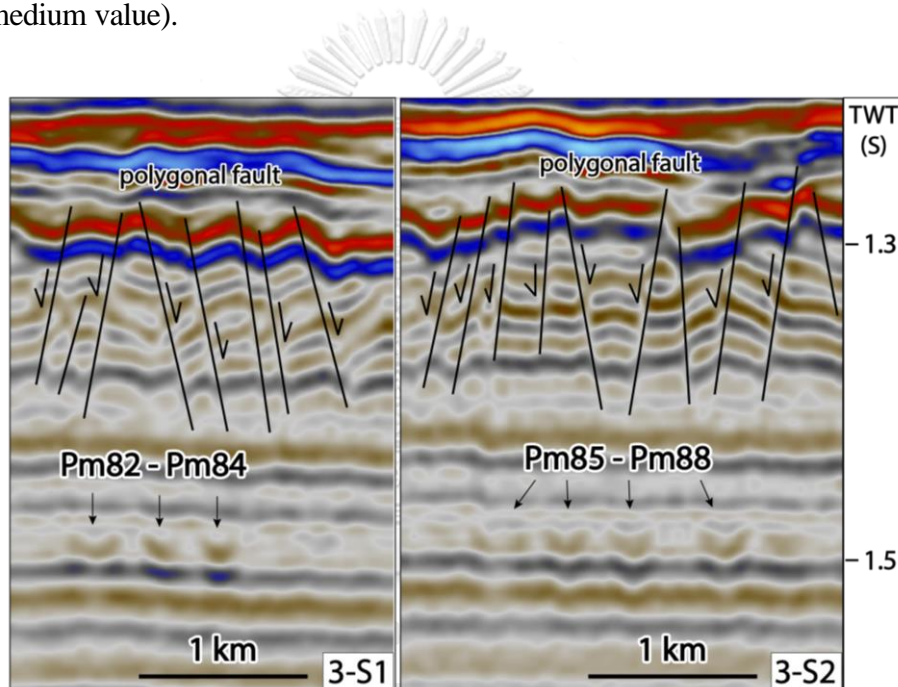


**Figure 43** Seismic sections show characteristics of paleo-pockmarks 82 to 88 (Pm82-Pm88). All paleo-pockmarks in these sections are U-shape pockmarks. Their size ranging from 163 to 225 m (width), and 18 to 22 ms (TWT) (depth). Polygonal faults are founded on the upper portion of the seismic section. See seismic profiles in Figure 42.

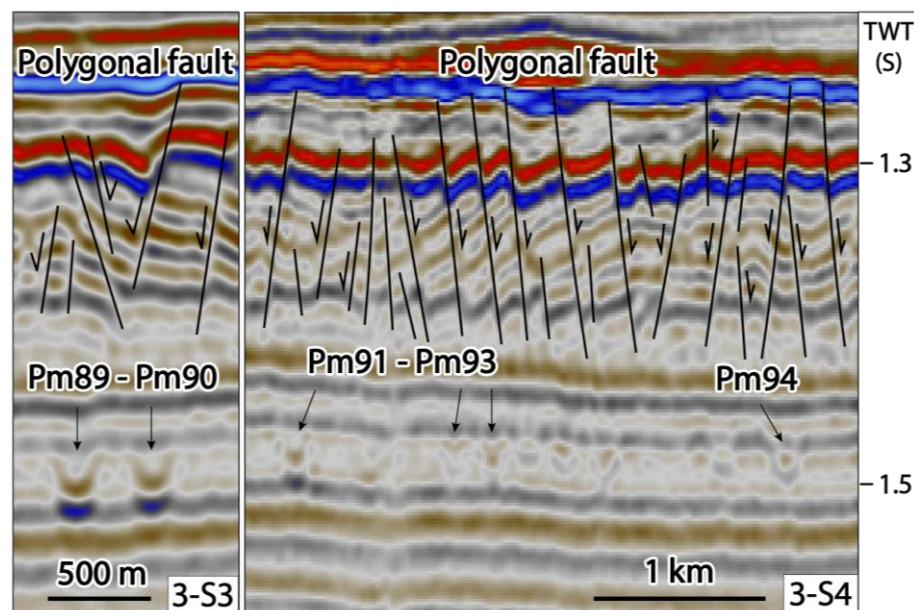


**Figure 44** Seismic sections show characteristics of paleo-pockmarks 89 to 94 (Pm89-Pm94). Paleo-pockmarks in these sections are V-shape to U-shape pockmarks. Their size ranges from 163 to 281 m (width), and 16 to 37 ms (TWT) (depth). Polygonal faults are founded on the upper portion of the seismic section.

**Table 4** The statistic information of representative paleo-pockmarks from zone 3

Name	Diameter (m)	Depth (ms) (TWT)	Shape		Section name
			Top view	Section view	
Pm82	222	20	Sub-round	U-shape	3-S1
Pm83	170	20	Sub-round	U-shape	
Pm84	173	22	Sub-round	U-shape	
Pm85	225	18	Sub-round	U-shape	3-S2
Pm86	163	19	Round	U-shape	
Pm87	170	19	Round	U-shape	
Pm88	212	22	Round	U-shape	3-S3
Pm89	194	29	Sub-round	U-shape	
Pm90	177	24	Sub-round	U-shape	
Pm91	201	24	Round	U-shape	3-S4
Pm92	163	16	Round	V-shape	
Pm93	191	21	Round	V-shape	
Pm94	281	37	Sub-round	U-shape	
<b>Average</b>	<b>195.54</b>	<b>22.38</b>			

#### 4.4 Density

Curvature dip attribute describes how much the curve deviates of edge and bottom of paleo-pockmarks from a horizontal plane. The result of this attribute clearly displays paleo-pockmark shapes on top view. The blue color (positive curvature) is identified as the edge of paleo-pockmarks, while the red color (negative curvature) is identified as the bottom of paleo-pockmarks (Figure 45f).

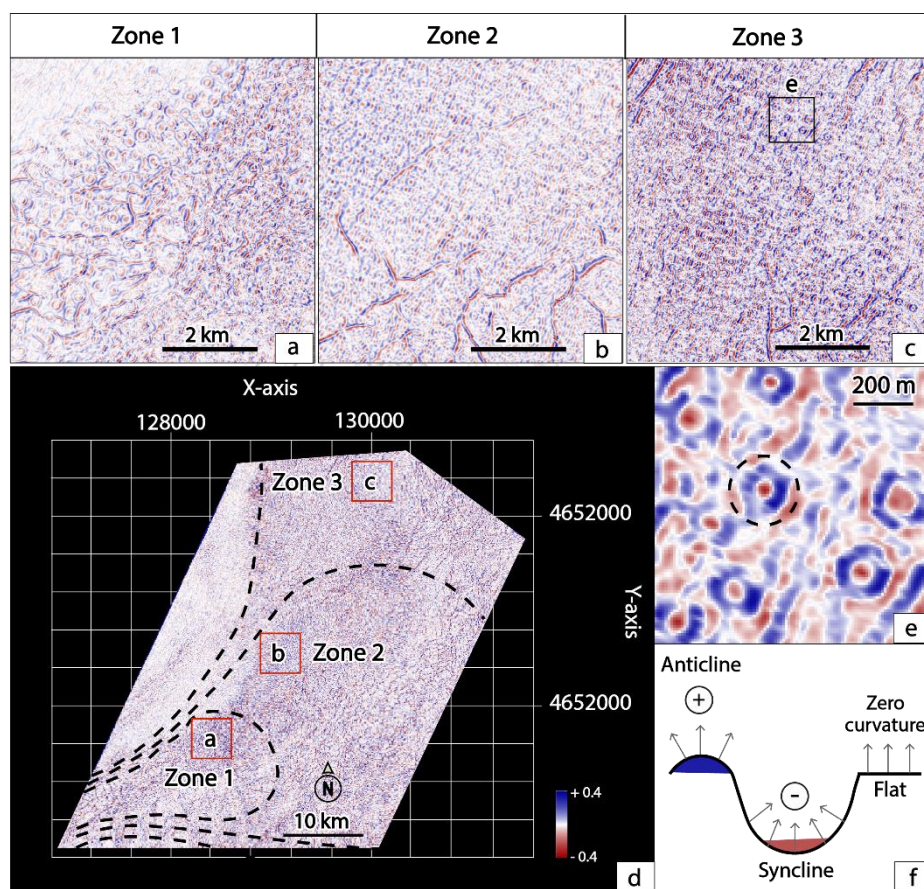


**Figure 45** Characteristics of paleo-pockmarks of three zones are described by curvature dip map, including (a) zone 1, (b) zone 2, and (c) zone 3 see the location in the red rectangle (d). Black dashed rectangles are the total area of three zones. Characteristics of paleo-pockmarks are shown in a dashed circle (blue color is pockmark edge and the red color is pockmark

The paleo-pockmark density is estimated by using the counting the number of paleo-pockmarks in 25 km<sup>2</sup>. The zones of paleo-pockmarks are chosen randomly such as zone 1, zone 2, and zone 3 see the location in (Figure 45d). First, zone 1 is in a proximal fan and covers an area of approximately 11 km<sup>2</sup>. The result of number counting in zone 1 shows 160 pockmarks in 25 km<sup>2</sup> area as shown in Figure 45a. Next, zone 2 is in middle fan covering an area around 225 km<sup>2</sup>. The result of number counting in zone 2 shows 336 pockmarks per 25 km<sup>2</sup> as shown in Figure 45b. The last zone, zone 3 is in a distal fan and cover an area around 110 km<sup>2</sup>. The result of number counting in zone 3 shows 103 pockmarks per 25 km<sup>2</sup> (Figure 45c). Thus, the aggregate of paleo-pockmark number from zone 1, zone 2, and zone 3 is more than 17,000 pockmarks.

#### **4.5 Well log analysis**

Well log analysis is used to describe a physical property of rock and study a depositional environment on a regional scale. The Great South Basin was surrounded by seven exploration wells. There are Hoiho-1, Kawau-1, Rakiura-1, Pukaki-1, Pakaha-1, Toroa-1, and Tara-1. All wells have several types of log, but this study uses only three main logs. The main well logs including gamma-ray log, resistivity log, neutron log, and density log. The results are divided into two major parts that are marker picking and well correlation.

##### **4.5.1 Marker picking**

The pattern of logs can identify rock type and depositional condition. Marker picking is the first step which we use to study log pattern and identify well top in the well log data. Pakaha-1 and Kawau-1 well were chosen to be an index well logs because two important reasons. First, Pakaha-1 well is the nearest well which located in the east of 3D seismic data, and it is used to correlate 3D seismic and well data. Pakaha-1 well does not have log data of Hoiho group because it was drilled on the high structure (horst). While Rakiura-1 has clearest log patterns from Hoiho group to Penrod group. Thus, both wells are chosen to study and describe characteristics of rock units. The result shows five major rock units as seen in Figure 46.



### **Unit A**

The gamma-ray log shows the serrated graph shift to the right side mostly (green graph). It means that lithology in this interval has a high clay mineral compound. Thus, this bed is identified as thin bed shale interbedded with very thin sandstone. Resistivity log shows low value, it means this rock is possible to have brine water. Density and neutron porosity log show high value. These logs indicate that the rock might be tight shale and sandstone. Thus, these properties indicate that this unit is possible to correlate to the Hoiho group.

### **Unit B**

Gamma-ray log in this unit has two major log patterns, including serrated graph shift to the left side (yellow graph) and serrated graph shift to the right side (green graph). These patterns indicate to a thick bed of sandstone (low clay content) interbedded with thin shale (high clay content) deposited in the upper part of the unit. This thick sandstone bed overlay on the thick bed of shale (high clay content) interbedded with thin sandstone which deposited in the lower part of the unit. Density and neutron porosity logs show two major patterns. The first pattern is high density and high neutron porosity as shown in the lower part of the unit. It can be interpreted that this rock unit is tight and high porosity. The second pattern shows a low density and high neutron porosity as shown in the upper part of the unit. It can be interpreted that this rock is sandstone with high porosity. Thus, these properties indicated that this unit is possible to correlate to the Pakaha group. This unit is possible to be one of good reservoir and seal in this basin.

### **Unit C**

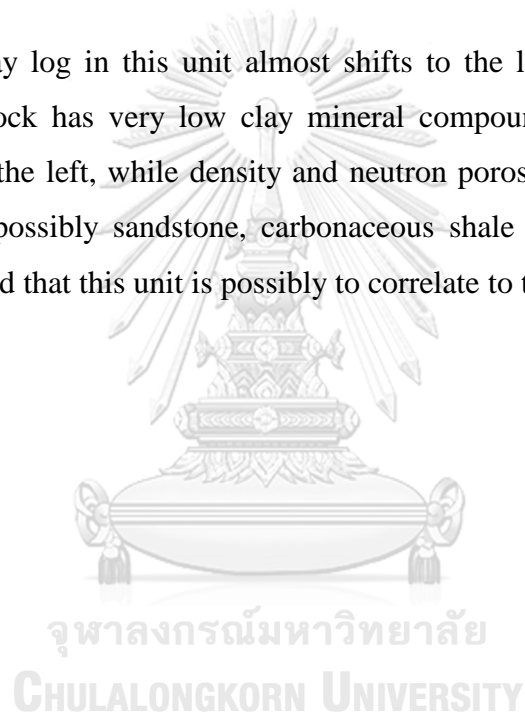
This unit shows serrated gamma-ray log shift to the left side (yellow graph). It means this rock is sandstone (low clay content) interbedded with thin shale (high clay content). Resistivity and density logs show low value. Its mean this rock possible to have brine water filled. Neutron porosity log is absent. Thus, these properties indicated that this unit is possible to correlate to the Laing formation.

**Unit D**

Gamma-ray log in this unit shift to the left side mostly (yellow graph). They show serrated graph pattern in the lower part and decrease to the upper part. It means this rock has a low clay mineral compound. Resistivity and density show low value or shift to the left, while neutron porosity log is absent. Its mean that this rock is possibly carbonaceous shale. Thus, these properties indicated that this unit is possible to correlate to the Tucker Cove formation.

**Unit E**

Gamma-ray log in this unit almost shifts to the left side (yellow graph). It means that this rock has very low clay mineral compound. Resistivity shows low value or shifts to the left, while density and neutron porosity log is absent. Its mean that this rock is possibly sandstone, carbonaceous shale or limestone. Thus, these properties indicated that this unit is possibly to correlate to the Penrod formation.



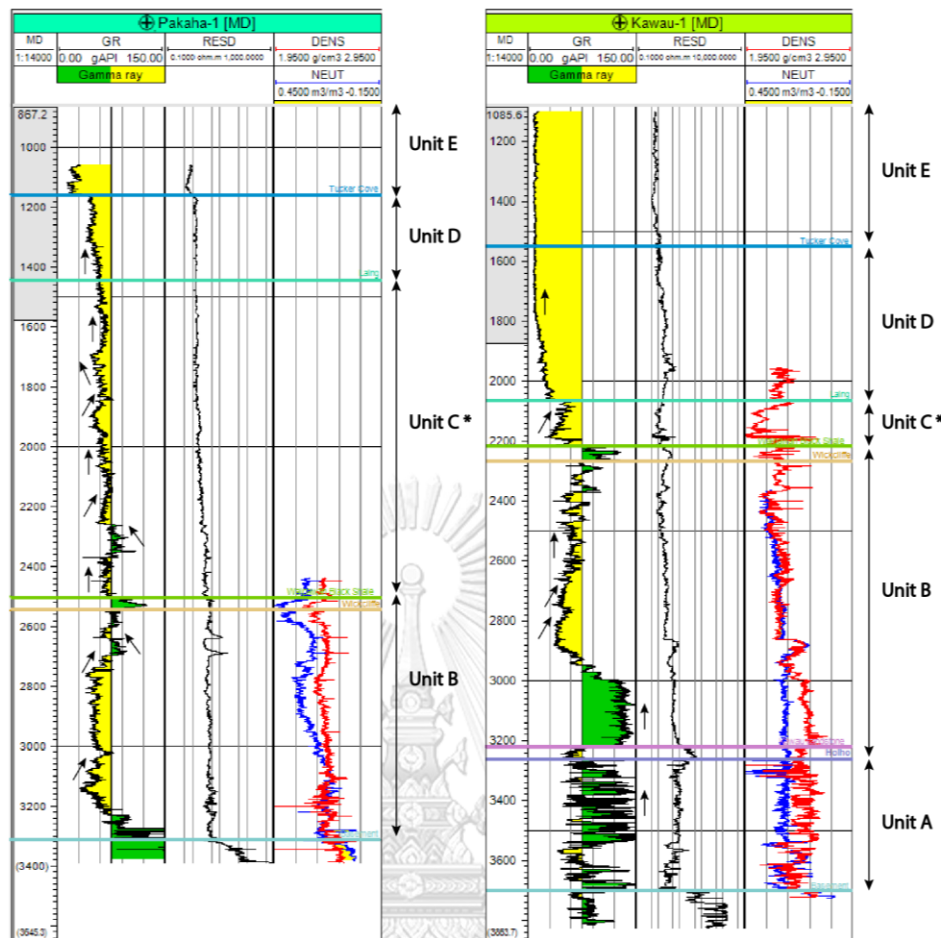


**Figure 46** Log patterns and marker picking of Pakaha-1 and Kawau-1 well. Paleo-pockmarks are founded on the surface of unit C (Laing formation). While unit B founded hydrocarbon in the Waipawan Black Shale (upper part of unit B).

#### 4.5.2 Well correlation and Depositional environment

Well correlation is used as the next step after marker picking. There are include three well data which located around the southern part and central part near the Great South Basin. The section of well correlation started with Pakaha-1 well located in the central part, following by Kawau-1 and Hoiho-1 well located in the southern part. This well correlation is used to interpret regional stratigraphy in the southern part or the proximal fan proportion. Moreover, characteristics of gamma-ray log is the main data which used to define the depositional environment of the sedimentary sequences. Based on log pattern of Kawau-1 well, the depositional



environment in the Great South Basin is divided within three main stages as shown in Figure 47.

The first stage, the gamma-ray log of Kawau-1 and Hoiho-1 well show the serrated pattern of shale aggradation interbedded with thin sandstone and coal. These rocks indicate to fluvial floodplain of non-marine Hoiho group (unit A) following by thin bed of sandstone of Kawau sandstone. In contrast, Hoiho and Kawau sandstone sequences are absented in the structure high (horst) of Pakaha-1 well data. The next stage, marine began to rise in the basin and sea level increase constantly. In the lower part of gamma-ray logs show the serrated pattern of shale aggradation. It indicates to the marine environment. While the upper part shows gamma ray with bell shape. This characteristic indicates to finning upward sequences of transgressive, tidal channel, and fluvial-deltaic channel. These sequences are indicated as Pakaha group (unit B). Following by deep marine stage of Rakiura group (unit C and unit D). Gamma-ray logs show different patterns, including serrated, symmetric, and bell pattern in Pakaha-1 well. While Kawau-1 and Hoiho-1 well show bell shape. It indicates that distal deep marine slope deposit in the central part of the basin (near Pakaha-1 well) following by progradation of clastic sediment and transgressive. While the southern part dominates by transgressive sand (near Kawau-1 and Hoiho-1 well). The final stage, gamma-ray logs of three well have a similar log pattern that gamma-ray logs show the cylindrical shape (low gamma-ray). This pattern indicates to channel fill around in the basin.

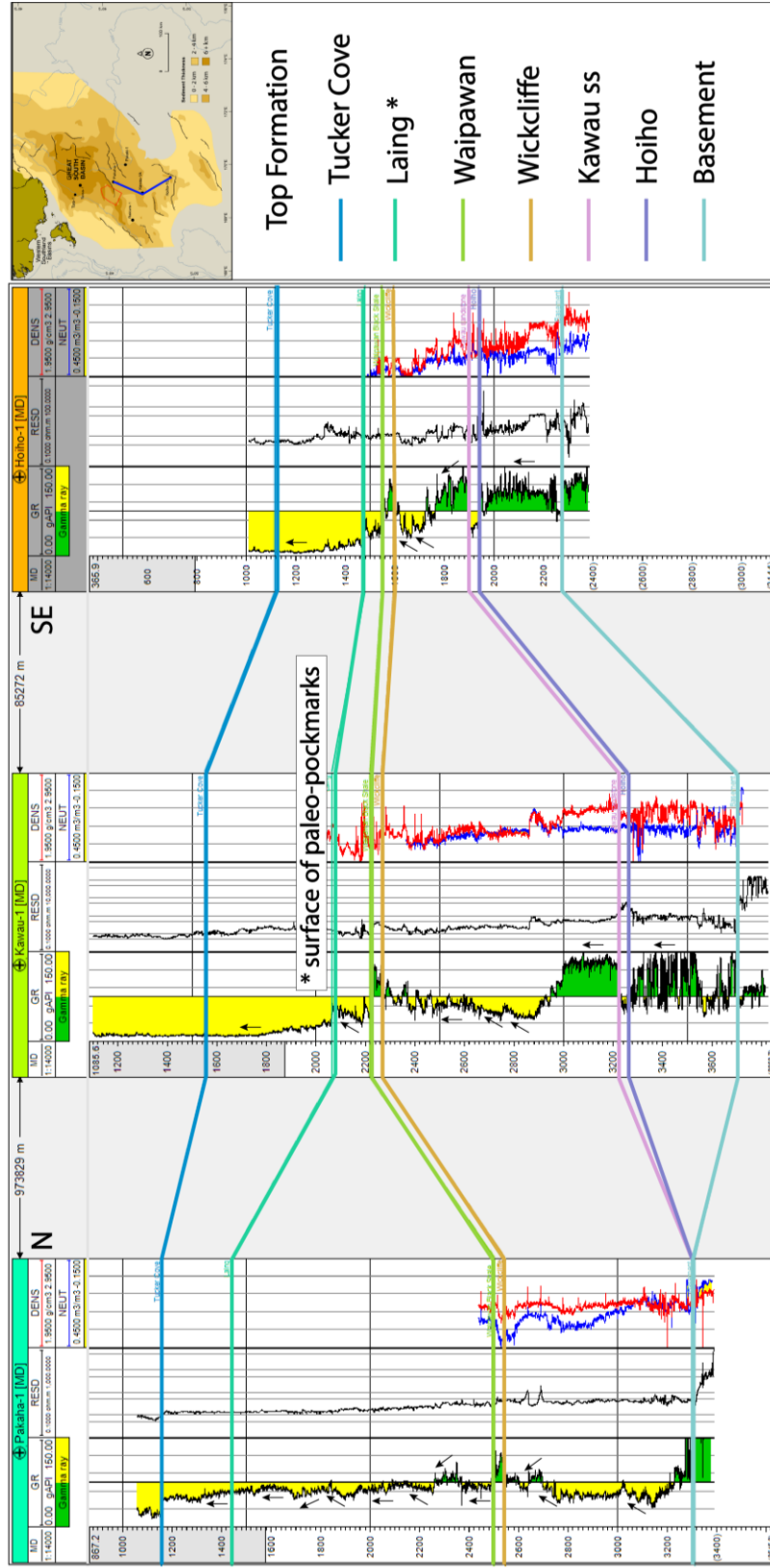


**Figure 47** Well correlation of 3 wells in the Great South Basin show the pattern of log pattern and regional correlation. Paleo-pockmarks are founded on the surface of Laing formation (middle Eocene time).

## CHAPTER 5

### DISCUSSIONS

From chapter 4, characteristics of paleo-pockmarks are the main key to discuss in this chapter. The major topics of discussion include pockmark classification, the possible fluid source, migration pathway, and petroleum application. All topics in this chapter are supported and compared with previous studies. For example, tectonic setting and stratigraphy in the Great South Basin, characteristics of pockmarks around the world, and other researches related to the main topics.

#### 5.1 Paleo-pockmark classification

##### 5.1.1 Type of the paleo-pockmarks

In 2002, Hovland et al. suggested the classification of common pockmarks which occur in seas, oceans, and some lakes worldwide by using the geometrical shapes of pockmarks (shape, size, and composite pattern). The types of pockmarks were identified within six major classes, for instance, unit pockmarks, normal pockmarks, elongated pockmarks, eyed pockmarks, a string of pockmarks, and complex pockmarks as described in chapter 1. Furthermore, Chen et al. (2015) used the same criteria to identify various types of pockmarks in the northern Zhongjiannan Basin, South China Sea. The numerous pockmarks in the northern Zhongjiannan Basin were divided within three major groups, for instance, 1) group one is identified from shape on top view, which are circular pockmarks, elliptical pockmarks, elongated pockmarks, crescent pockmarks, comet pockmarks, and irregular pockmarks; 2) group two is identified from size, which are small pockmarks, normal pockmarks, giant pockmarks, and mega-pockmarks; 3) group three is identified from composite pattern, which is composite pockmarks, pockmark strings, and pockmark group as shown in chapter 2. Thus, this study uses the geometrical shapes of pockmarks to classify paleo-pockmarks in the study area.

The paleo-pockmark characteristics in the study area show similar shapes, but it shows different sizes as shown in chapter 4. Three zones of paleo-pockmarks are chosen by the random selection. The ninety-four paleo-pockmarks are chosen randomly to show their shapes and their sizes both on the top view and section view.

All zones (zone 1, zone 2, and zone 3) show the same characters that are round to sub-round in shapes on the top view, with V-shape and U-shape in the seismic sections. In addition, the sizes of paleo-pockmarks in the study area seem to have diverse sizes in each zone. The size of paleo-pockmark in each zone is shown in Table 2, Table 3, and Table 4 in chapter 4. The average size in zone 1 is around 340 meters (204 to 481 m) in wide, and 24 ms (15 to 45 ms) (TWT) in depth. While in the zone 2 paleo-pockmarks are 226 meters (131 to 350 m) in wide, and 26 ms (15 to 45 ms) (TWT) in depth. The average size in zone 3 is 195 meters (163 to 281 m) in wide and 22 ms (16 to 37 ms) (TWT) in depth. The paleo-pockmarks in zone 1 seem to have the larger size than the other zones. Thus, this study will be focused on the characteristics of pockmarks which have round (circular) to sub-round shapes on the top view. From the previous studies (e.g.)(Chen et al., 2015; Hovland et al., 2002), they suggested three types of pockmarks having round or sub-round in shape on the top view similar to this area. So, the pockmarks in the study area could be classified as a unit pockmark, normal pockmarks, and eyed pockmarks based on Hovland et al. (2002). Although these pockmarks have a similar shape, they have different mechanism of formation. Thus, the next paragraphs intend to discuss the pockmark type related to mechanism of paleo-pockmark formation in this area.

### **A unit pockmarks**

A unit pockmark is round shape pockmarks with size less than 5 meters (Hovland et al., 2010). The size of unit pockmark is smaller than normal pockmarks and eyed pockmarks (Hovland et al., 2002; Hovland et al., 2010). Furthermore, the size of a unit pockmark is also smaller than the paleo-pockmarks in the study area. This type of pockmarks could be founded as an isolated feature or associated with large pockmarks. For example, a group of unit pockmark associated with elongated pockmarks in the southeastern flank of Emerald Basin (Josenhans et al., 1978), the unit pockmarks and normal pockmarks in the Norwegian Trough (Hovland et al., 2010). However, the ancient unit pockmarks are not clearly found in the 3D seismic data at the Great South Basin, but they may be founded by using another high-resolution data. Thus, it is impossible that paleo-pockmarks in the study area will be

classified as the unit pockmarks because the size of paleo-pockmarks is larger than to be unit pockmarks.

### **Eyed pockmarks**

In the early period, eyed pockmarks were categorized as a small pockmark because they had a size ranging from 3 to 5 meters in width (Judd and Hovland, 2009). This type of pockmarks shows oval to circular in shapes like a unit pockmark and normal pockmarks. Judd and Hovland (2009) founded that this pockmark includes a patch of high reflection in the central pockmark. They suggested that the possible materials which deposited in the center of this pockmark are coarse sediments, dead and living shells, and carbonate precipitation (Hovland et al., 2002; Hovland et al., 2010). However, the paleo-pockmarks in the study area show clearly V-shape to U-shape in the seismic section without any material deposited in the central portion. Thus, the paleo-pockmarks in the study area cannot be classified as the eyed pockmarks.

### **Normal pockmarks**

Normal pockmarks are the common pockmarks which are founded in various geological setting (Hovland et al., 2002). The shape of this pockmarks shows round to sub-round in shape on top view in generally with conical shape (V-shape to U-shape) in seismic section (Andresen, 2012; Chenrai and Huuse, 2017; Hovland et al., 2002; King and MacLEAN, 1970; Pilcher and Argent, 2007). In the early period, Hovland et al. (2002) defined the size of normal pockmarks could be ranging from 10 to 700 meters in wide, and deep from 1 to 45 meters. After that, Pilcher and Argent (2007) founded the large circular depression which has size more than contemporary pockmarks on the West African continental margin. Then, normal pockmarks were divided within three types based on their size, that is 1) “normal pockmarks” have size ranging from 10 to 250 meters (Pilcher and Argent, 2007); 2) “giant pockmarks” have size ranging from 250 to hundreds of meters (Pilcher and Argent, 2007); 3) “Mega-pockmarks” have size ranging from one to few kilometers (Chen et al., 2015; Sun et al., 2011) as shown in (Figure 48).

The comparison between typical normal pockmarks and paleo-pockmarks in the study area show the similarity both shapes and sizes. That is round to sub-round in shape on the top view and conical shape in seismic section. The ninety-four paleo-pockmarks in the study area show the size ranging from 131 to 481 meters in diameters and 15 to 45 ms (TWT) in depth. The average measurement of paleo-pockmarks in the study area is 244 meters in width and 24 ms (TWT) in depth. The size (diameter and depth) of paleo-pockmarks in the study area is plotted in the graph (Figure 48). The result shows the size of paleo-pockmarks is located in the common trend (compared with 57 publishes) and covers more than two orders of magnitude (normal pockmarks and giant pockmarks). Thus, the paleo-pockmarks in the study area are possible to be normal pockmarks and giant pockmarks base on their shape and their size. The differentiation of three types of pockmarks is compared and concluded in Table 5.

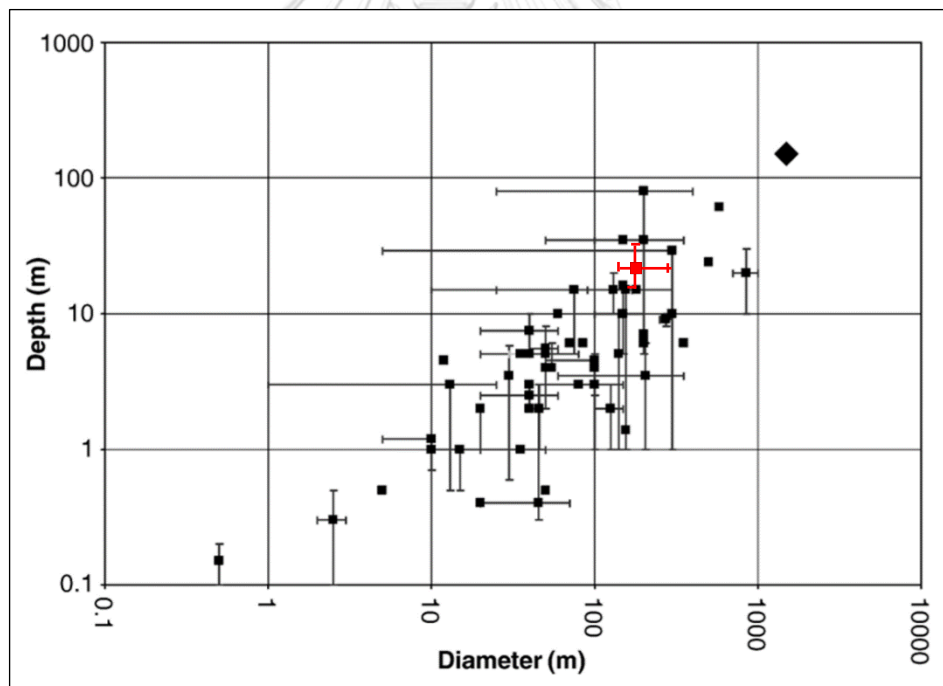


**Figure 48** Graph illustrates the order of dimension of pockmarks from 57 published. Single points are pockmark measurement or average measurement. Error bars show the range of size from each field. Red point and red error bars show the boundary of size ranging of the paleo-pockmarks in the study area. modified from (Pilcher and Argent, 2007)

**Table 5 The characteristic comparison of three type pockmarks**

<b>Pockmark type</b>	<b>Size</b>	<b>Shape</b>	<b>Specific feature</b>
Unit pockmarks	Small	Round to Sub-round	Homogeneous sediment inside
Eyed pockmarks	N/A	Round to Sub-round	Lithology different at the center
Normal pockmarks	Large	Round to Sub-round	Homogeneous sediment inside

### **5.1.2 Density of the paleo-pockmarks and their location**

The absolute abundance of pockmarks is predicted by several methods, such as quantitative estimate (King and MacLEAN, 1970), statistical analysis (Mazzini et al., 2017; Tasianas et al., 2018). This part is attempted to find the comparative density of paleo-pockmark in the study area (low or high density). The densities of pockmarks were suggested at different values from previous studies. For example, Pilcher and Argent (2007) founded random pockmarks distributed in their study area with approximately 0.15 and 1.4 pockmarks per a square kilometer. This value seems to be low-density pockmarks. On the other hand, King and MacLean (1970) defined high-density pockmarks which is 45 to 200 pockmarks in a square kilometer. In 2009, Webb et al. (2009) suggested high-density pockmarks occur in the inner Oslofjord, Norway. The pockmarks from their study have a high density of 500 pockmarks per 179 square kilometers (2.79 pockmarks / km<sup>2</sup>). While Mazzini et al. (2017) founded numerous pockmarks occur in extensive area with 10 to 20 pockmarks per a square kilometer. Moreover, Tasianas et al. (2018) founded high-density pockmarks occur approximately 700 pockmarks per a square kilometer. Thus, this study uses the comparison between paleo-pockmark in the study area and other studies around the world to support the results.

The density of the paleo-pockmarks in the study area is predicted by using quantitative estimate or number counting in five square kilometers areas. The reason to use five square kilometers area is to avoid the data biases. The results consist of three selected areas from zone 1 (proximal fan), zone 2 (middle fan), and zone 3



(distal fan). The paleo-pockmark density in zone 1 displays approximately 160 pockmarks per twenty-five square kilometers ( $6.4$  pockmarks /  $\text{km}^2$ ). While zone 2 displays 336 pockmarks per twenty-five square kilometers ( $13.44$  pockmarks /  $\text{km}^2$ ), and zone 3 shows 103 pockmarks per five square kilometers ( $4.12$  pockmarks /  $\text{km}^2$ ). The paleo-pockmark density in the study area is compared with previous studies. The result found that the density rate of the paleo-pockmarks is classified as a high-density pockmark area. The density rate shows approximately 5 to 70 pockmarks per a square kilometer based on density rate of the previous study (King and MacLEAN, 1970; Mazzini et al., 2017). Moreover, the paleo-pockmark density in zone B seems to be the highest density zone than zone 1 and zone 3. While zone 3 is the lowest density than zone 1 and zone 2 (Figure 49).

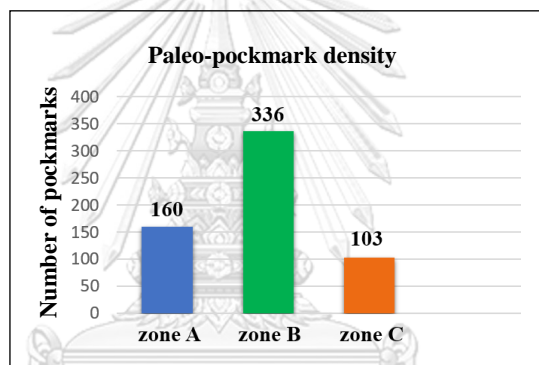


**Figure 49** The bar graph shows the comparison of paleo-pockmark density in five square kilometers areas ( $\text{pm} / 25 \text{ km}^2$ ) from zone 1, zone 2, and zone 3. It should be noted that zone B seems to be the highest density, while zone C has the lowest density than the other zones.

Regarding to distributed location, paleo-pockmarks manifest on the surface of Laing formation (Rakiura group) in middle Eocene time. Laing formation shows characteristics of low-angle clinoform facies indicating delta environment deposited from slope to basin (from southwest to northeast direction). In 2010, ExxonMobil (2010) reported characteristics of sediments in Laing formation which are divided into two facies. There are shelf facies and basinal facies. The shelf facies include sandstone and siltstone interbedded with thin shale and claystone layer which located in the lower part of Laing formation. While basinal facies include mostly claystone,

shale, and limestone which located in the upper part of Laing formation where paleo-pockmark occurred. Seismic characteristics of fine-grained sediment of Laing formation show characteristics of onlap feature overlain on progradational clino-form (Figure 50). Thus, it means fine-grained sediment in the upper part of Laing formation are transported from the marine environment. The characteristics of both facies relate with the seismic profile in chapter 4. The evidence of the progradational pattern of clastic sediment in the lower part of Laing formation as shown in Figure 24. Progradational pattern locates beneath the paleo-pockmarks area of zone 1 (proximal fan) and zone 2 (middle fan). Furthermore, paleo-pockmark sizes in zone 1 has the largest size than zone 2 and zone 3, while zone 2 has the smallest size than other zones. It is possible that the size and density of paleo-pockmarks both zone 1 and zone 2 are controlled by lithology or fluid pathway. From the result, it can be concluded that these paleo-pockmarks related to their distribution (fan shape like pattern) and their characteristics (shape, size, and density).

The differentiation of density and size of paleo-pockmarks in each zone is described by using the Turbidite Facies Model (Bouma Sequence) of a submarine fan. Shanmugam (2016) concluded that sediment in sub-marine fan includes five divisions, including Ta, Tb, Tc, Td, and Te, respectively. Coarse-grained sediment (Ta) deposits at the proximal fan and grade to fine-grained sediment (Te) at the distal fan (Figure 51). Paleo-pockmarks at the proximal fan (zone 1) has a size larger than the middle (zone 2) and distal fan (zone 3). The reason is fluid will be migrated through coarse-grained sediment better than fine-grained sediment and generate large size pockmarks in the area. While paleo-pockmarks at the middle fan (zone 2) has a higher density than the other zones because fine-grained sediment has high porosity and it is possible to accumulate fluid in the sedimentary layer more than coarse-grained sediment.

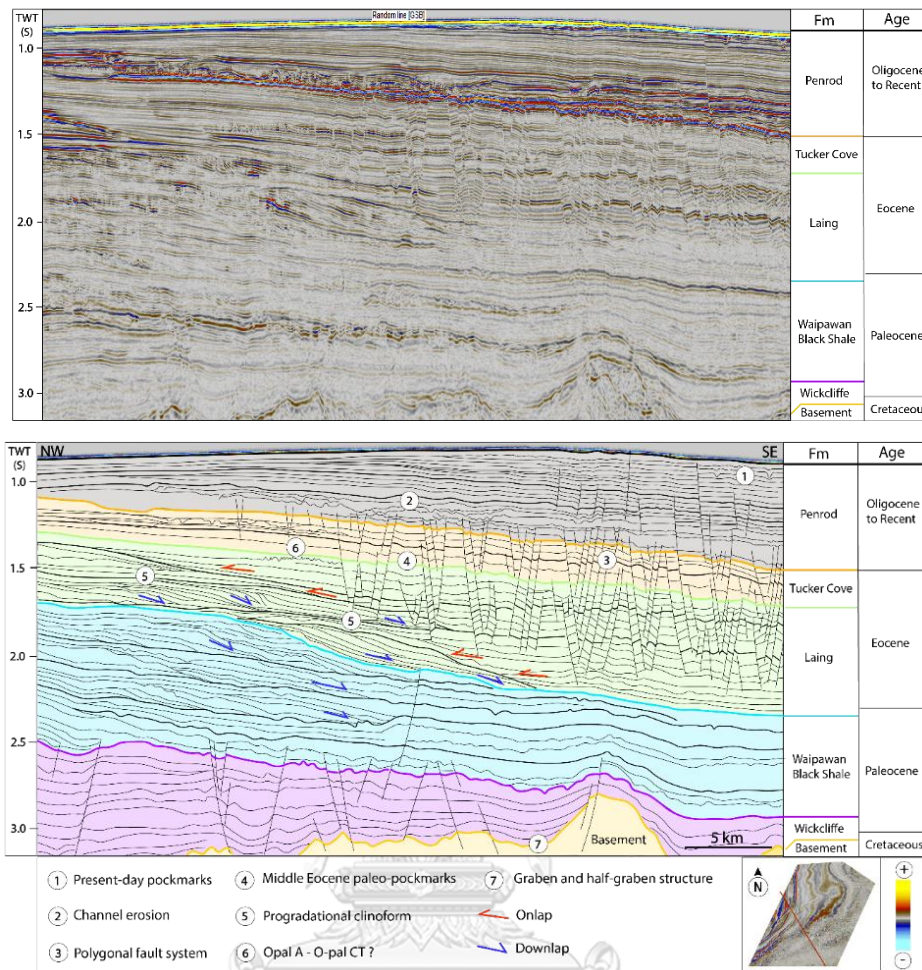


**Figure 50** Seismic sections show termination patterns of sedimentary layers in the Great South Basin. The upper part of Waipawan Black Shale (blue layer) shows downlap pattern (blue arrows) from NW to SE direction. Laing formation (green layer) shows onlap pattern (red arrow) on Waipawan Black Shale formation. While Tucker Cove formation (yellow layer) and Penrod Group (grey layer) show parallel pattern overlay on Laing formation.

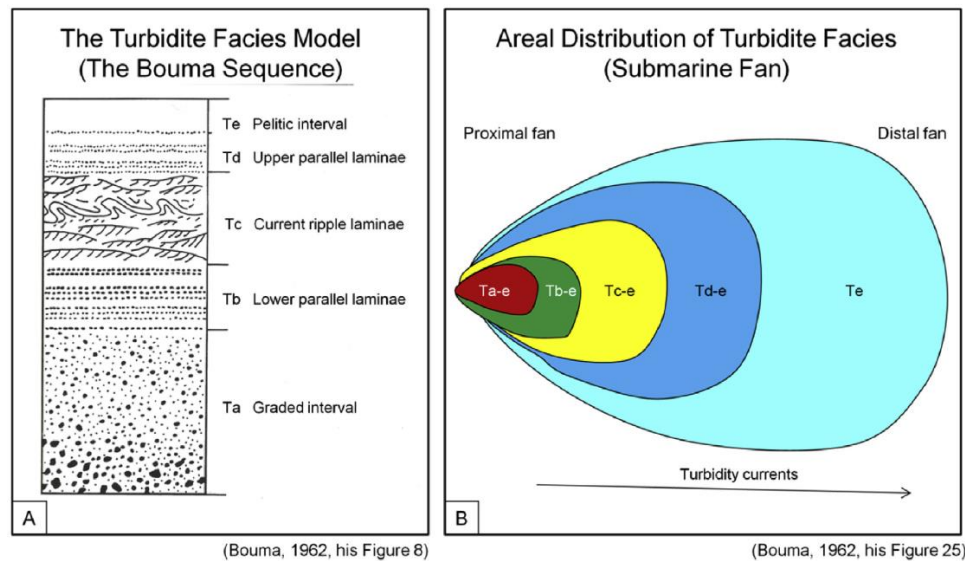


**Figure 51** Turbidite facies model (Bouma Sequence) shows characteristics of sediment in a sub-marine fan. This sediment sequences relate with size and density of paleo-pockmarks in the study area (Shanmugam, 1997).

## 5.2 The possible fluid sources

In this part, the possible fluid types which can create paleo-pockmarks in the study area is discussed. Four types of fluid include pore water, hydrothermal fluid, thermogenic methane, and biogenic methane are chosen for discussion about the possible fluid sources of paleo-pockmarks in the study area. These fluid types are founded commonly and related to the fluid flow process in the offshore area worldwide. Discussion of the possible fluid source of paleo-pockmarks is described in detail below.

### 5.2.1 Pore water

Pore water is water that is trapped between sediment grain when fine-grained sediment deposited (Judd and Hovland, 2009). It is possible to migrate through fractures, burrows, or pore spaces between sediment grains when the sedimentary layer is compressed by external factors (Hammond, 2001). Pore water is one of the important fluid sources of pockmark generation. For example, porewater is the main fluid source of pockmarks (Chenrai and Huuse, 2017; Harrington, 1985; King and MacLEAN, 1970). However, compaction of sedimentary formation could not be the

main trigger for pore water accumulation, but they are occur associated with another condition. For instant, earthquake (Hovland et al., 2002), sea level change (Luo et al., 2015), and rapid sediment loading (Chenrai and Huuse, 2017).

Two main keys are used to consider the suitability of pore water to be the fluid source of paleo-pockmarks in the study area. First, it should have the formation of pore water in the study area. Most pore water accumulates with the fine-grained sediments such as clay and silt (Harrington, 1985). Based on Pakaha-1 and Rakiura-1 wells indicate that paleo-pockmarks in the study area occurs on the surface of Laing formation (unit C) and overlay on Wickliffe formation which were dominated by shale and claystone. If these layers are saturated with water, pore water is possible to be one of the fluid sources of paleo-pockmarks in the study area. However, seismic characteristics of fluid flow features (e.g. fractures, burrows), and their mechanism are not observed on the 3D seismic data. Seismic sections (Figure 23 and 24) show an increase of layer of fine-grained sediment from proximal to the distal fan (Southwest to Northeast direction). While the size and density of paleo-pockmarks are varied, zone A has the largest size and zone B has the highest density. Thus, porewater is possible to be one of the fluid sources of paleo-pockmarks in the study area.

### **5.2.2 Hydrothermal fluid**

A hydrothermal system is one of the important processes for studying fluid plumping system and ore-deposit (Hovland et al., 2005; Judd and Hovland, 2009). Hydrothermal activity is a process of heated subsurface water circulation (Colín-García et al., 2016). Subsurface water is heated near magma and volcanic rock (batholiths, sills, and dykes) with temperature up to 1200°C (Judd and Hovland, 2009). Hydrothermal activity occurs both oceanic and continental crust, including mid-oceanic ridges, back-arc basins, and on submarine volcanic arcs (Hovland et al., 2005; Norton, 1984). Hydrothermal venting is one of the main processes which could form pockmarks on the seabed (Judd and Hovland, 2009). Seismic characteristics of volcanic activities are not founded in the Great South Basin. It means there is no heat source of hydrothermal activity in the study area. The standard temperature in the sedimentary formation could not be a heat source for hydrothermal fluid. Thus,

hydrothermal fluid is not reasonable to be the fluid source of paleo-pockmarks in the study area.

### **5.2.3 Biogenic Methane**

Methane is one of the important origins of fluid flow feature worldwide. Methane is divided into two major types, there are biogenic methane and abiogenic methane. Biogenic methane is derived from organic matter, while abiogenic methane derived from another process that are not related with organic matter (e.g. hydrothermal system) (Schoell, 1988). Biogenic methane is reported as one of the main fluid origins for fluid expulsion (Nakajima et al., 2014; Nickel et al., 2012). They are generated by several processes and divided within two major types. Including thermogenic methane and bacterial or microbial methane (Schoell, 1988).

ExxonMobil (2010) founded trace gas in Pakaha-1 well. Also New Zealand Petroleum and Minerals (2014) reported trace oil and gas in other exploration wells in the later time. Trace oil and gas are founded in two exploration wells including Tara-1 and Taroa-1 wells. Source rocks of the Great South Basin include 1) late Cretaceous fluvial and marine coaly sediments (Hoiho Group), and 2) late Cretaceous to Eocene marine mudstones and shales (Wickliffe, Waipawan Black Shale, and Taratu Formations) (NZP&M, 2015) in Figure 52. It means organic matter in source rock is possible to be the source of biogenic methane in the study area. Thus, biogenic methane is chosen to discuss in term of the possible fluid source for paleo-pockmarks in the study area. Definition and properties of both methane are discussed in detail below.

#### **a) Thermogenic methane**

Thermogenic methane is generated by thermal cracking of kerogens. They are produced during late catagenesis to early metagenesis (zone of oil and gas generation) with high-temperature (157° to 221°C) (Stolper et al., 2014) as presented in Figure 53. Thermal maturity of hydrocarbon is calculated by using geothermal gradient (39°C/km) and seabed temperature (5°C) of the Great South Basin. Initially, two formations of source rock are focused that is late Cretaceous coal formation of Hoiho group and late Paleocene shale of Waipawan Black Shale. The reason for choosing



these group or formation is they are found in Pakaha-1 well and Pukaki-1 well see in Figure 13 (Chapter 2), which are the nearest well from 3D seismic data. Hoiho group deposits in the lower portion at around 3.0 to 3.2 km (data from Pukaki-1 well) with temperature around 132 to 142°C. While Waipawan Black Shale deposits at around 2.50 to 2.54 km (data from Pakaha-1 well) with temperature around 110 to 112°C. These data could conclude that thermogenic gas could not be generated with low temperature. Furthermore, there are no seismic characteristics of the fluid pathway (e.g. fault) for middle Eocene paleo-pockmarks. If thermogenic gas is the main fluid source in the study area. They need to migrate through the fluid pathway (e.g. fault) and generate pockmarks above it similar to the study of Pilcher and Argent (2007).

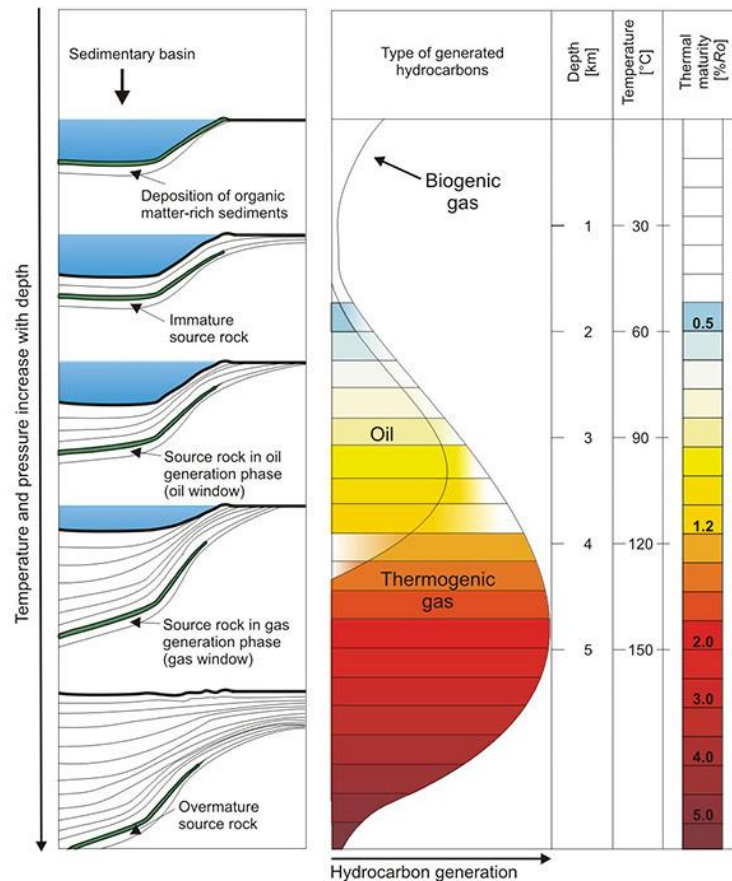


**Figure 52** Schematic model of hydrocarbon maturation shows stage of biogenic gas and thermogenic gas, which occur in different temperature and pressure (Bjørlykke, 1989).

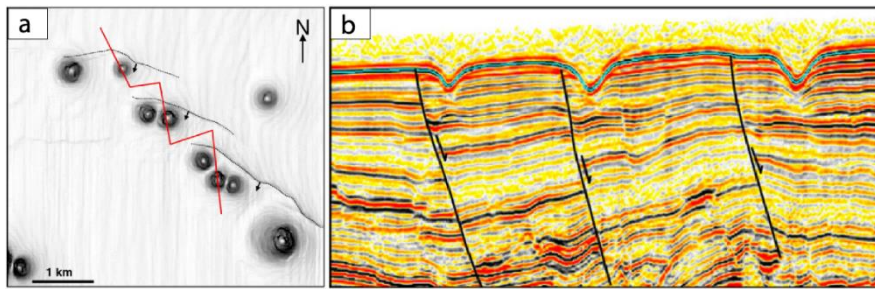


**Figure 53** Example of pockmarks migrated through normal fault and generate pockmarks on the hanging wall (Pilcher and Argent, 2007).

### b) Bacterial or Microbial methane

Bacterial or microbial methane is generated by bacterial activity which deposits in regional scale (Schoell, 1988; Welhan, 1988). They will be generated during early diagenesis stage (zone of biogenic gas generation) with low-temperature (less than 60°C) (Stolper et al., 2014) as present in Figure 53. Microbial methane is derived from two processes, including carbon dioxide reduction (CO<sub>2</sub> reduction) and fermentation (Schoell, 1988). CO<sub>2</sub> reduction occurs in the low sediment temperature, while fermentation occurs in warmer sediment temperature. Microbial methane is possible to occur by mixing process between CO<sub>2</sub> reduction and fermentation. Characteristics of paleo-pockmarks in the study area show high density and wide distribution. Mostly high-density pockmarks are created by a large amount of liquid and gaseous hydrocarbons in the potential petroleum area (Anka et al., 2012). As a result, the maximum temperature of Waipawan Black Shale (35°C) as shown in part a) is possible to produce microbial methane which has a wide distribution in the study area.

### 5.3 Migration pathway

Migration pathway of pockmarks is founded in various types worldwide. For example, Gay et al. (2004) suggested that the first-order polygonal fault is possible a migration pathway of fluid generated pockmarks on the surface. Gay et al. (2006) founded linear pockmarks manifest on the length of the buried channel. This channel acts as a fluid migration pathway and generates linear pockmarks above it. Pilcher and Argent (2007) founded pockmarks occur on the hanging along fault strike. These faults create the conduit for fluid escaping from the fluid source and generate

pockmarks at the seafloor. In this part the possible migration pathway of the paleo-pockmarks in the study area, is discussed and focus on two seismic features in the area including 1) polygonal fault system and major faults, and 2) progradational clinoform.

### **5.3.1 Polygonal fault system**

In the Great South Basin, there are no relationship between pockmarks and polygonal fault in the area. Seismic sections in chapter 4 show paleo-pockmarks layer are cut by polygonal faults around 1.5 s (TWT) as shown in zone 1 and some part in zone 2 (Figure 48, 30, and 34). In addition, paleo-pockmarks in zone 3 are found beneath the polygonal fault system (Figure 42 and 43). This result supports that polygonal faults in the area are not the migration pathway of the paleo-pockmarks. In contrast, polygonal fault system is used as an indicator to confirm diagenesis process of the fine-grained sediment formation in the study area.

### **5.3.2 Progradational clinoform**

The progradational pattern of clastic sediment may act as a reservoir rock in the area similar to the buried channel (Gay et al., 2006). This clinoforms are covered by fine-grained marine sediments of Laing Formation in middle Eocene time. This sediment deposits on the slope to shelf area and act as a seal membrane. The seismic section in chapter 4 (Figure 24) shows thickness increase from proximal fan to distal fan (southwest to northeast direction). It means the thickness of the seal has a relationship with the size and density of paleo-pockmark in the area. Paleo-pockmarks in zone 1 has a larger size than the other zone. While paleo-pockmarks in zone 2 has a higher density than the other zone. Seismic characteristics of migration pathway (gas chimney, pipe, or conduit) of middle Eocene paleo-pockmarks are not founded in the seismic data. It is possible that the fluid (methane gas) possible to migrate through the sedimentary layer and create pockmarks on the surface of Laing Formation.

## **5.4 Other external factors**

### **5.4.1 Sea-level change**

Paleocene-Eocene Thermal Maximum (PETM) is the important effect of climatic warming and sea-level change worldwide. This event effect to increase of temperature more than 5°C and ice-melting (Sluijs et al., 2006). Uruski (2017)

suggested comparison graph between global sea-level curve and local sea-level curve in the Great South Basin, New Zealand (Figure 55). This graph shows a decrease of global sea-level in the long-term period from Paleocene to Eocene time, while the local sea-level curve shows sea-level drop for short-term around middle Eocene. The decrease of sea-level around middle Eocene is possible to be the important trigger of decreasing of hydrostatic pressure in the Great South Basin. When hydrostatic pressure drops, the pressure of the fluid under the seal layer will migrate and expulse to the seabed. Thus, the decrease of sea-level is possible to be the trigger of paleo-pockmark expulsion in the study area.

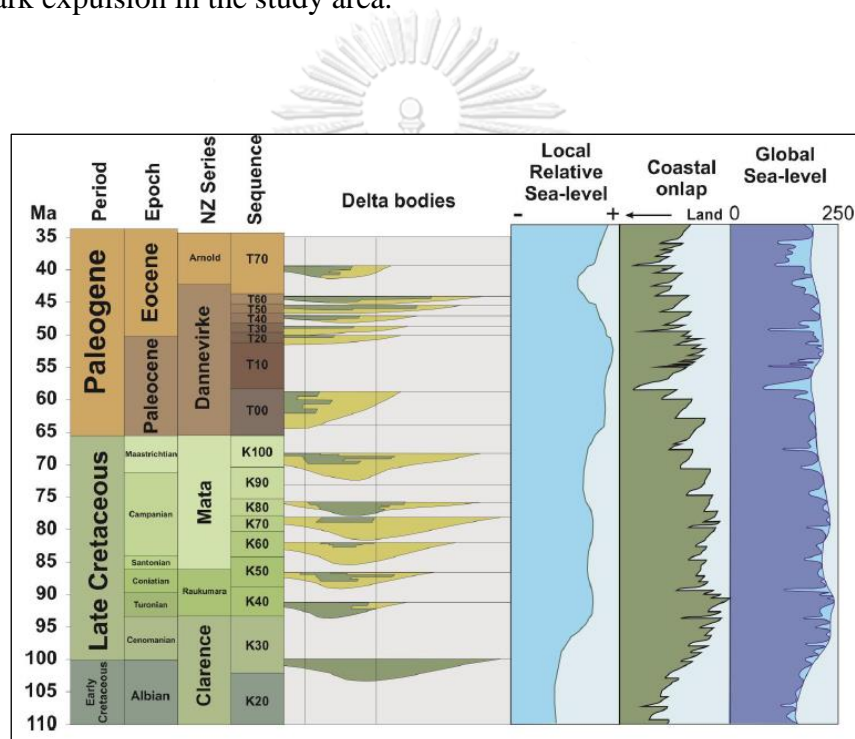


**Figure 54** The comparison between global sea-level curve and local sea-level curve in the Great South Basin shows sea-level drop for short-term around middle Eocene (Uruski, 2017).

### 5.5 Mechanism of middle Eocene Paleo-pockmarks

The main possible fluid origin of middle Eocene paleo-pockmarks is microbial methane in the sedimentary formation. Microbial methane is produced in low temperature ( $< 60\text{ }^{\circ}\text{C}$ ) condition near the middle Eocene seafloor (less than 1 km). Temperature in the sedimentary formation increases from the seabed to the deeper

part depend on local geothermal gradient ( $\sim 40$  °C/km) and seafloor temperature ( $\sim 6$  °C) during middle Eocene time. Mechanism of middle Eocene paleo-pockmarks are divided into four stages from early middle Eocene time to recent (Figure 55).

**a) Early middle Eocene**

Fine-grained sediment and organic matter deposited on the seabed in the early stage. Then, bacteria accumulated and decomposed organic matter in the sedimentary layer. Bacterial activities produce microbial methane by carbon dioxide reduction and fermentation in the anoxic condition.

**b) Basin floor fan develop**

Coarse-grained and fine-grained sediment began deposited in the slope area and created basin floor fan along the southwest to northeast direction. Coarse-grained sediment is transported and deposited when the energy drops at the proximal fan, and fine-grained sediment are migrated to the distal fan.

**c) Middle Eocene seabed**

Basinal facies of Laing formation deposited overlain on basin floor fan. Thick bed of fine-grained marine sediment created overburden pressure in the basin. The overburden pressure lead to expel of microbial methane in the lower part. Microbial methane migrated through sedimentary layer of basin floor fan and thick bed of fine-grained marine sediment. Fluid expelled through sedimentary layer and created numerous pockmarks on the middle Eocene seafloor.

**d) Present day seabed**

Sea-level increase and carbonate sediment of Tucker Cover formation and Penrod group deposited overlain on Laing formation. Middle Eocene paleo-pockmarks are buried by younger sediment. Following by fine-grained sediment compaction which created polygonal fault system on the upper part of Laing formation and the lower part of Tucker Cove formation.

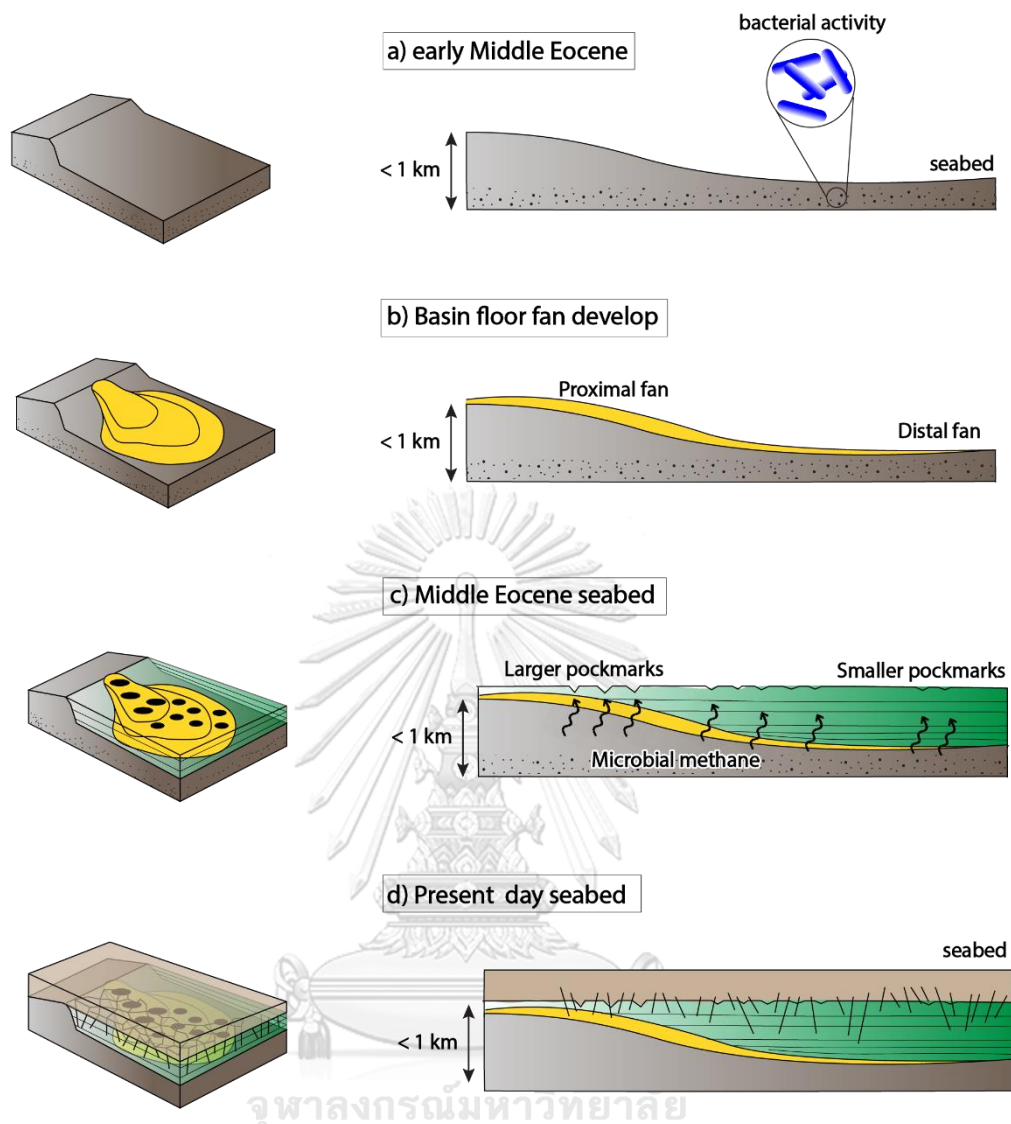


**Figure 55** Model of Mechanism of middle Eocene paleo-pockmarks in the study area during early middle Eocene to recent.

## 5.6 Petroleum application

Pockmarks are used as an indicator of a fluid flow process in the petroleum field (Andresen, 2012; Hovland et al., 2002) and for the study of the climate change (Judd and Hovland, 1992). Pockmarks characteristics can help to identify the fluid source in the area (e.g. gas associated with methane and porewater). For example, high-density normal pockmarks as shown in the Great South Basin are pockmarks founded mostly in the large gas field, same as the Barents Sea (Nickel et al., 2012) and the North Sea (Mazzini et al., 2017). While low-density pockmark characteristics which occur associated with porewater found in New Zealand (Chenrai and Huuse,



2017) (Figure 6). Even if the range of high-density and low-density pockmarks is uncertain, but the characteristic of pockmark distribution can predict fluid source of pockmark formation in the area.

In addition, the study of paleo-pockmarks in the Great South Basin suggests that it is possible to found methane gas in the study area. This methane gas is possible produced by microbial activity around late Paleocene to middle Eocene time. Microbial methane is produced in low-temperature condition with low total organic carbon (TOC). Moreover, it is possible to indicate the timing and maturation of hydrocarbon and fluid flow system in the area. The hydrocarbon status is immature because temperature lower than 60°C. It means microbial methane has not potential to be a commercial petroleum field in the Great South Basin, New Zealand.



## CHAPTER 6

### CONCLUSIONS

This study aims to describe the seismic characteristics of middle Eocene paleo-pockmarks and predict the fluid origin and mechanism of paleo-pockmarks at the Great South Basin, New Zealand. 2D and 3D seismic data and well log data are used as the main data in this study. The finding of this study is that numerous middle Eocene paleo-pockmarks are found on the fine-grained marine sediment of Liang formation. Paleo-pockmark layer is overlain by younger sediments of Tucker Cove formation and Penrod group. The high amplitude anomalies of paleo-pockmark formation coincide with a fan shaped-like feature from the southwest to the northeast direction (from proximal to distal fan). The clinofolds reflections underneath the paleo-pockmark layer would act as the migration pathway of fluid to the paleo-pockmarks area.

Middle Eocene paleo-pockmarks are divided into three zones, including zone 1 (proximal fan), zone 2 (middle fan), and zone 3 (distal fan). The paleo-pockmarks are classified as “normal pockmarks” with a sub-round to round shaped pockmark on top view and V-shaped to U-shaped pockmark from profile section. Their sizes are mainly ranging from 131 to 481 m in diameter and 15 to 45 ms (TWT) in depth. The smallest paleo-pockmarks are founded in zone 2 (middle fan) having diameter and depth approximately 131 m and 16 ms (TWT), respectively. The largest paleo-pockmarks are founded in zone 1 (proximal fan) having diameter and depth approximately 481 m and 15 ms (TWT), respectively. The paleo-pockmark density in zone 1 displays approximately 6.4 pockmarks per square kilometer. While zone 2 displays 13.44 pockmarks per square kilometer, and zone 3 shows 4.12 pockmarks per square kilometer. Moreover, the paleo-pockmark density in zone 2 seems to be the highest density zone than zone 1 and zone 3. While zone 3 is the lowest density than zone 1 and zone 2. It is possible that the size and density of paleo-pockmarks both zone 1 and zone 2 are controlled by lithology or fluid pathway.

Distribution of paleo-pockmarks is interpreted to be caused by two possible fluid origins. First, microbial methane is the main fluid origins which is produced by

bacterial activity at low temperature ( $< 60\text{ }^{\circ}\text{C}$ ) condition. Microbial methane can create high-density pockmarks with wide distribution similar to the study area. Moreover, pore water within the sedimentary formation is interpreted to be one of another possible fluid origins distributed to the paleo-pockmarks in the study area.



## REFERENCES

- Andresen, K.J. 2012. Fluid flow features in hydrocarbon plumbing systems: What do they tell us about the basin evolution? Marine Geology 332: 89-108.
- Andresen, K.J., and Huuse, M. 2011. 'Bulls-eye' pockmarks and polygonal faulting in the Lower Congo Basin: relative timing and implications for fluid expulsion during shallow burial. Marine Geology 279: 111-127.
- Ballance, P. 2009. New Zealand geology: an illustrated guide. Geoscience Society of New Zealand.
- Bertoni, C., Cartwright, J., and Hermanrud, C. 2013. Evidence for large-scale methane venting due to rapid drawdown of sea level during the Messinian Salinity Crisis. Geology 41: 371-374.
- Bøe, R., Rise, L., and Ottesen, D. 1998. Elongate depressions on the southern slope of the Norwegian Trench (Skagerrak): morphology and evolution. Marine Geology 146: 191-203.
- Boetius, A., et al. 2000. A marine microbial consortium apparently mediating anaerobic oxidation of methane. Nature 407: 623.
- Cartwright, J. 2007. The impact of 3D seismic data on the understanding of compaction, fluid flow and diagenesis in sedimentary basins. Journal of the Geological Society 164: 881-893.
- Chand, S., Mienert, J., Andreassen, K., Knies, J., Plassen, L., and Fotland, B. 2008. Gas hydrate stability zone modelling in areas of salt tectonics and pockmarks of the Barents Sea suggests an active hydrocarbon venting system. Marine and Petroleum Geology 25: 625-636.
- Chapman, R.E. 1987. Fluid flow in sedimentary basins: a geologist's perspective. Geological Society, London, Special Publications 34: 3-18.
- Chen, J., et al. 2015. Morphologies, classification and genesis of pockmarks, mud volcanoes and associated fluid escape features in the northern Zhongjiannan Basin, South China Sea. Deep Sea Research Part II: Topical Studies in Oceanography 122: 106-117.
- Chenrai, P., and Huuse, M. 2017. Pockmark formation by porewater expulsion during rapid progradation in the offshore Taranaki Basin, New Zealand. Marine and Petroleum Geology 82: 399-413.
- Colín-García, M., et al. 2016. Hydrothermal vents and prebiotic chemistry: a review. Boletín de la Sociedad Geológica Mexicana 68: 599-620.
- Constable, R.M., Langdale, S., and Allan, T.M.H. 2010. Development of a sequence stratigraphic framework in the Great South Basin Trans.). In (Ed.),^(Eds.), (ed., Vol. pp.). PTTEP New Zealand Ltd, Mitsui E&P Australia Pty Ltd and Shell GSB Ltd. (Reprinted from.
- Cowley, R., and O'brien, G. 2000. Identification and interpretation of leaking hydrocarbons using seismic data: A comparative montage of examples from the major fields in Australia's northwest shelf and Gippsland basin. The APPEA Journal 40: 119-150.
- de Mahiques, M.M., Schattner, U., Lazar, M., Sumida, P.Y., and Souza, L.A. 2017. An extensive pockmark field on the upper Atlantic margin of Southeast Brazil: spatial analysis and its relationship with salt diapirism. Heliyon 3: e00257.
- ExxonMobil. 2010. Great South Basin 3D/2D Seismic Interpretation Report, PEP 50117

- Trans.). In (Ed.),^(Eds.), (ed., Vol. pp.). New Zealand Government. (Reprinted from.
- Gay, A., Lopez, M., Cochonat, P., Séranne, M., Levaché, D., and Sermondadaz, G. 2006. Isolated seafloor pockmarks linked to BSRs, fluid chimneys, polygonal faults and stacked Oligocene–Miocene turbiditic palaeochannels in the Lower Congo Basin. Marine Geology 226: 25-40.
- Gay, A., Lopez, M., Cochonat, P., and Sermondadaz, G. 2004. Polygonal faults–furrows system related to early stages of compaction - upper Miocene to recent sediments of the Lower Congo Basin. Basin Research 16: 101-116.
- Gorman, R., Reid, S., Chiswell, S., and Smith, M. 2005. Marine weather and sea conditions of the Great South Basin Trans.). In (Ed.),^(Eds.), (ed., Vol. pp.). National Institute of Water & Atmospheric Research Ltd. (Reprinted from.
- Hammond, D. 2001. Pore water chemistry.
- Harrington, P. 1985. Formation of pockmarks by pore-water escape. Geo-Marine Letters 5: 193-197.
- Hovland, M. 1983. Elongated depressions associated with pockmarks in the western slope of the Norwegian Trench. Marine Geology 51: 35-46.
- Hovland, M., Gardner, J.V., and Judd, A. 2002. The significance of pockmarks to understanding fluid flow processes and geohazards. Geofluids 2: 127-136.
- Hovland, M., Heggland, R., De Vries, M., and Tjelta, T. 2010. Unit-pockmarks and their potential significance for predicting fluid flow. Marine and Petroleum Geology 27: 1190-1199.
- Hovland, M., and Svensen, H. 2006. Submarine pingoes: Indicators of shallow gas hydrates in a pockmark at Nyegga, Norwegian Sea. Marine Geology 228: 15-23.
- Hovland, M., et al. 2005. Complex pockmarks with carbonate-ridges off mid-Norway: Products of sediment degassing. Marine Geology 218: 191-206.
- Hovland, M., Talbot, M.R., Qvale, H., Olaussen, S., and Aasberg, L. 1987. Methane-related carbonate cements in pockmarks of the North Sea. Journal of Sedimentary Research 57: 881-892.
- Josenhans, H.W., King, L.H., and Fader, G.B. 1978. A side-scan sonar mosaic of pockmarks on the Scotian Shelf. Canadian Journal of Earth Sciences 15: 831-840.
- Judd, A., and Hovland, M. 1992. The evidence of shallow gas in marine sediments. Continental Shelf Research 12: 1081-1095.
- Judd, A., and Hovland, M. 2009. Seabed fluid flow: the impact on geology, biology and the marine environment. Cambridge University Press.
- Judd, A.G. 2003. The global importance and context of methane escape from the seabed. Geo-Marine Letters 23: 147-154.
- Killops, S., Cook, R., Sykes, R., and Boudou, J. 1997. Petroleum potential and oil-source correlation in the Great South and Canterbury Basins. New Zealand Journal of Geology and Geophysics 40: 405-423.
- King, L.H., and MacLEAN, B. 1970. Pockmarks on the Scotian shelf. Geological Society of America Bulletin 81: 3141-3148.
- Koson, S., Chenrai, P., and Choowong, M. 2014. Seismic attributes and their applications in seismic geomorphology. Bulletin of Earth Sciences of Thailand 6: 1-9.
- Kuhasubpasin, B. 2017. Reservoir Property Analysis From Well Log Data

Of North Cape Formation,

- Taranaki Basin, Nwe Zealand. Bachelor's degree, Geology Department of Geology, Faculty of Science, Chulalongkorn University, Chulalongkorn University.
- Luo, M., et al. 2015. Estimating the time of pockmark formation in the SW Xisha Uplift (South China Sea) using reaction-transport modeling. Marine Geology 364: 21-31.
- Mazzini, A., et al. 2017. A climatic trigger for the giant Troll pockmark field in the northern North Sea. Earth and Planetary Science Letters 464: 24-34.
- Milkov, A. 2000. Worldwide distribution of submarine mud volcanoes and associated gas hydrates. Marine Geology 167: 29-42.
- Minerals, N.Z.P. 2014. New Zealand Petroleum Basins. 38-104.
- Morgan, D., Cartwright, J., and Imbert, P. 2015. Perturbation of polygonal fault propagation by buried pockmarks and the implications for the development of polygonal fault systems. Marine and Petroleum Geology 65: 157-171.
- Morley, C.K., et al. 2017. New style of honeycomb structures revealed on 3D seismic data indicate widespread diagenesis offshore Great South Basin, New Zealand. Marine and Petroleum Geology 86: 140-154.
- Murchison, R.I. 1827. On the Coal-field of Brora in Sutherlandshire, and some other Stratified Deposits in the North of Scotland. Transactions of the Geological Society of London 2: 293-326.
- Nakajima, T., et al. 2014. Formation of pockmarks and submarine canyons associated with dissociation of gas hydrates on the Joetsu Knoll, eastern margin of the Sea of Japan. Journal of Asian Earth Sciences 90: 228-242.
- Nicholas, W., Nichol, S., Kool, J., Carroll, A., and Rollet, N. 2016. Comment on “Evidence for the biotic origin of seabed pockmarks on the Australian continental shelf” by RJ Mueller [Marine and Petroleum Geology (2015). Marine and Petroleum Geology 69: 266-268.
- Nickel, J.C., di Primio, R., Mangelsdorf, K., Stoddart, D., and Kallmeyer, J. 2012. Characterization of microbial activity in pockmark fields of the SW-Barents Sea. Marine Geology 332: 152-162.
- Norton, D.L. 1984. Theory of hydrothermal systems. Annual Review of Earth and Planetary Sciences 12: 155-177.
- NZP&M. 2015. Great South-Canterbury Province. In Minerals, N.Z.P. (ed.), New Zealand Petroleum Basins, pp. 50-63. New Zealand Petroleum & Minerals.
- Odundun, O., and Nton, M. 2012. Facies interpretation from well logs: Applied to SMEKS field, offshore western Niger Delta. pp. AAPG international conference and exhibition.
- Omosanya, K.O., and Harishidayat, D. 2019. Seismic geomorphology of Cenozoic slope deposits and deltaic clinoforms in the Great South Basin (GSB) offshore New Zealand. Geo-Marine Letters 39: 77-99.
- Pernes, R.A.S. 2013. Well-logging Correlation–Analysis and correlation of well logs in Rio Grande do Norte basin wells.
- Pigott, J.D., Kang, M.-H., and Han, H.-C. 2013. First order seismic attributes for clastic seismic facies interpretation: Examples from the East China Sea. Journal of Asian Earth Sciences 66: 34-54.
- Pilcher, R., and Argent, J. 2007. Mega-pockmarks and linear pockmark trains on the West African continental margin. Marine Geology 244: 15-32.



- Puchała, R. 2014. Morphology and origin of modern seabed features in the central basin of the Gulf of Thailand.
- Riboulot, V., et al. 2013. Sea-level change and free gas occurrence influencing a submarine landslide and pockmark formation and distribution in deepwater Nigeria. Earth and Planetary Science Letters 375: 78-91.
- Schoell, M. 1988. Multiple origins of methane in the Earth. Chemical geology 71: 1-10.
- Serra, O. 1984. Fundamentals of Well-log Interpretation: The interpretation of logging data. Elsevier Science Limited.
- Shanmugam, G. 1997. The Bouma sequence and the turbidite mind set. Earth-Science Reviews 42: 201-229.
- Skarke, A., Ruppel, C., Kodis, M., Brothers, D., and Lobecker, E. 2014. Widespread methane leakage from the sea floor on the northern US Atlantic margin. Nature Geoscience 7: 657-661.
- Sluijs, A., et al. 2006. Subtropical Arctic Ocean temperatures during the Palaeocene/Eocene thermal maximum. Nature 441: 610.
- Stolper, D., et al. 2014. Formation temperatures of thermogenic and biogenic methane. Science 344: 1500-1503.
- Sun, Q., Wu, S., Hovland, M., Luo, P., Lu, Y., and Qu, T. 2011. The morphologies and genesis of mega-pockmarks near the Xisha Uplift, South China Sea. Marine and Petroleum Geology 28: 1146-1156.
- Tasianas, A., et al. 2018. High-resolution 3D seismic study of pockmarks and shallow fluid flow systems at the Snøhvit hydrocarbon field in the SW Barents Sea. Marine Geology 403: 247-261.
- Uruski, C. 2017. Stacked Deltas in the Great South Basin Trans.). In (Ed.),^(Eds.), (ed., Vol. pp.). OMV New Zealand Ltd: OMV New Zealand Ltd. (Reprinted from.
- Welhan, J.A. 1988. Origins of methane in hydrothermal systems. Chemical Geology 71: 183-198.



จุฬาลงกรณ์มหาวิทยาลัย  
**CHULALONGKORN UNIVERSITY**

## VITA

<b>NAME</b>	Arunee Karaket
<b>DATE OF BIRTH</b>	21 Jan 1992
<b>PLACE OF BIRTH</b>	Chachoengsao
<b>HOME ADDRESS</b>	1/8 Moo.3, Phimpha, Bangpakong, Chachoengsao



จุฬาลงกรณ์มหาวิทยาลัย  
CHULALONGKORN UNIVERSITY